Supporting information

Towards Understanding Oxygen Heterocycle-Forming Cyclases: A Selectivity Study of The Pyran Synthase PedPS7

Lisa Wagner, [a] Jörg Stang,[a] Sebastian Derra,[a] Tim Hollmann[a] and Frank Hahn*[a]

[a]*Professur für Organische Chemie (Lebensmittelchemie), Fakultät für Biologie, Chemie und Geowissenschaften, Department of Chemistry, Universität Bayreuth, 95447 Bayreuth, Germany*

*E-mail: frank.hahn@uni-bayreuth.de

Contents

Methods and materials

Chemistry & Analytics

UPLC-MS analysis was performed on a WATERS Acquity Ultra Perfomance LC (column: HSS C18, pore size 100 Å, particle size 1.8 µm, 2.1 x 50 mm; PDA detector; SQ detector). Mode of ionisation was ESI+ and found mass is given. Reversed phase-UPLC-applications were performed with membrane-filtrated and double distilled water as well as commercially available UPLC-grade methanol or acetonitrile.

NMR spectra were recorded with BRUKER Avance III HD 500 or an Avance 300 with the residual solvent signal as internal standard ($CDCl_3$, ^1H: 7.26 ppm, ^{13}C: 77.2 ppm; C_6D_6, ^1H: 7.16 ppm). Multiplicities are described using the following abbreviations: s = singlet, d = doublet, t = triplet, q = quartet, m = multiplet, b = broad. The multiplicities are elucidated using the distortionless enhancement by polarization transfer (DEPT) spectral editing technique, with secondary pulses at 90° and 135°. Multiplicities are reported using the following abbreviations: q (quarternary carbon), t (tertiary carbon = methine), s (secondary carbon = methylene), p (primary carbon = methyl).

High resolution mass spectra are obtained with a Q Exactive (THERMO SCIENTIFIC) *via* loop-mode injection. Ionization is achieved by ESI. Semi-preparative HPLC was performed with a WATERS HPLC (600 controller, 2487 Dual wavelength absorbance detector) using a C18-SP stationary phase. Chiral HPLC analysis was performed using a WATERS Alliance 2695 Separations Module (column: OJ-H, particle size 5 µm, 4.6 mm x 250 mmL) with a WATERS 2487 Dual Wavelength Absorbance Detector and using an isocratic gradient with hexane:*iso*-propanole 90:10.

Solvents, columns, operating procedures and retention times (t_R) are given with the corresponding experimental and analytical data. (Abbreviations: DCM = dichloromethane, DMF = dimethylformamide, EtOAc = ethyl acetate).

Biochemistry

All chemicals and antibiotics were purchased from SIGMA-ALDRICH and ROTH. Cell disruption was conducted by sonication (Sonoplus Typ UW3100 and Sonoplus HD3100 with probe MS-73 or KE-76) from BANDELIN. Protein purification was performed on an ÄKTA pure system (GE HEALTHCARE). His-bind Ni chelate chromatography resin was purchased from NOVAGEN. PD-10 desalting columns from GE HEALTHCARE were used for buffer exchange. Protein concentration was measured on a Varioskan LUX multimode microplate reader (THERMO SCIENTIFIC).

Chemical synthesis

The synthesis of all compounds was described in reference [1,2], except for the synthetic racemic mixture *syn-rac*-**35**, which is shown below.

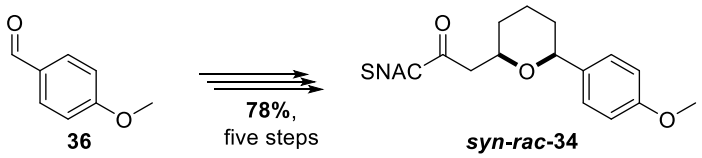

1-(4-Methoxyphenyl)hex-5-en-1-ol (*rac*-37)

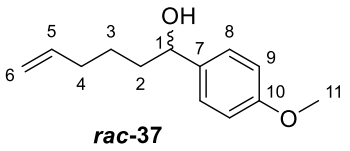

To a suspension of magnesium (219 mg, 9.00 mmol, 3.0 eq.) in THF (12.0 mL) was slowly added 5-bromo-1-pentene (710 µL, 6.00 mmol, 2.0 eq.) and the suspension was stirred for 1 h under reflux. After cooling to room temperature, the supernatant was carefully dropped into a 0 °C cold solution of anisaldehyde (**36**) (365 µL, 3.00 mmol, 1.0 eq.) in THF (28.0 mL, 0.11 M) and stirred at this temperature for 3 h. To terminate the reaction, saturated NH_4Cl solution (20.0 mL) was added carefully. The resulting phases were separated and the aqueous one extracted with Et_2O (3× 10.0 mL). The combined organic phases were washed with saturated NaCl solution (1× 50.0 mL), dried over Na_2SO_4 and filtered. After removing the solvent *in vacuo* and flash chromatography (SiO_2, cyclohexane:EtOAc / 10:1 → 8:1), the product *rac*-**37** (616 mg, 2.99 mmol, quantitative) was obtained as colourless oil.

R_f : (cyclohexane:EtOAc / 10:1) = 0.28.

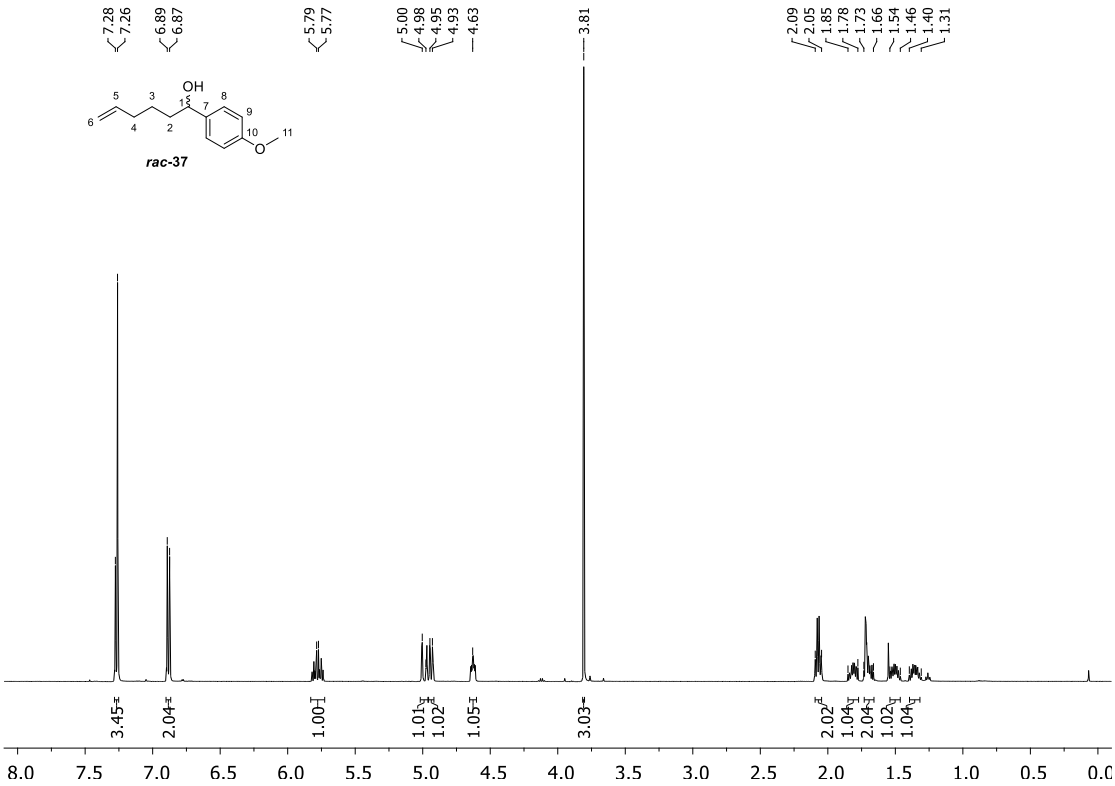

Figure S1. ^1H NMR analysis of the purified product *rac*-**37** ($CDCl_3$, 500 MHz).

^{1}H NMR (500 MHz, $CDCl_3$): δ = 7.27 (d, *J* = 8.6 Hz, 2H, 8-CH), 6.88 (d, *J* = 8.6 Hz, 2H, 9-CH), 5.78 (ddt, *J* = 16.9, 10.2, 6.7 Hz, 1H, 5-CH), 4.99 (ddt, *J* = 17.0, 2.0, 1.6 Hz, 1H, 1× 6-CH), 4.94 (ddt, *J* = 10.2, 2.0, 1.2 Hz, 1H, 1× 6-CH), 4.63 (dt, *J* = 7.2, 3.1 Hz, 1H, 1-CH), 3.81 (s, 3H, 11-CH_3), 2.09-2.05 (m, 2H, 4-CH_2), 1.85-1.78 (m, 1H, 1× 2-CH_2), 1.73-1.66 (m, 2H, 1× 2-CH_2 and OH), 1.54-1.46 (m, 1H, 1× 3-CH_2), 1.40-1.31 (m, 1H, 1× 3-CH_2) ppm.

The analytical data correspond to those in the literature [3].

Ethyl-(*E*)-7-hydroxy-7-(4-methoxyphenyl)hept-2-enoate (***rac*-38**)

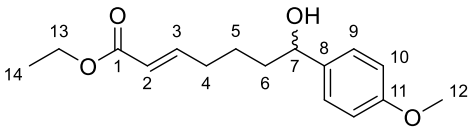

***rac*-38**

To a solution of alcohol *rac*-**37** (515 mg, 2.5 mmol, 1.0 eq.) and ethyl acrylate (633 µL, 7.5 mmol, 3.0 eq.) in CH_2Cl_2 (25 mL, 0.1 M) was added HOVEYDA-GRUBBS-II catalyst (39.0 mg, 62.5 µmol, 2.5 mol%) and the solution was stirred under reflux. After 2 h, the same amount of catalyst was added again and the solution was stirred for another 2 h. After cooling to room temperature and removing of the solvent *in vacuo*, the residue was purified by flash chromatography (SiO_2, cyclohexane:EtOAc / 3:1). The product *rac*-**38** (677 mg, 2.43 mmol, 97%) was obtained as brown oil.

R_f : (cyclohexane:EtOAc / 3:1) = 0.32.

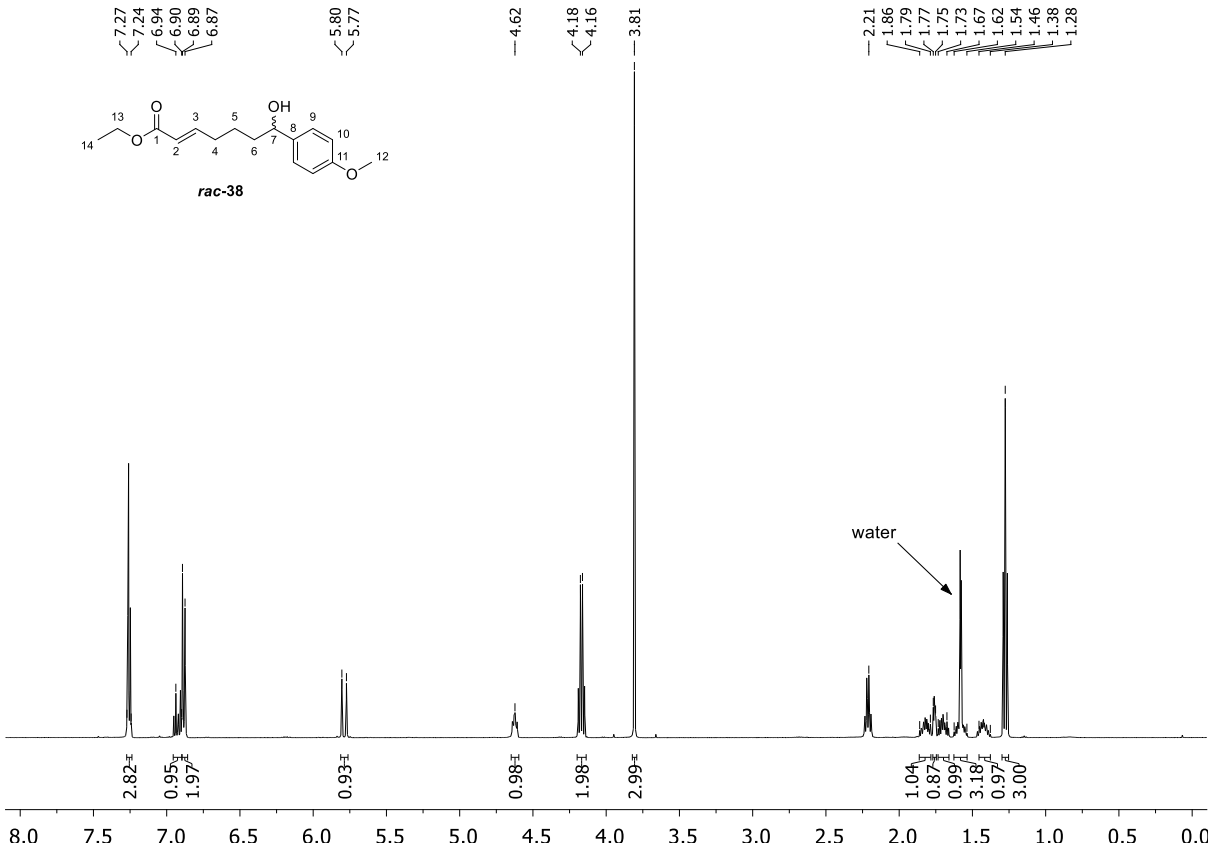

Figure S2. ^{1}H NMR analysis of the purified product *rac*-**38** ($CDCl_3$, 500 MHz).

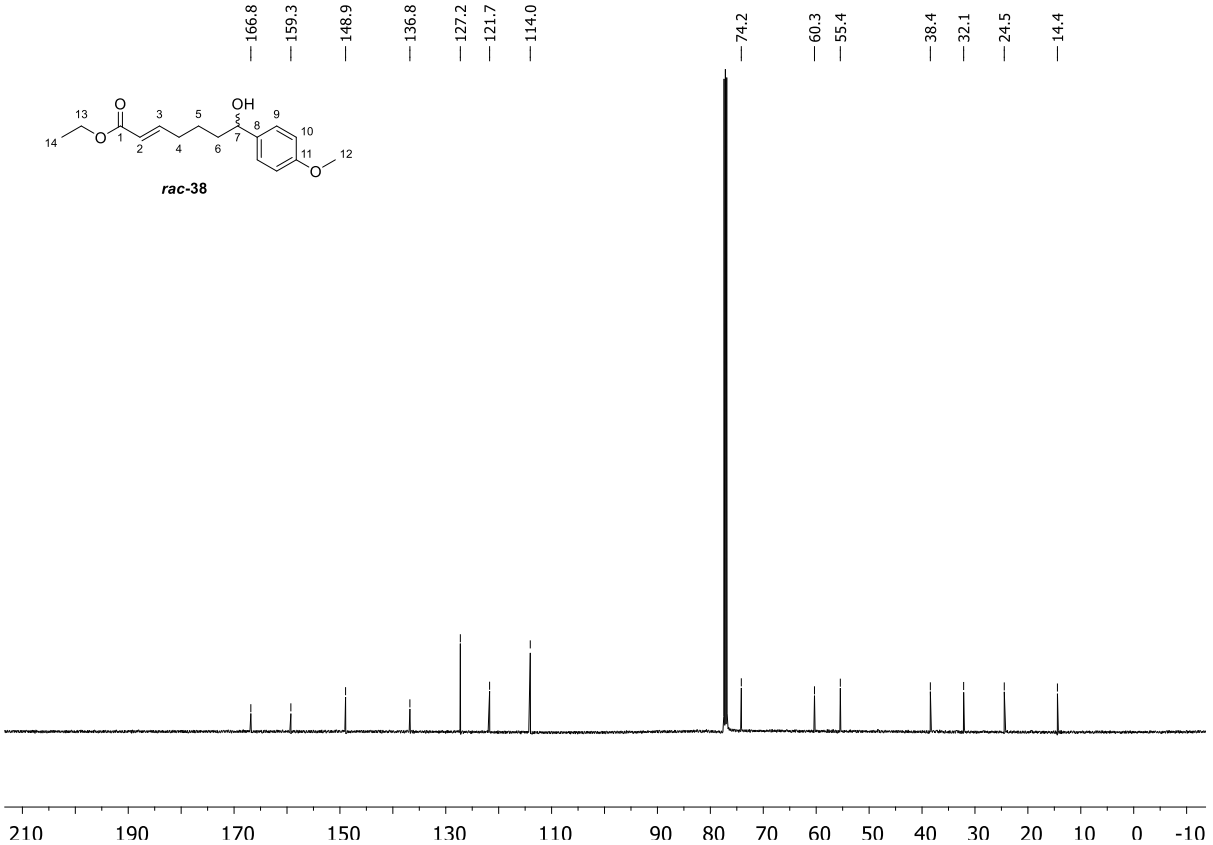

Figure S3. ^{13}C NMR analysis of the purified product *rac*-**38** ($CDCl_3$, 125 MHz).

^{1}H NMR (500 MHz, $CDCl_3$): δ = 7.27-7.25 (m, 2H, 2× 9-CH), 6.92 (dt, *J* = 15.7, 6.9 Hz, 1H, 3-CH), 6.88 (d, *J* = 8.8 Hz, 2H, 2× 10-CH), 5.79 (dt, *J* = 15.7, 1.5 Hz, 1H, 2-CH), 4.62 (t, *J* = 7.2 Hz, 1H, 7-CH), 4.17 (q, *J* = 7.1 Hz, 2H, 13-CH_2), 3.81 (s, 3H, 12-CH_3), 2.21 (ddt, *J* = 7.4, 6.9, 1.5 Hz, 2H, 4-CH_2), 1.86-1.79 (m, 1H, 1× 6-CH_2), 1.77-1.75 (m, 1H, OH), 1.73-1.67 (m, 1H, 1× 6-CH_2), 1.62-1.54 (m, 1H, 1× 5-CH_2), 1.46-1.38 (m, 1H, 1× 5-CH_2), 1.28 (t, *J* = 7.1 Hz, 3H, 14-CH_3) ppm.
^{13}C NMR (125 MHz, $CDCl_3$): δ = 166.8 (q, C-1), 159.3 (q, C-11), 148.9 (t, C-3), 136.8 (q, C-8), 127.2 (t, 2× C-9), 121.7 (t, C-2), 114.0 (t, 2× C-10), 74.2 (t, C-7), 60.3 (s, C-13), 55.4 (p, C-12), 38.4 (s, C-6), 32.1 (s, C-4), 24.5 (s, C-5), 14.4 (p, C-14) ppm.
HRMS (ESI$^+$): *m/z* for $C_{16}H_{21}O_3$ $[M+H-H_2O]^+$: calculated 261.14852, found 261.14816.

Ethyl-2-(6-(4-methoxyphenyl)tetrahydro-2*H*-pyran-2-yl)-acetate (*syn*-*rac*-39)

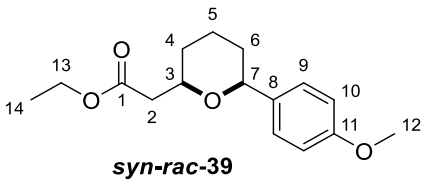

To a solution of ethyl ester *rac*-**38** (540 mg, 1.95 mmol, 1.0 eq.) in CH_2Cl_2 (20 mL, 0.1 M) at 0 °C KO*t*Bu (241 mg, 2.15 mmol, 1.1 eq.) was added slowly and the solution was stirred at this temperature for 1 h. To stop the reaction, saturated NH_4Cl solution (15.0 mL) was added. The resulting phases were separated and the aqueous one extracted with CH_2Cl_2 (3× 10.0 mL). The combined organic phases were washed with saturated NaCl solution (1× 40.0 mL), dried over $MgSO_4$ and filtered. After removing the solvent *in vacuo*, the product *syn*-*rac*-**39** (513 mg, 1.84 mmol, 95%) was obtained without further purification as yellow-orange oil.

R_f : (cyclohexane:EtOAc / 3:1) = 0.45.

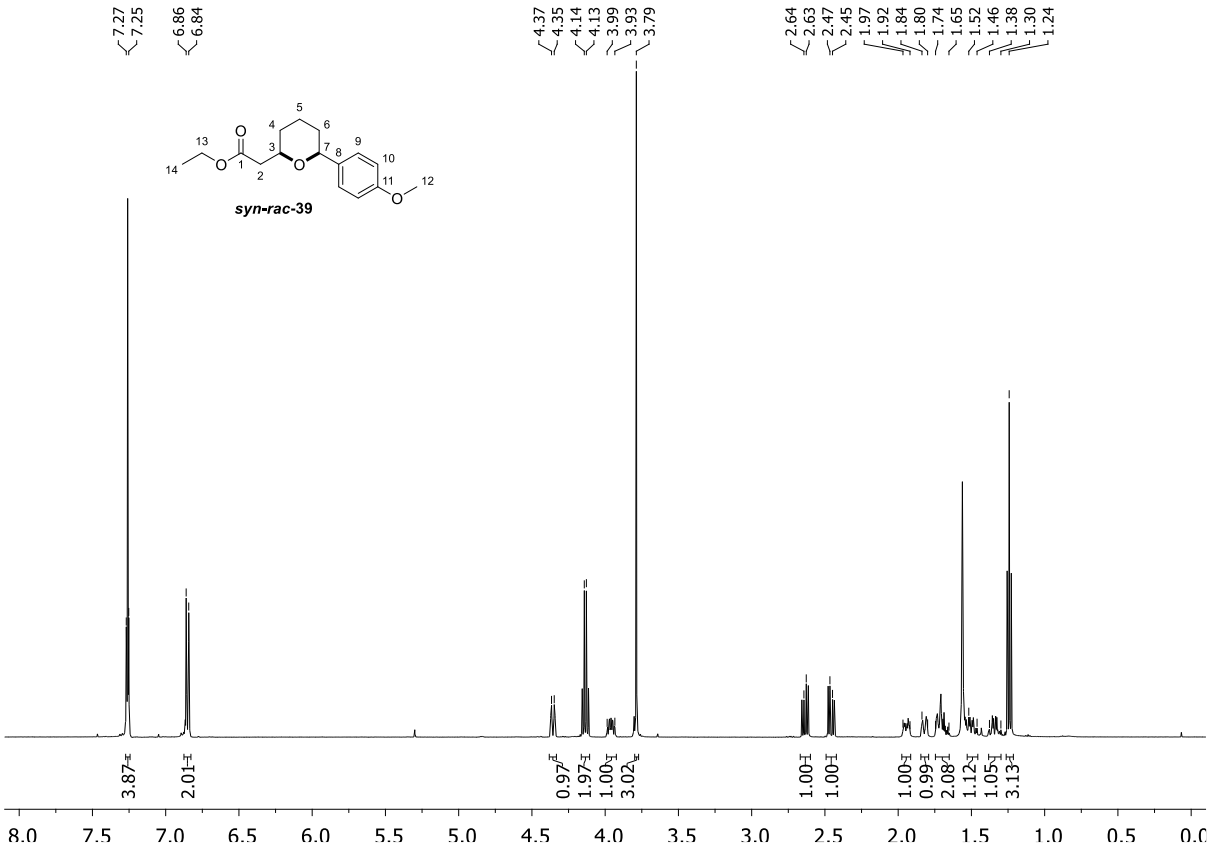

Figure S4. ^{1}H NMR analysis of the purified product *syn-rac*-**39** ($CDCl_3$, 500 MHz).

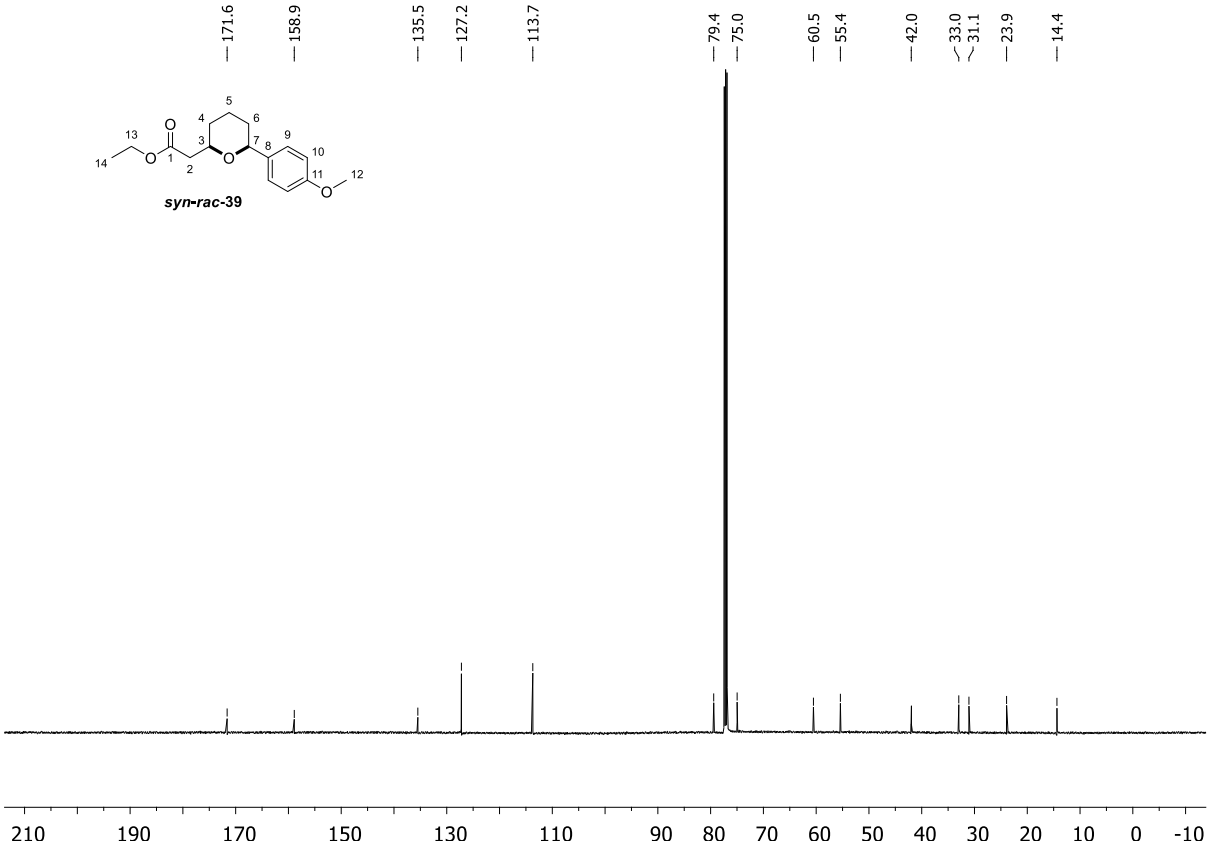

Figure S5. ^{13}C NMR analysis of the purified product *syn-rac*-**39** ($CDCl_3$, 125 MHz).

^{1}H NMR (500 MHz, $CDCl_3$): δ = 7.27-7.25 (m, 2H, 2 × 9-CH), 6.85 (d, *J* = 8.8 Hz, 2H, 2 × 10-CH), 4.36 (dd, *J* = 11.3, 2.1 Hz, 1H, 7-CH), 4.14 (q, *J* = 7.1 Hz, 2H, 13-CH_2), 3.99-3.93 (m, 1H, 3-CH), 3.79 (s, 3H, 12-CH_3), 2.64 (dd, *J* = 15.0, 7.1 Hz, 1H, 1 × 2-CH_2), 2.46 (dd, *J* = 15.0, 6.1 Hz, 1H, 1 × 2-CH_2), 1.97-1.92 (m, 1H, 1 × 5-CH_2), 1.84-1.80 (m, 1H, 1 × 6-CH_2), 1.75-1.65 (m, 2H, 1 × 4-CH_2 and 1 × 5-CH_2), 1.52-1.46 (m, 1H, 1 × 6-CH_2), 1.38-1.30 (m, 1H, 1 × 4-CH_2), 1.24 (t, *J* = 7.1 Hz, 3H, 14-CH_3) ppm.

^{13}C NMR (125 MHz, $CDCl_3$): δ = 171.6 (q, C-1), 158.9 (q, C-11), 135.5 (q, C-8), 127.2 (t, 2× C-9), 113.7 (t, 2× C-10), 79.4 (t, C-7), 75.0 (t, C-3), 60.5 (s, C-13), 55.4 (p, C-12), 41.9 (s, C-2), 33.0 (s, C-6), 31.0 (s, C-4), 23.9 (s, C-5), 14.4 (p, C-14) ppm.

HRMS (ESI$^+$): *m/z* for $C_{16}H_{23}O_4$ $[M+H]^+$: calculated 279.15909, found 279.15873.

2-(6-(4-methoxyphenyl)tetrahydro-2*H*-pyran-2-yl)acetic acid (*syn-rac*-40)

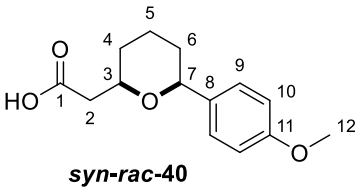

***syn-rac*-40**

The ethyl ester *syn-rac*-**39** (420 mg, 1.50 mmol, 1.0 eq.) was placed in a methanol:water mixture (3:1, 15 mL, 0.1 M). After addition of LiOH (108 mg, 4.50 mmol, 3.0 eq.), the solution was heated to 50 °C and stirred overnight. After concentration *in vacuo*, the residue was taken up in aqueous HCl solution (10.0 mL, 1 M) and extracted with EtOAc (3× 10.0 mL). The combined organic phases were dried over $MgSO_4$, filtered and the solvent was removed *in vacuo*. The product *syn-rac*-**40** (382 mg, crude) was used directly without further purification. Only a small amount was recrystallised for analytical purposes (cyclohexane) and obtained from this as white solid.

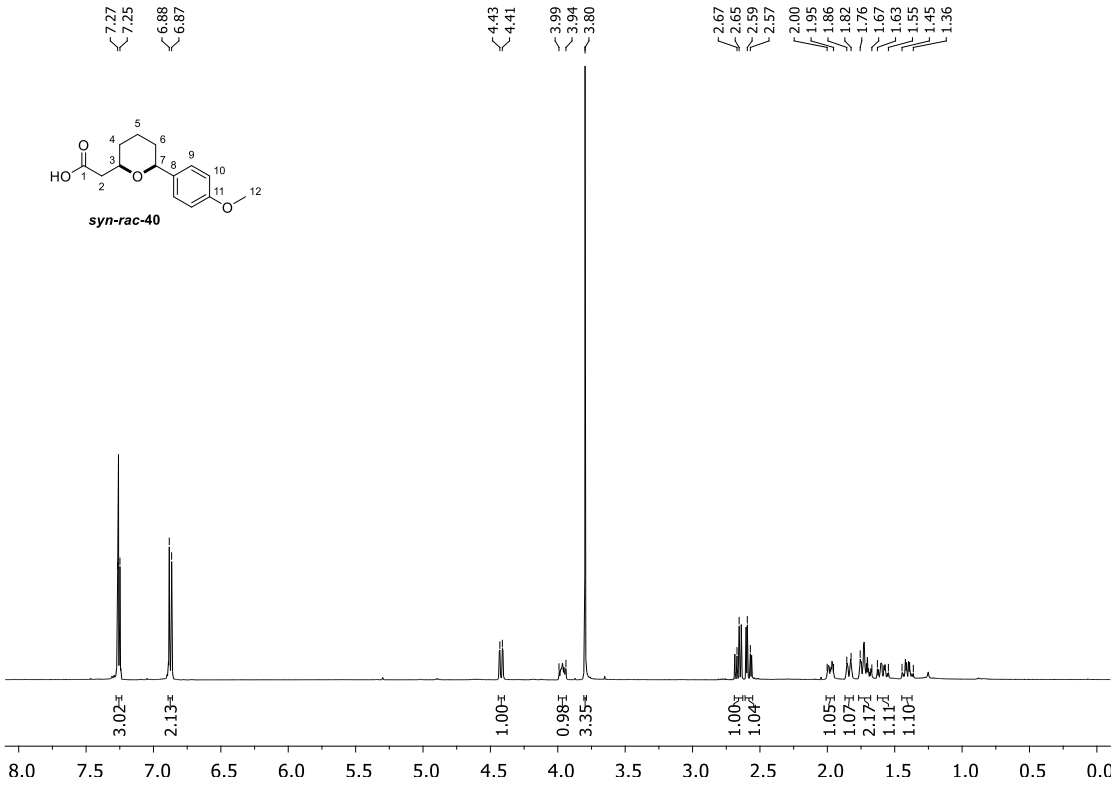

Figure S6. ^{1}H NMR analysis of the purified product *syn-rac*-**40** ($CDCl_3$, 500 MHz).

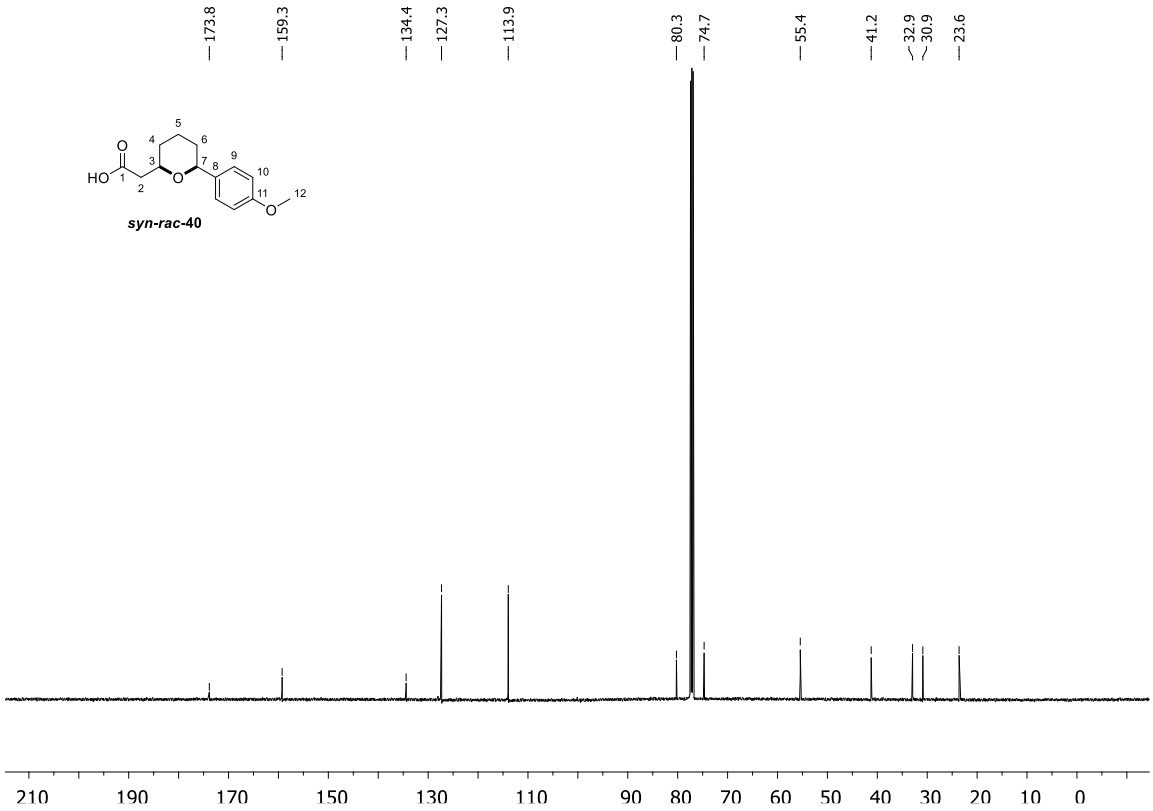

Figure S7. ^{13}C NMR analysis of the purified product *syn-rac*-**40** ($CDCl_3$, 125 MHz).

^{1}H NMR (500 MHz, $CDCl_3$): δ = 7.27-7.25 (m, 2H, 2× 9-CH), 6.88-6.87 (m, 2H, 2× 10-CH), 4.42 (dd, *J* = 11.3, 2.1 Hz, 1H, 7-CH), 3.99-3.94 (m, 1H, 3-CH), 3.80 (s, 3H, 12-CH_3), 2.66 (dd, *J* = 15.9, 7.9 Hz, 1H, 1× 2-CH_2), 2.58 (dd, *J* = 15.9, 4.6 Hz, 1H, 1× 2-CH_2), 2.00-1.95 (m, 1H, 1× 5-CH_2), 1.86-1.82 (m, 1H, 1× 6-CH_2), 1.76-1.67 (m, 2H, 1× 4-CH_2 and 1× 5-CH_2), 1.63-1.55 (m, 1H, 1× 6-CH_2), 1.45-1.36 (m, 1H, 1× 4-CH_2) ppm.

^{13}C NMR (125 MHz, $CDCl_3$): δ = 173.8 (q, C-1), 159.3 (q, C-11), 134.4 (q, C-8), 127.3 (t, 2× C-9), 113.9 (t, 2× C-10), 80.3 (t, C-7), 74.7 (t, C-3), 55.4 (p, C-12), 41.2 (s, C-2), 32.9 (s, C-6), 30.9 (s, C-4), 23.5 (s, C-5) ppm.

HRMS (ESI$^+$): *m/z* for $C_{14}H_{19}O_4$ $[M+H]^+$: calculated 251.12779, found 251.12775.

Melting point: 123 °C.

S-(2-acetamidoethyl)-2-(6-(4-methoxyphenyl)tetrahydro-2*H*-pyran-2-yl)ethanethioate (*syn-rac*-35)

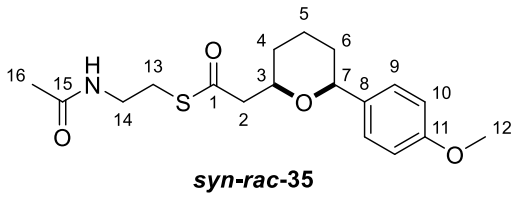

***syn-rac*-35**

The carboxylic acid *syn-rac*-**40** (382 mg, 1.50 mmol, 1.0 eq.) was placed together with HSNAC (268 mg, 2.25 mmol, 1.5 eq.) in CH_2Cl_2 (7.50 mL, 0.2 M) and the solution was cooled to 0 °C. To this were added DMAP (18.3 mg, 0.15 mmol, 0.1 eq.) and EDC×HCl (431 mg, 2.25 mmol, 1.5 eq.). After warming to room temperature, the solution was stirred for 2 h. To terminate the reaction, saturated NH_4Cl (10.0 mL) solution was added. The resulting phases were separated and the aqueous one extracted with CH_2Cl_2 (3× 8.00 mL). The combined organic

phases were dried over $MgSO_4$ and filtered. After removing the solvent *in vacuo* and flash chromatography (SiO_2, EtOAc), the product *syn-rac*-**35** (448 mg, 1.27 mmol, 85%, two steps) was obtained as orange oil.

R_f : (EtOAc) = 0.43.

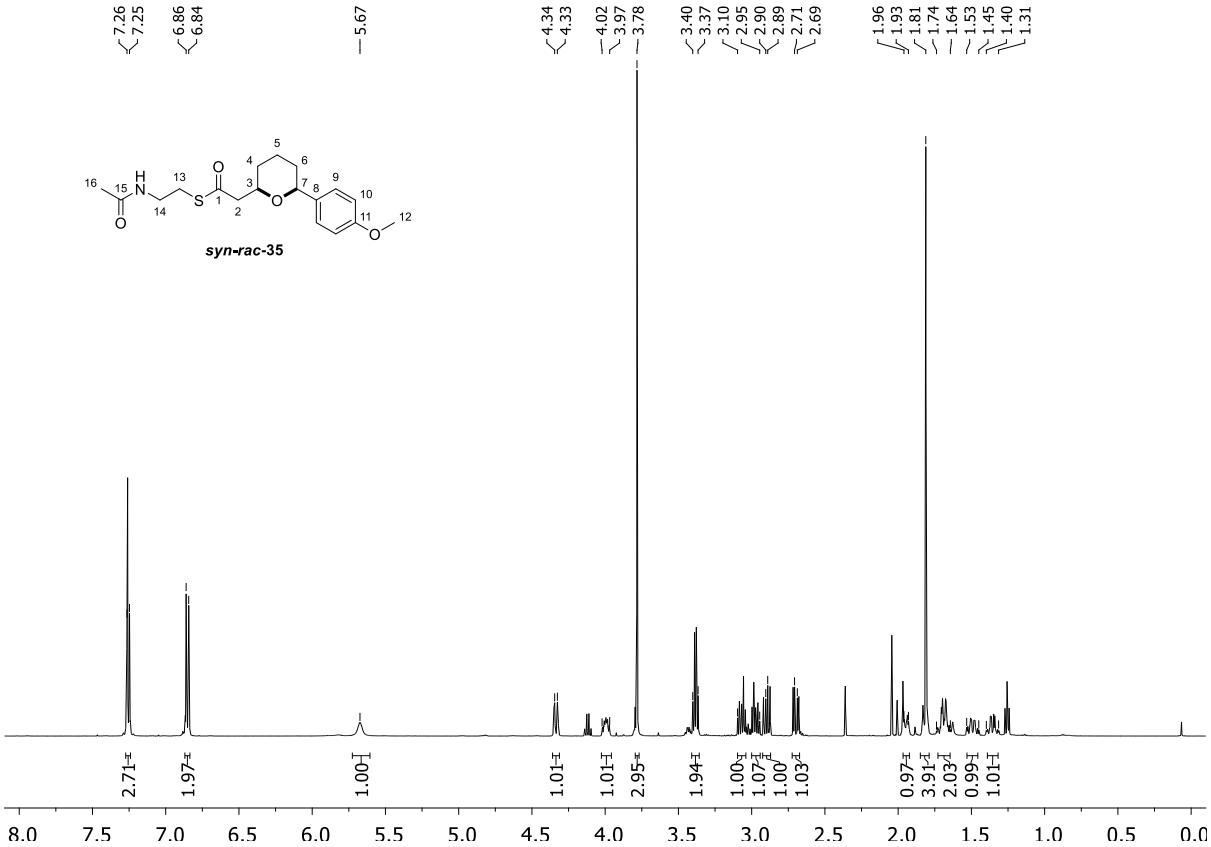

Figure S8. ^{1}H NMR analysis of the purified product *syn-rac*-**35** ($CDCl_3$, 500 MHz).

^{1}H NMR (500 MHz, $CDCl_3$): δ = 7.27-7.25 (m, 2H, 2× 9-CH), 6.83-6.81 (m, 2H, 2× 10-CH), 4.70 (br, 1H, NH), 4.15 (dd, *J* = 10.7, 2.0 Hz, 1H, 7-CH), 3.99-3.88 (m, 1H, 3-CH), 3.30 (s, 3H, 12-CH_3), 3.17 (ddd, *J* = 12.6, 6.5, 1.8 Hz, 2H, 14-CH_2), 2.86-2.72 (m, 3H, 13-CH_2 and 1× 2-CH_2), 2.41 (dd, *J* = 14.6, 4.7 Hz, 1H, 1× 2-CH_2), 1.56-1.52 (m, 2H, 1× 5-CH_2 and 1× 6-CH_2), 1.43 (s, 3H, 16-CH_3), 1.35-1.35 (m, 3H, 1× 4-CH_2 and 1 × 5-CH_2 and 1× 6-CH_2), 1.10-1.02 (m, 1H, 1× 4-CH_2) ppm.
The analytical data correspond to those in the literature [2].

Transesterification of assay products

The compound mixtures **3-L,7-L-34**+**3-D,7-D-34** (reference and after enzymatic reaction with AmbDH3) and **3-L,7-L-34**+**3-D/L,7-D/L-34** (after enzymatic reaction with PedPS7) are transesterified to the corresponding SEt thioester. The SNAC thioester (4.0 mg, 11.4 µmol, 1.0 eq) is dissolved in DMF (570 µL). Ethanethiol (7.7 µL, 107 µmol, 9.4 eq) and DIPEA (9.2 µL, 52.4 µmol, 4.6 eq) are added. After stirring for 2 d at room temperature saturated NaCl-solution is added and three times extracted with Et_2O. The combined organic layers are washed with 5% LiCl-Solution and concentrated under reduced pressure. The crude product is purified by flash chromatography on silica gel (cyclohexane:EtOAc / 19:1) and analysed *via* NMR spectroscopy and chiral HPLC.

Cloning, gene expression and enzyme purification

Sequence of the *pedPS7* gene

CATATGAGCACCCTGGTTAGCACCGAAGGTGTTAGCCGTTTCAAGGGCGAAGAGTTTTTCCTGCGTGACCACAGC
GGTATGCTGCCGGCGGCGGTGTACCTGGAAATGGTTCGTGCGTTCGCGGAGGGCAAGCACGAACGTAAAATCACC
GGCCTGAGCCACGTGGTTTGGCCGAAGGTGCTGCTGGTTAGCGGCGAGGGCCGTGAAGTGCGTACCTGCCTGACC
AACGTTGACCGTAGCGCGTTTCTGATTAGCGCGTGCGAGCAGAGCAGCGAAGGTCCGCAAGAGGTGACCTACTGC
CAGGGCAACCTGCTGCTGCCGGAAGTGATGGAAGAACCGGGTGCGGCGCTGGCGATTGAAGCGATTGCGTATCGT
TGCCCGAGCGTGCTGGAGGCGAAACAATGCGATCGTCTGCTGCAAAGCACCCATGGTCCGGCGCTGATGAGCGTT
CAGCAACTGCGTTACAGCGACCGTGAAGCGCTGGCGCTGCTGCAACTGCCGGATGAGCTGCAGATGGGTTGGGAC
GATTATGGTTGGCACCCGAGCCTGCTGAACGGTGCGATTCTGGCGAGCGTGGTTTGGTGCCTGGCGCGTGCGCCG
CGTAGCCGTGCGGGTCTGCCGATGCCGTTCAGCCTGGACCGTCTGCGTGTGTTCCAACCGTTTGAACGTCAGATG
CAAGCGTATGTTCGTCGTCATGGTAGCGCGCGTAGCCTGGGCGAGAACCTGGAAAAGGTGGACATTGATCTGCTG
GATAGCCAGGGTCGTTGCCTGGCGAGCCTGGAAGGTTTCACCCTGGTTTTTGCGCCGGATGCGAATCGTCTGGTT
TAAGAATTC

The expression plasmid *pedPS7_pET28a(+)* was used for expression of *pedPS7* in *E. coli* BL21(DE3) under analogous conditions as for *ambDH3* in [2]. 1 g of *E. coli* BL21(DE3) cells carrying *pedPS7_pET28a(+)* were suspended in 10 mL HEPES buffer (25 mM HEPES, 100 mM NaCl, pH 6.8 if not otherwise stated). Cell disruption was performed on ice by sonication (45% amplitude, 10 cycles, 30 s sonication, 30 s pause). After centrifugation (10000 g, 4 °C, 30 min), the obtained crude lysate was filtered (cellulose acetate, 0.45 µm) and either used for enzymatic conversions or purified *via* Ni-NTA affinity chromatography.

The lysate was passed through a HisTrap™ FF Ni-NTA column (in combination with a FPLC Äkta Pure System). The column was washed with wash buffer until the absorption was under 50 mAU. Elution of the target protein could be observed during a linear gradient elution with elution buffer (30 mM Tris, 500 mM NaCl, 500 mM imidazole, 10% glycerol, pH 7.5) from 0 to 100% in 25 mL. The protein-containing fractions were united and the elution buffer replaced by HEPES buffer (25 mM HEPES, 100 mM NaCl, pH 7.2) using PD-10 desalting column. If necessary the purified enzyme was concentrated and immediately used for activity assays. The identity of PedPS7 was confirmed by ESI-MS/MS analysis.

Gene expression of *ambDH3* and purification of the enzyme were performed according to reference [1].

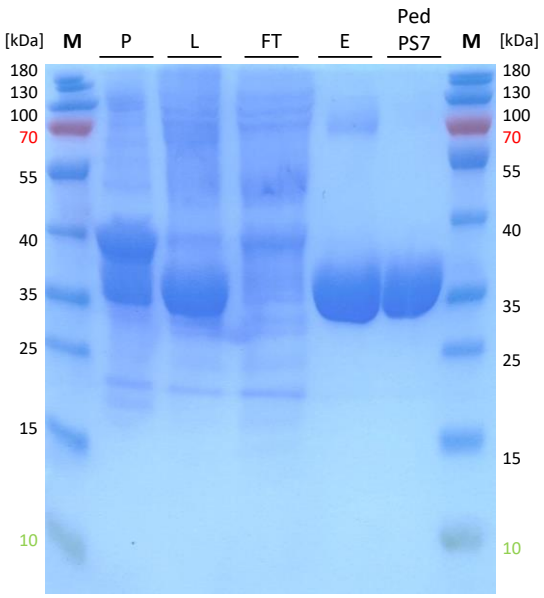

Figure S9. Purification of His_6-PedPS7 fusion protein (33 kDa). M: marker (kDa), P: pellet, L: lysate, FT: flow-through, E: elution fractions with imidazole, PedPS7: purified and concentrated enzyme solution.

Substrate tolerance of PedPS7 and AmbDH3

Small-scale conversions and UPLC-MS analysis

All reactions were performed in a 2 mL tube containing substrate (0.1 mg, concentration 2 or 4 mM) and enzyme in HEPES buffer at 30 °C and 300 rpm. After 16 h the assays were extracted with 500 µL EtOAc. The organic solvent was evaporated, the remaining solid dissolved in MeOH and analysed by UPLC-MS. The conversion values were calculated using calibration straights recorded for **8** and **18**. Multiple rounds of conversion were conducted for **28**, **29** and **30** to maximise the amount of material for further ^{1}H NMR analysis. Incubation experiments with the 2-D,3-D,7-D-selective AmbDH3 served as additional reference experiments to assign the *cis*-THPs.

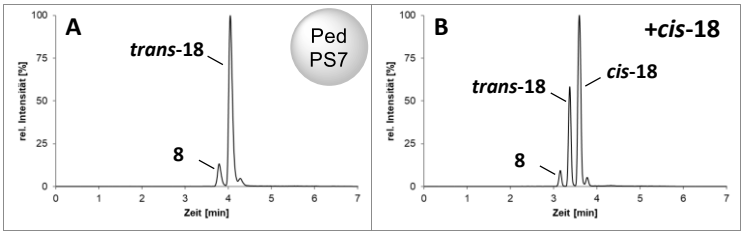

Figure S10. UPLC-MS analysis of (**A**) the conversion of **8** by PedPS7 and (**B**) spiking with *cis*-**15**. M(**8**)=324, M(**18**)=324, t_R(**8**)=3.78 min in **A** and 3.17 min in **B**, t_R(*trans*-**18**)=4.04 min in **A** and 3.38 min in **B**, t_R(*cis*-**18**)=3.59 min in **B**. Conditions of enzyme assay: 0.1 mg (332 nmol) of **8** in HEPES buffer (substrate concentration 4 mM) and 10.0 mg/mL His$_6$-PedPS7. The differences in the retention times are caused by a column exchange.

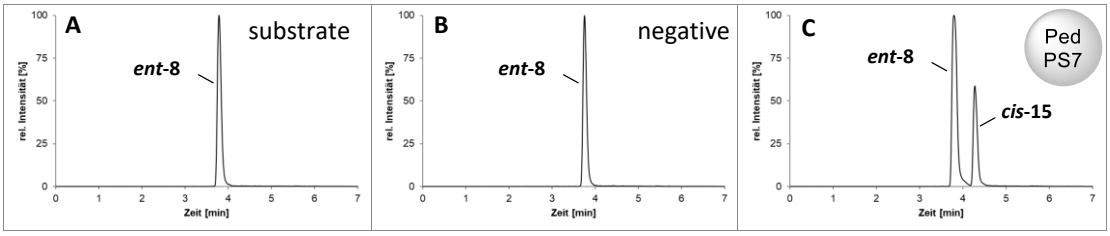

Figure S11. UPLC-MS analysis of (**A**) substrate ***ent*-8**, (**B**) negative control (incubation without enzyme) and (**C**) conversion of ***ent*-8** by PedPS7. M(***ent*-8**)=324, M(**15**)=324, t_R(***ent*-8**)=3.78 min, t_R(*cis*-**15**)=4.27 min. Conditions of enzyme assay: 0.1 mg (332 nmol) of ***ent*-8** in HEPES buffer (substrate concentration 2 mM (**B**) and 4 mM (**C**)) and 10.0 mg/mL His$_6$-PedPS7 (**C**).

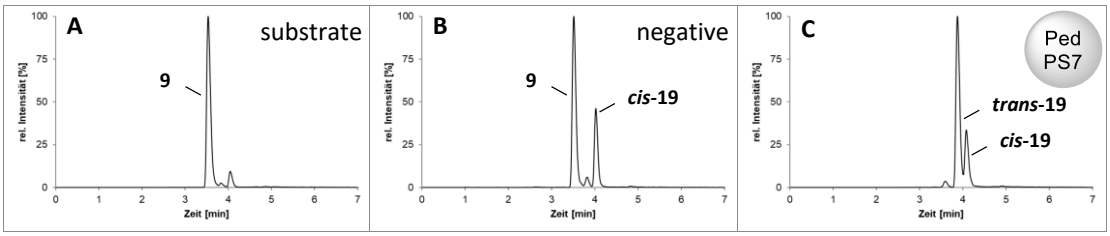

Figure S12. UPLC-MS analysis of (**A**) substrate **9**, (**B**) negative control (incubation without enzyme), (**C**) conversion of **9** by PedPS7. M(**9**)=310, M(**19**)=310, t_R(**9**)=3.51 min, t_R(*trans*-**19**)=3.87 min, t_R(*cis*-**19**)=4.08 min. Conditions of enzyme assay: 0.1 mg (348 nmol) substrate **9** in HEPES buffer (substrate concentration 2 mM (**B**) and 4 mM (**C**)) and 10.0 mg/mL His$_6$-PedPS7 (**C**).

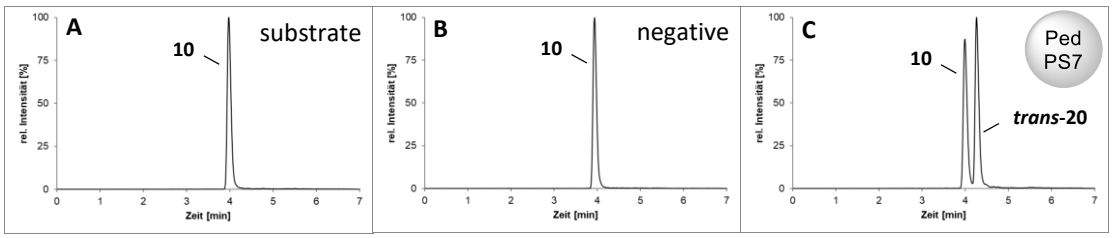

Figure S13. UPLC-MS analysis of (**A**) substrate **10**, (**B**) negative control (incubation without enzyme), (**C**) conversion of **10** by PedPS7. M(**10**)=338, M(**20**)=338, t_R(**10**)=3.99 min, t_R(*trans*-**20**)=4.20 min. Conditions of enzyme assay: 0.1 mg (317 nmol) substrate **10** in HEPES buffer (substrate concentration 2 mM (**B**) and 4 mM (**D**)) and 10.0 mg/mL His_6-PedPS7 (**C**).

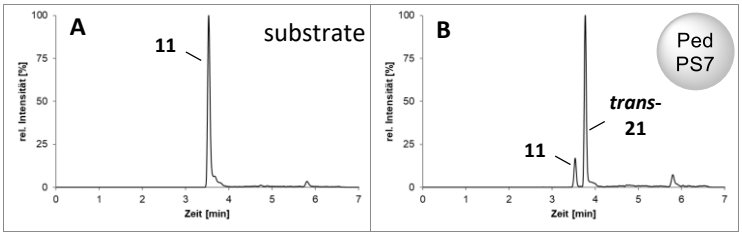

Figure S14. UPLC-MS analysis of (**A**) substrate **11**, (**B**) conversion of **11** by PedPS7. M(**11**)=338, M(**21**)=338, t_R(**11**)=3.53 min, t_R(*trans*-**21**)=3.76 min. Conditions of enzyme assay: 0.1 mg (317 nmol) substrate **11** in HEPES buffer (substrate concentration 2 mM) and 2.7 mg/mL His_6-PedPS7 (**C**).

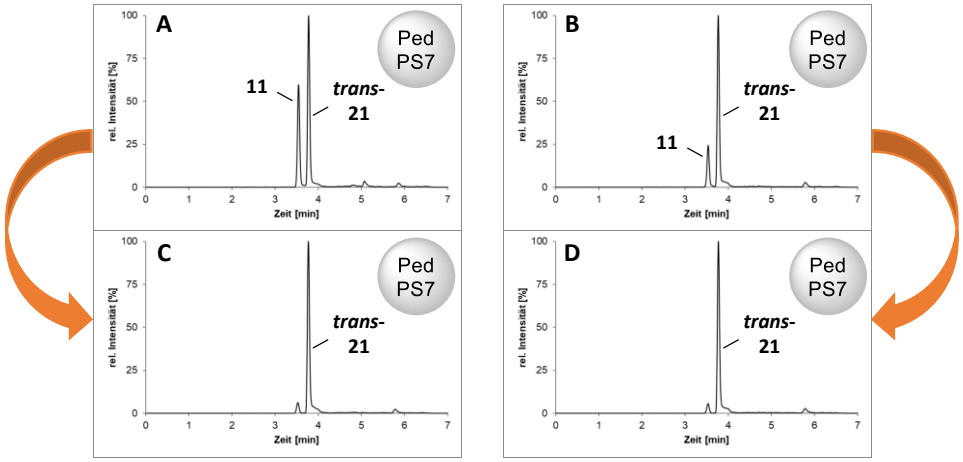

Figure S15. UPLC-MS analysis of conversion of **11** by PedPS7 after one (**A+B**) and two (**C+D**) reaction cycles. M(**11**)=338, M(**21**)=338, t_R(**11**)=3.53 min, t_R(*trans*-**21**)=3.77 min. Conditions of enzyme assay: 5× 0.1 mg (317 nmol) substrate **11** in HEPES buffer 6.8 (**A**), HEPES glycerol buffer pH 7.2 (**B**) and HEPES buffer pH 7.2 (**C+D**) (substrate concentration 2 mM) and 1.6–7.0 mg/mL His_6-PedPS7.

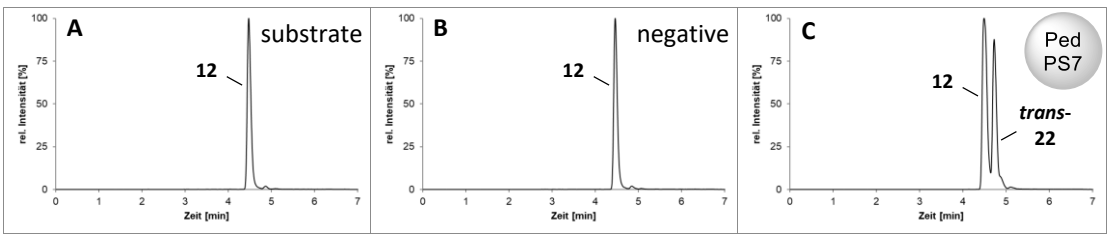

Figure S16. UPLC-MS analysis of (**A**) substrate **12**, (**B**) negative control (incubation without enzyme), (**C**) conversion of **12** by PedPS7. M(**12**)=366, M(**22**)=366, t_R(**12**)=4.49 min, t_R(*trans*-**22**)=4.72 min. Conditions of enzyme assay: 0.1 mg (292 nmol) substrate **12** in HEPES buffer (substrate concentration 2 mM (**B**) and 4 mM (**C**)) and 10.0 mg/mL His_6-PedPS7 (**C**).

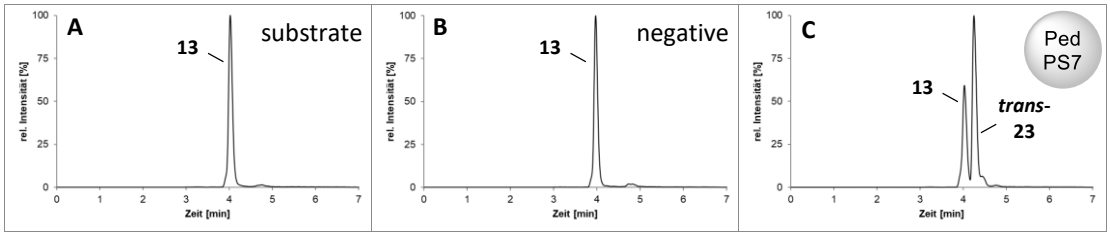

Figure S17. UPLC-MS analysis of (**A**) substrate **13**, (**B**) negative control (incubation without enzyme), (**C**) conversion of **13** by PedPS7. M(**13**)=372, M(**23**)=372, t_R(**13**)=4.02 min, t_R(*trans*-**23**)=4.24 min. Conditions of enzyme assay: 0.1 mg (287 nmol) substrate **13** in HEPES buffer (substrate concentration 2 mM (**B**) and 4 mM (**C**)) and 10.0 mg/mL His_6-PedPS7 (**C**).

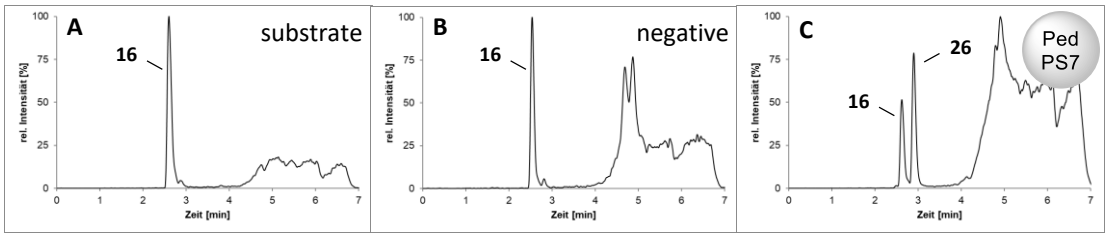

Figure S18. UPLC-MS analysis of (**A**) substrate **16**, (**B**) negative control (incubation without enzyme), (**C**) conversion of **16** by PedPS7. M(**16**)=291, M(**26**)=291, t_R(**16**)=2.62 min, t_R(**26**)=2.90 min. Conditions of enzyme assay: 0.1 mg (408 nmol) substrate **16** in HEPES buffer (substrate concentration 2 mM (**B**) and 4 mM (**C**)) and 10.0 mg/mL His_6-PedPS7 (**C**).

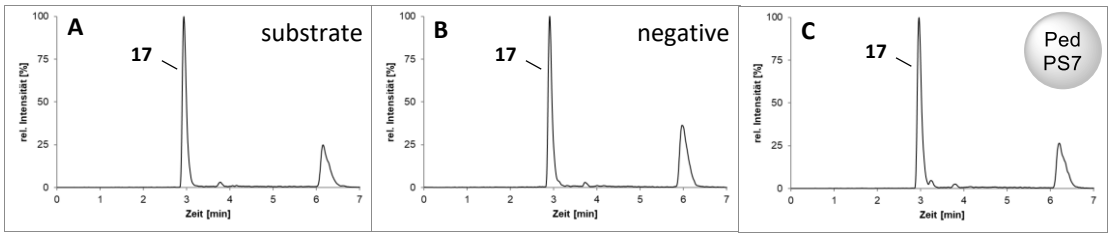

Figure S19. UPLC-MS analysis of (**A**) substrate **17**, (**B**) negative control (incubation without enzyme), (**C**) conversion of **17** by PedPS7. M(**17**)=282, M(**27**)=282, t_R(**17**)=2.96 min, t_R(**27**)=3.80 min. Conditions of enzyme assay: 0.1 mg (386 nmol) substrate **17** in HEPES buffer (substrate concentration 2 mM (**B**) and 4 mM (**C**)) and 10.0 mg/mL His_6-PedPS7 (**C**).

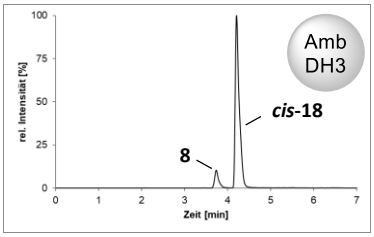

Figure S20. UPLC-MS analysis of the conversion of **8** by AmbDH3. M(**8**)=324, M(**18**)=324, t_R(**8**)=3.72 min, t_R(*cis*-**18**)=4.19 min. Conditions of enzyme assay: 0.1 mg (332 nmol) substrate **8** in HEPES buffer (substrate concentration 2 mM) and 5.0 mg/mL His_6-AmbDH3. This reaction has been reported various times with reliable quantitative conversion.[1,2]

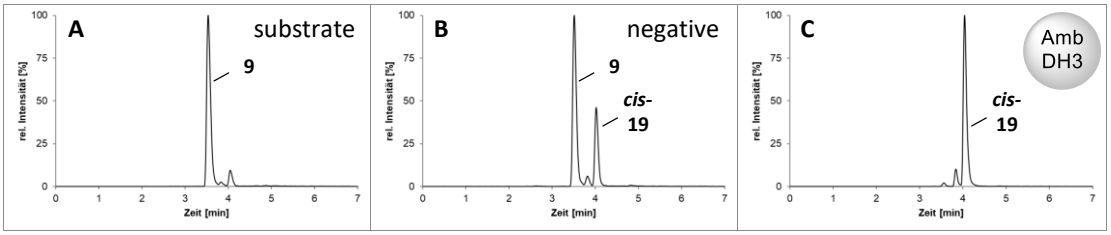

Figure S21. UPLC-MS analysis of (**A**) substrate **9**, (**B**) negative control (incubation without enzyme), (**C**) conversion of **9** by AmbDH3. M(**9**)=310, M(**19**)=310, t_R(**9**)=3.51 min, t_R(*cis*-**19**)=4.03 min. Conditions of enzyme assay: 0.1 mg (348 nmol) substrate **9** in HEPES buffer (substrate concentration 2 mM) and 10.0 mg/mL His_6-AmbDH3.

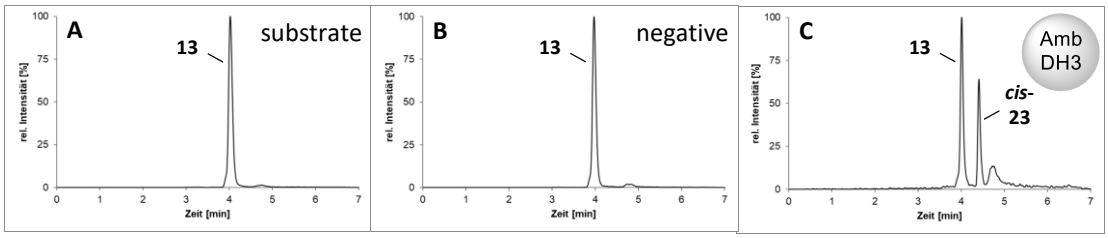

Figure S22. UPLC-MS analysis of (**A**) substrate **13**, (**B**) negative control (incubation without enzyme), (**C**) conversion of **13** by AmbDH3. M(**13**)=372, M(**23**)= 372, t_R(**13**)=4.01 min, t_R(*cis*-**23**)=4.41 min. Conditions of enzyme assay: 0.1 mg (287 nmol) substrate **13** in HEPES buffer (Conditions of enzyme assay: 2 mM) and 10.0 mg/mL His_6-AmbDH3.

Semipreparative-scale conversions and NMR analysis

For semipreparative scale conversions, substrates **8**, **11**, **14**, **15**, **28**, **29**, **30** and **31** (5 mg, final concentration 1 or 2 mM) were incubated with the PedPS7 solution (purified enzyme or filtered lysate) at 300 rpm and 30 °C in a 50 mL flask. After 16 h, the solution was transferred to a 50 mL tube and the flask was washed with EtOAc. After extraction with EtOAc (3x), the organic layers were combined. The solvent was evaporated, the remaining solids dissolved in MeOH and analysed *via* UPLC-MS or NMR spectroscopy. The synthesis and analytical data of all starting materials are reported in reference [2]. The ^{1}H NMR spectra of the crude products were used to assign the configuration of the formed THPs and to estimate the conversion.

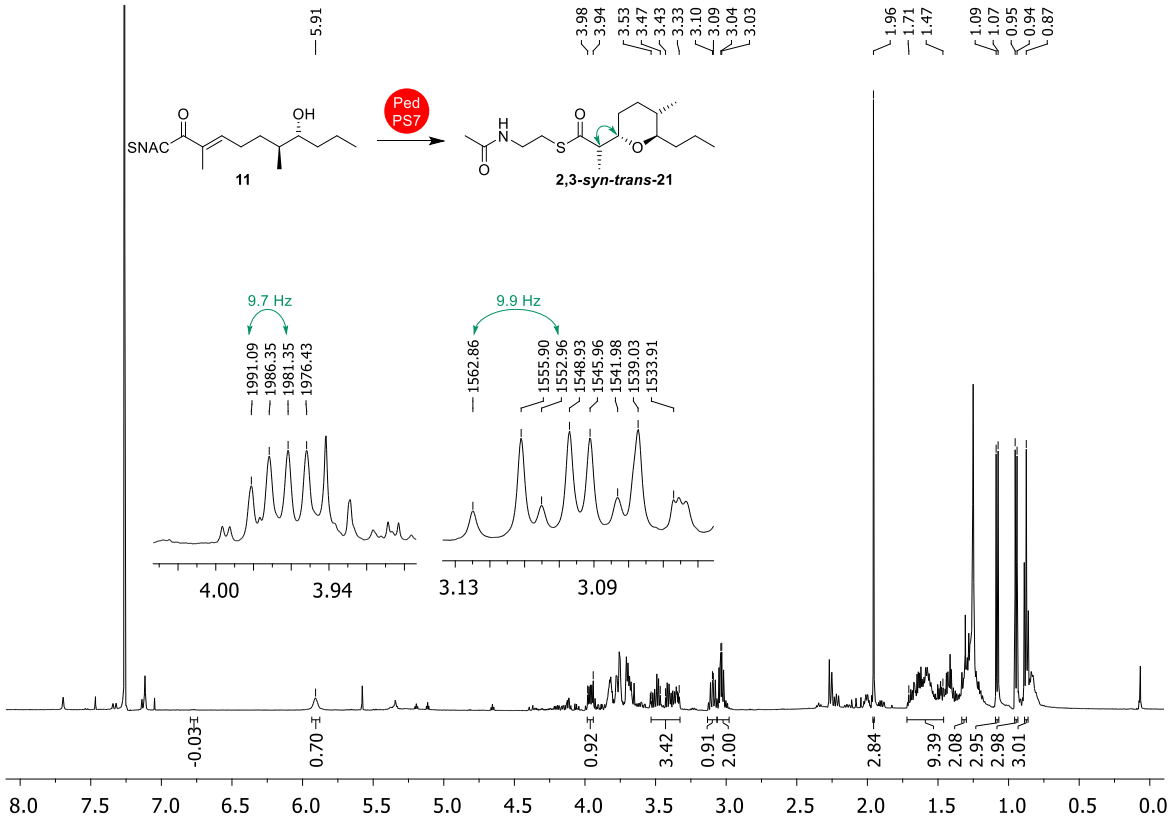

Figure S23. ^{1}H NMR analysis of the conversion experiment of PedPS7 and substrate **11** ($CDCl_3$, 500 MHz). It shows the 2,6-*trans*-THP characteristic shift of δ(**3-H**) = 3.96 and δ(**7-H**) = 3.35 ppm. The vicinal coupling constant $^{3}J_{2H\text{-}3H}$ of 9.7–9.9 Hz confirms the relative *syn*-configuration at C-2-C-3.[4] An *anti*-configuration would give a vicinal coupling constant $^{3}J_{2H\text{-}3H}$ of 10.8–11.2 Hz.[5,6] The conversion can only be estimated due to overlapping signals.

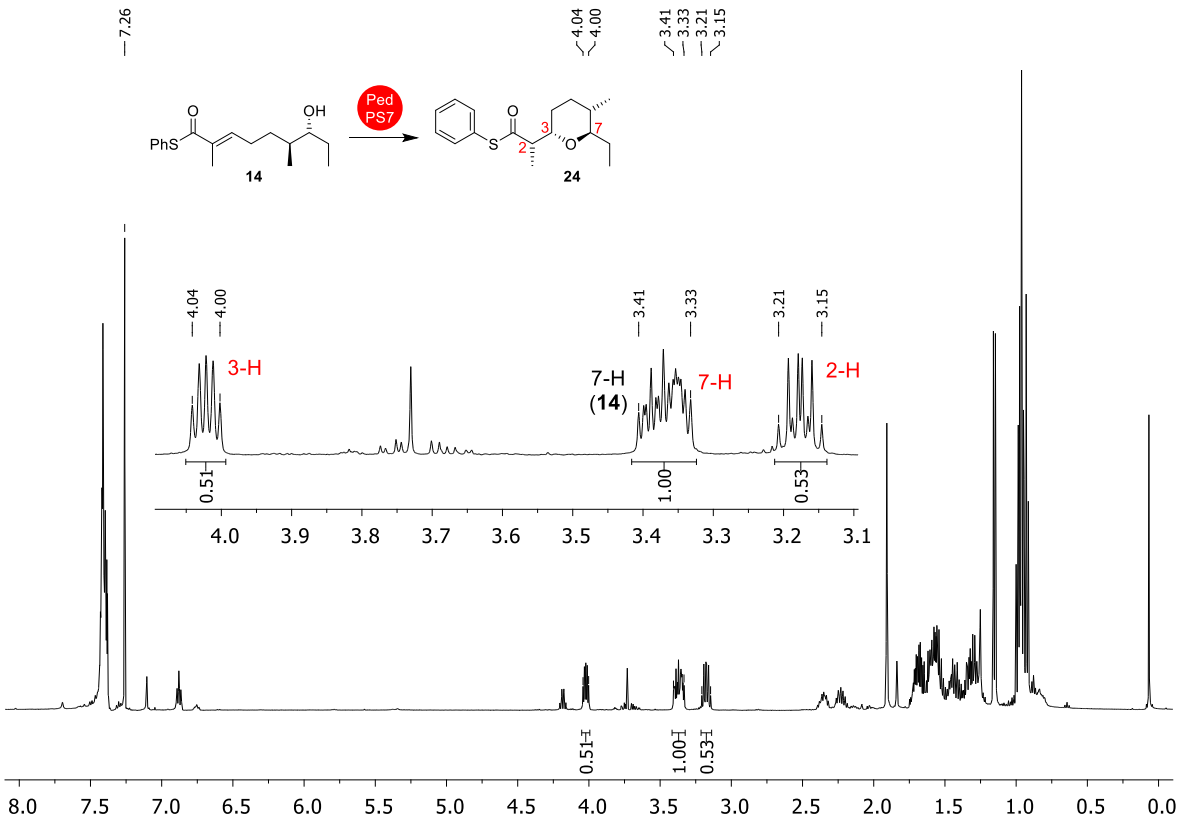

Figure S24. ^{1}H NMR analysis of the conversion experiment of PedPS7 and substrate **14** after one reaction cycle ($CDCl_3$, 500 MHz). The signals for determination of the conversion are annotated.

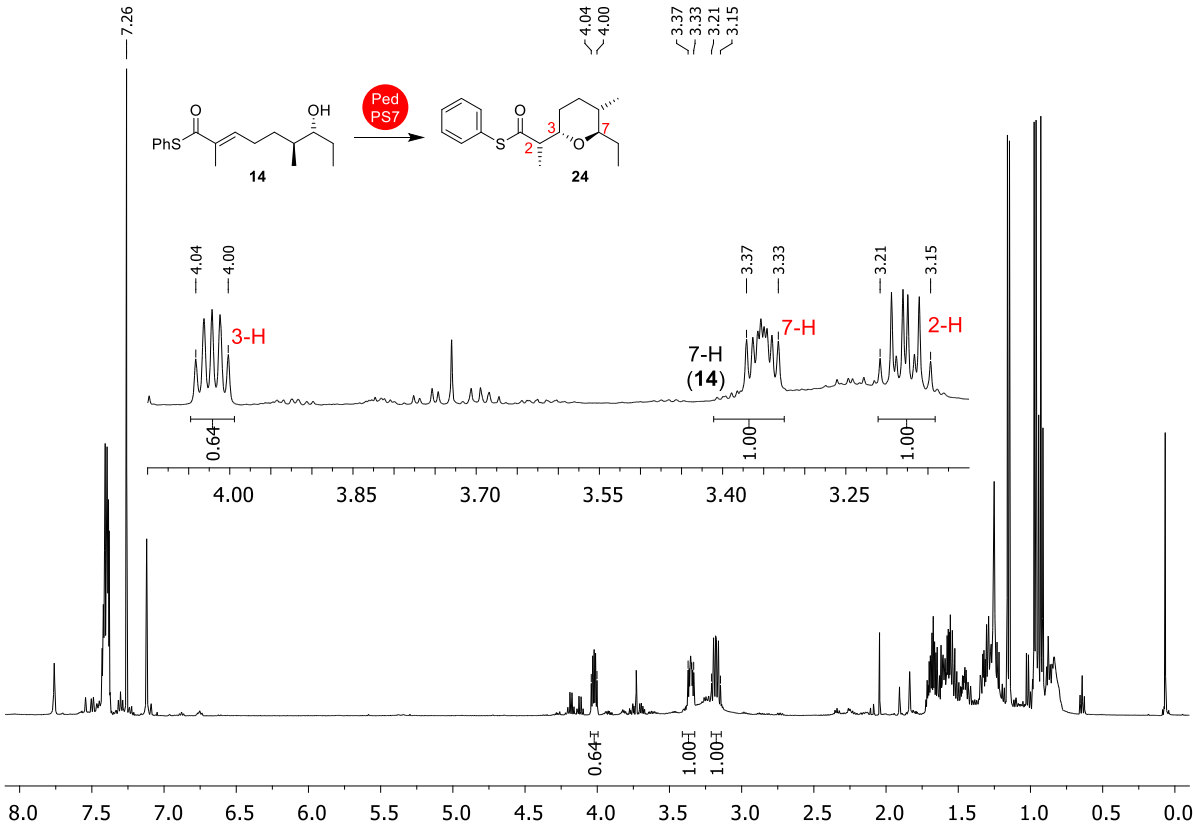

Figure S25. ^{1}H NMR analysis of the conversion experiment of PedPS7 and substrate **14** after two reaction cycles shows nearly full conversion ($CDCl_3$, 500 MHz). The signals for determination of the conversion are annotated.

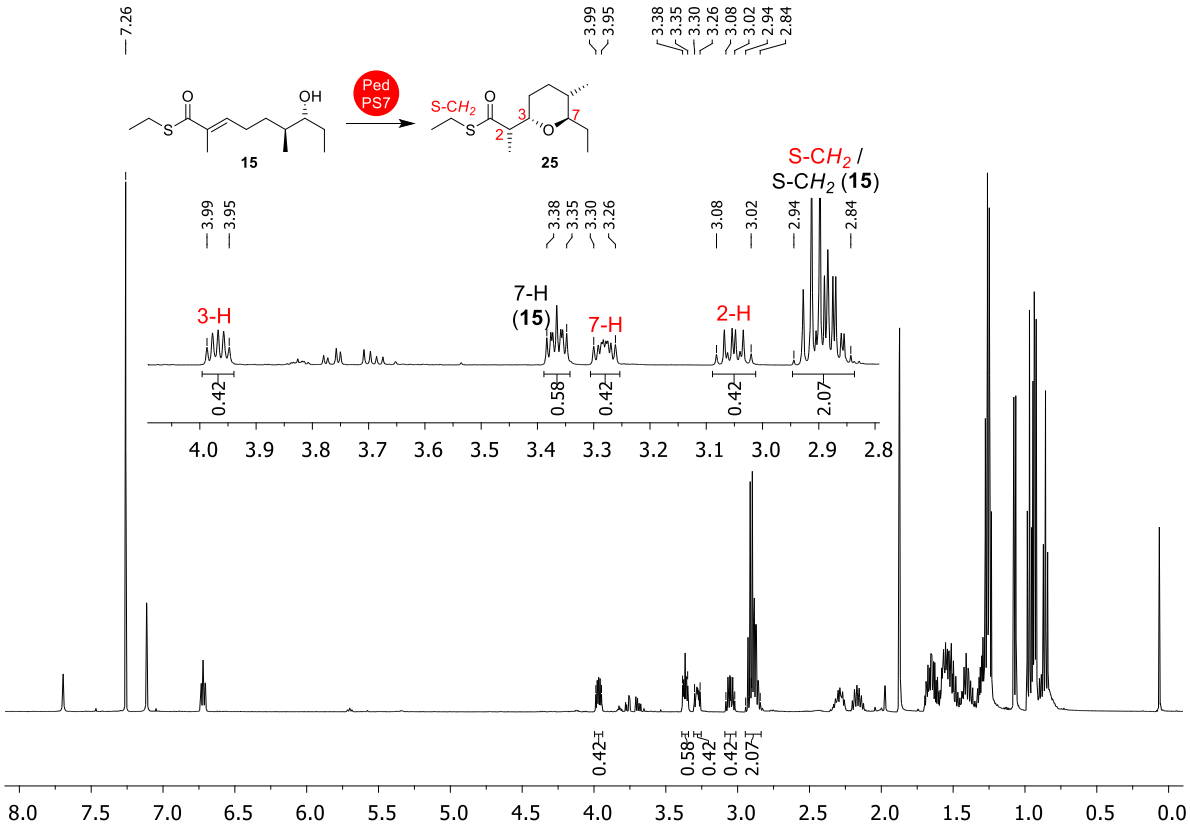

Figure S26. ^{1}H NMR analysis of the conversion experiment of PedPS7 and substrate **15** after one reaction cycle ($CDCl_3$, 500 MHz). The signals for determination of the conversion are annotated.

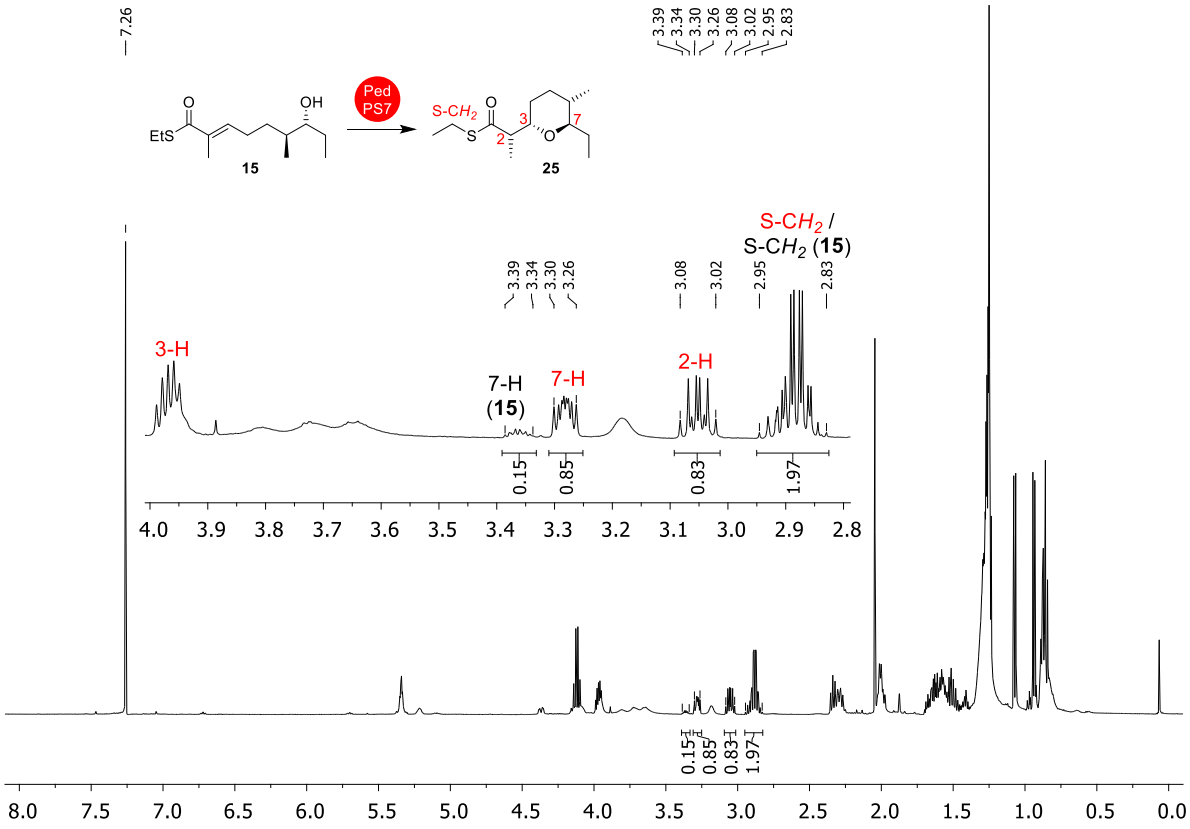

Figure S27. ^{1}H NMR analysis of the conversion experiment of PedPS7 and substrate **15** after two reaction cycles shows a conversion of ~85% ($CDCl_3$, 500 MHz). The signals for determination of the conversion are annotated.

Compound purification and configurational analysis

The obtained crude materials after enzymatic reaction were purified by flash chromatography on silica gel (EtOAc (for **18** and **28**); EtOAc:dichloromethane / 2:1 (for **29** and **30**); hexane:EtOAc / 20:1 (for **24** and **35**)) or by RP-HPLC (for **25**). The pooled product fractions were obtained as a colourless solid and analysed *via* NMR spectroscopy and chiral HPLC. The ^{1}H NMR spectra of the purified products were used to assign the configuration of the formed THPs.

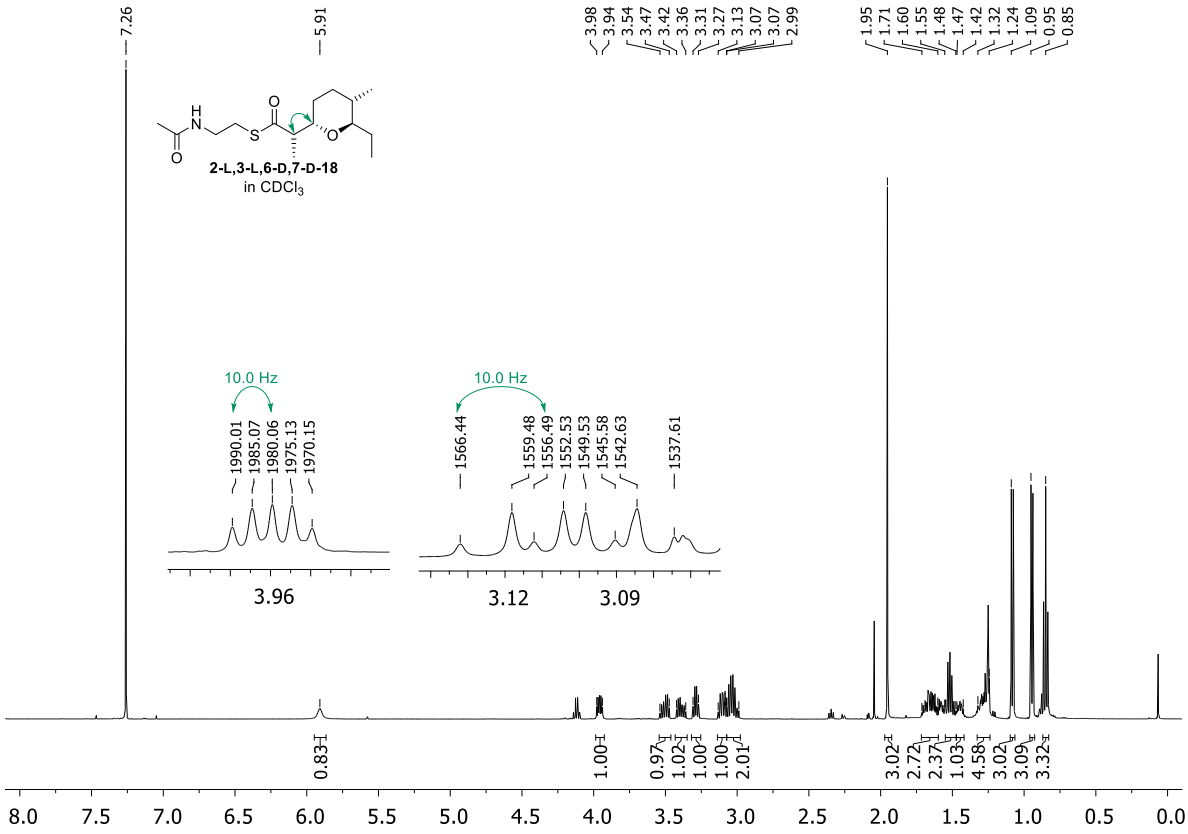

Figure S28. ^{1}H NMR analysis of the purified product **2-L,3-L,6-D,7-D-18** from incubation of **8** with PedPS7 ($CDCl_3$, 500 MHz). It shows the 2,6-*trans*-THP characteristic shift of δ(**3-H**) = 3.96 and δ(**7-H**) = 3.29 ppm. The vicinal coupling constant $^{3}J_{2H\text{-}3H}$ = 10.0 Hz confirms the shown configuration at C-2.[4] Traces of EtOAc are visible.

^{1}H NMR (500 MHz, $CDCl_3$): δ [ppm] = 5.91 (s, 1H, N*H*CH_2), 3.96 (ddd, *J* = 10.0, 5.0, 4.9 Hz, 1H, OC*H*CH_2CH_2), 3.54–3.47 (m, 1H, 1× NHC*H*$_2$), 3.42–3.36 (m, 1H, 1× NHC*H*$_2$), 3.31–3.27 (td, *J* = 6.4 Hz, 1H, OC*H*CH_2CH_3), 3.10–3.07 (dq, *J* = 10.0, 3.1 Hz, 1H, CC*H*CH_3), 3.07–2.99 (m, 2H, C*H*$_2$S), 1.95 (s, 3H, OCC*H*$_3$), 1.71–1.60 (m, 2H, OCHC*H*$_2$$CH_2$), 1.55–1.48 (m, 2H, C*H*$_2$$CH_3$), 1.47–1.42 (m, 1H, CH_2C*H*CH_3), 1.32–1.24 (m, 2H, C*H*$_2$$CHCH_3$), 1.09 (d, *J* = 7.0 Hz, 3H, CCHC*H*$_3$), 0.95 (d, *J* = 6.8 Hz, 3H, CH_2CHC*H*$_3$), 0.85 (t, *J* = 7.4 Hz, 3H, CH_2C*H*$_3$).

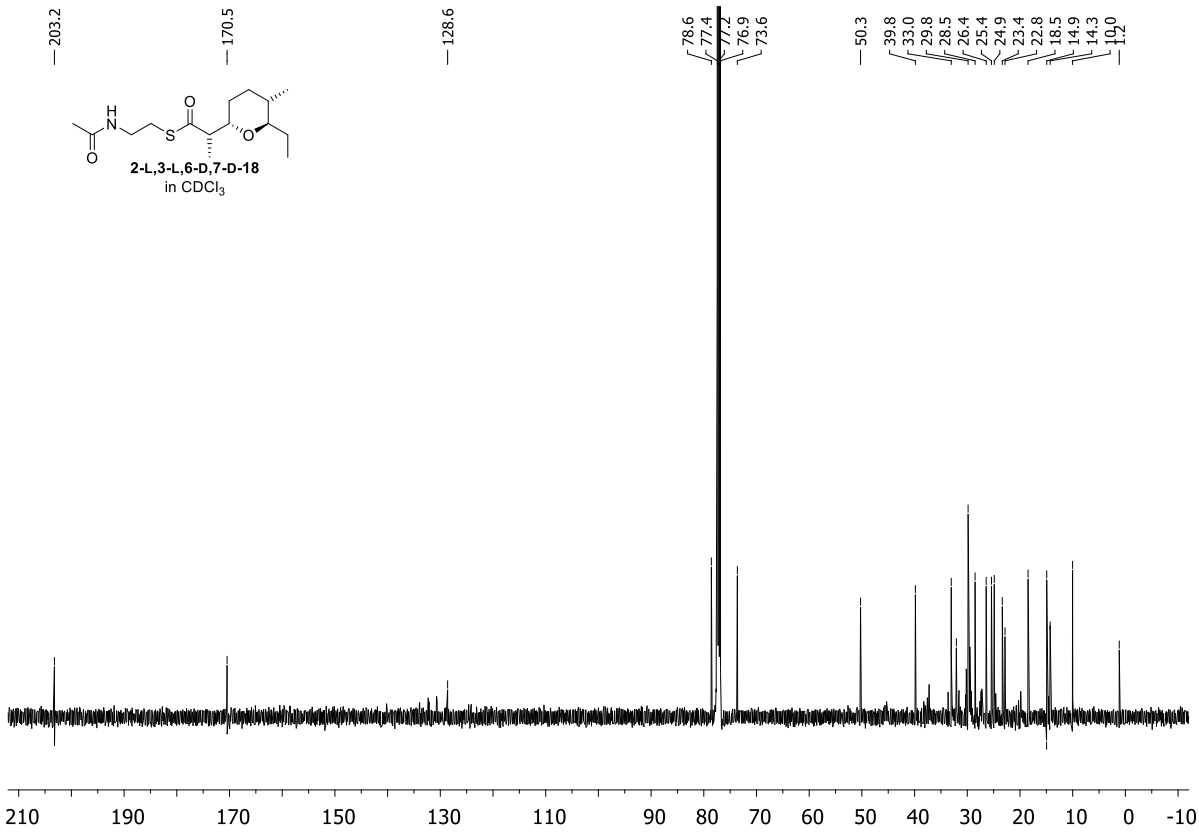

Figure S29. ^{13}C NMR analysis of the product **2-L,3-L,6-D,7-D-18** after conversion of **8** by PedPS7 ($CDCl_3$, 125 MHz).

^{13}C NMR (125 MHz, $CDCl_3$): δ [ppm] = 203.2 (q, S*C*O), 170.5 (q, CH_3*C*O), 78.6 (t, C(O)CH*C*HO), 73.6 (t, CH*C*HOCH_2), 50.3 (t, CO*C*HCH_3), 39.9 (s, NH*C*H_2), 33.0 (t, CH_2*C*HCH_3), 29.9 (s, *C*H_2CHCH_3), 28.5 (s, *C*H_2S), 26.4 (s, CHO*C*$H_2$$CH_2$), 25.4 (s, CHO*C*$H_2$$CH_2$), 23.4 (p, *C*$H_3$CO), 18.5 (p, CH_2CH*C*H_3), 14.3 (p, COCH*C*H_3), 10.0 (p, CH_2*C*H_3).

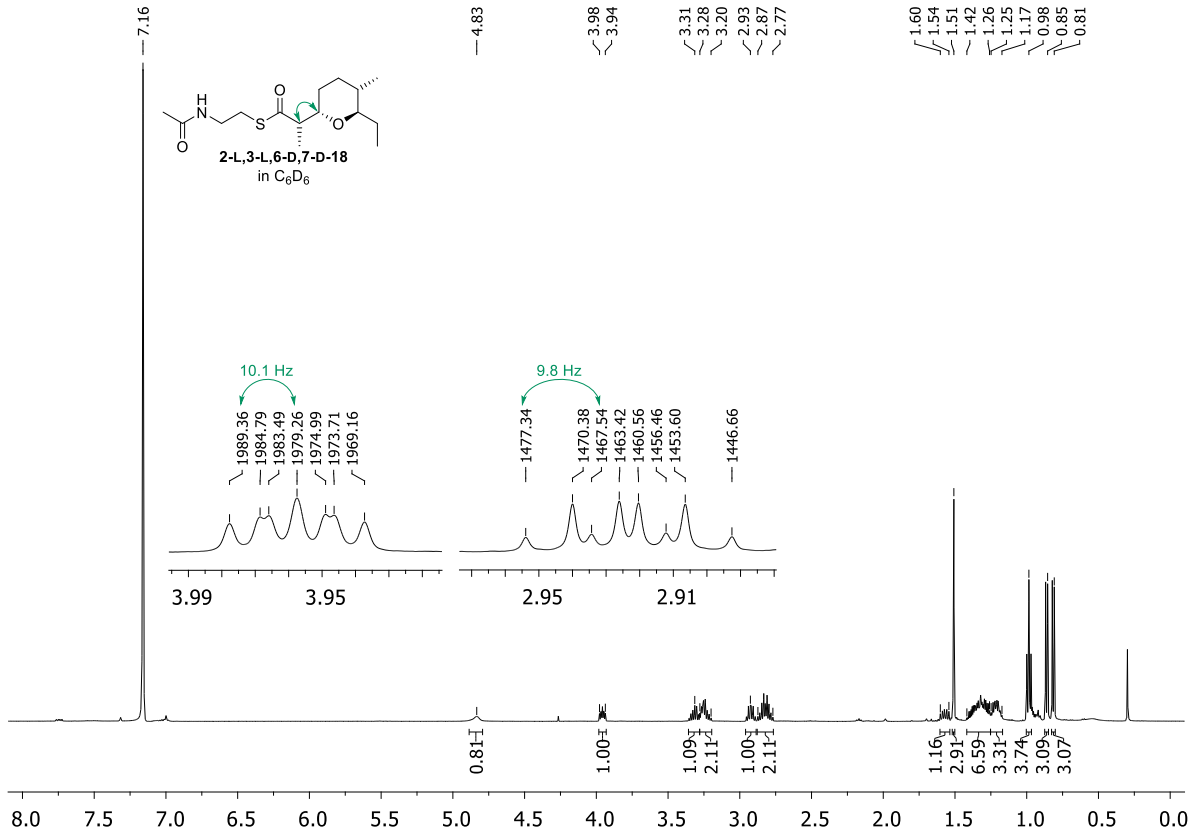

Figure S30. ^{1}H NMR analysis of the product **2-L,3-L,6-D,7-D-18** after incubation of PedPS7 and substrate **8** (C_6D_6, 500 MHz). It shows the 2,6-*trans*-THP characteristic shift of δ(**3-H**) = 3.96 and δ(**7-H**) = 3.30 ppm. The vicinal coupling constant $^{3}J_{2H\text{-}3H}$ = 10.0 Hz confirms the shown configuration at C-2.[4]

^{1}H NMR (500 MHz, C_6D_6): δ [ppm] = 4.83 (s, 1H, N*H*CH_2), 3.98–3.94 (ddd, *J* = 10.1, 5.9, 4.6 Hz, 1H, OC*H*CH_2CH_2), 3.31 (td, J = 13.3, 6.6 Hz, 1H, OC*H*CH_2CH_3), 3.28–3.20 (m, 2H, NHC*H*$_2$), 2.93 (dq, *J* = 9.8, 7.0 Hz, 1H, CC*H*CH_3), 2.87–2.77 (m, 2H, C*H*$_2$S), 1.60–1.54 (m, 1H, CH_2CHCH_3), 1.51 (s, 3H, OCC*H*$_3$), 1.42–1.26 (m, 4H, C*H*$_2$$CHCH_3$, $OCHCH_2CH_2$), 1.25–1.17 (m, 2H, C*H*$_2$$CH_3$), 0.98 (t, *J* = 7.4 Hz, 3H, CH_2CH_3), 0.85 (d, *J* = 7.0 Hz, 3H, $CCHCH_3$), 0.79 (d, *J* = 6.8 Hz, 3H, CH_2CHCH_3).

HRMS (ESI^+) *m/z* for $C_{15}H_{28}NO_3S$ $[M+H]^+$: calculated 302.1790, found 302.1779.

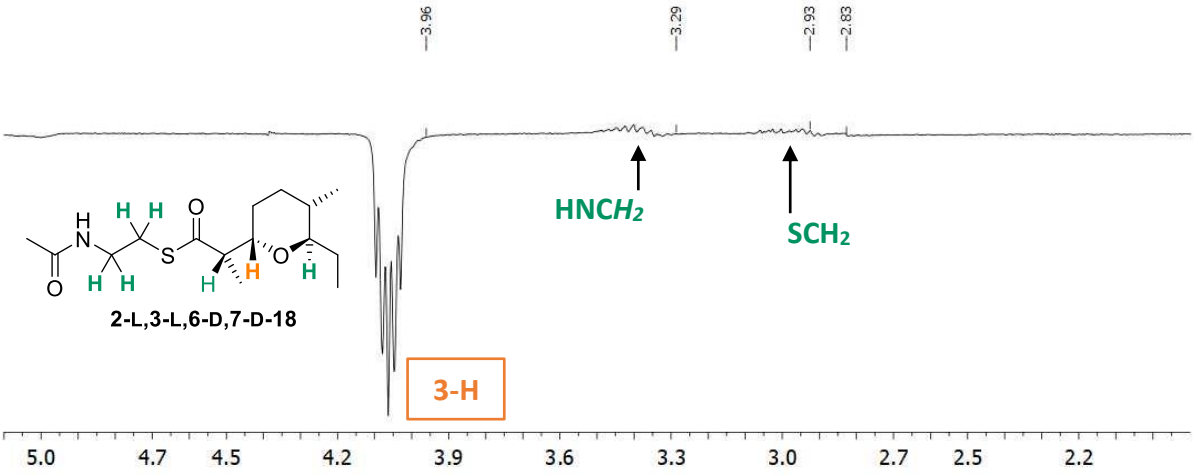

Figure S31. Section of the 1D-NOE spectrum of purified **2-L,3-L,6-D,7-D-18** with saturation at 3.96 ppm (**3-H**) (C_6D_6, 300 MHz). No correlation with **7-H** at δ = 3.31 ppm is observed. The full 1D NOE spectrum is shown in Figure S32.

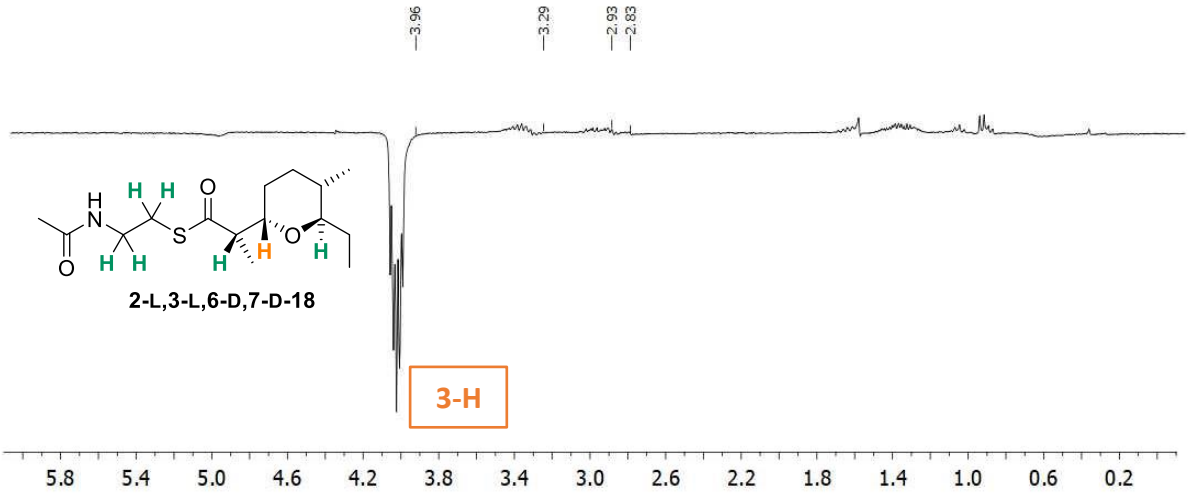

Figure S32. Full 1D-NOE spectrum of purified **2-L,3-L,6-D,7-D-18** with saturation at 3.96 ppm (**3-H**) (C_6D_6, 300 MHz).

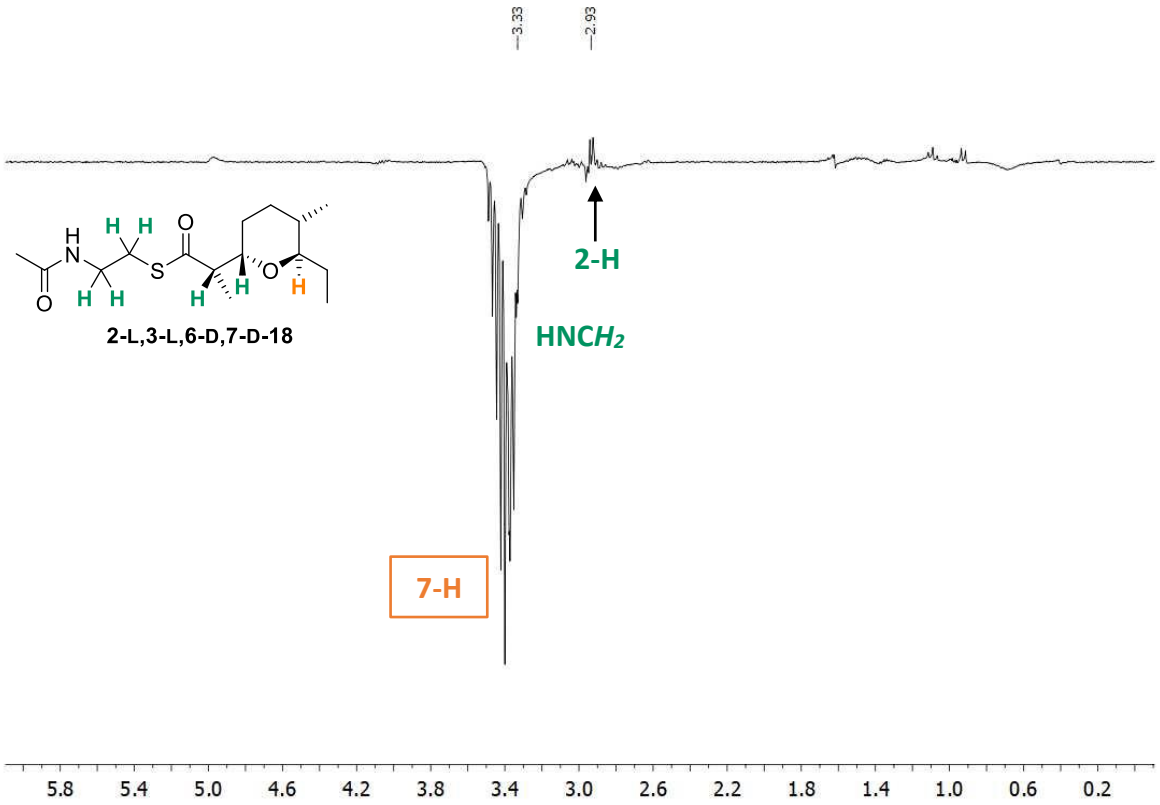

Figure S33. 1D NOE spectrum of purified **2-L,3-L,6-D,7-D-18** with saturation at 3.31 ppm (**7-H**) (C_6D_6, 300 MHz). No correlation with **3-H** at δ = 3.96 ppm and a weak correlation with **2-H** at δ = 2.93 ppm is observed.

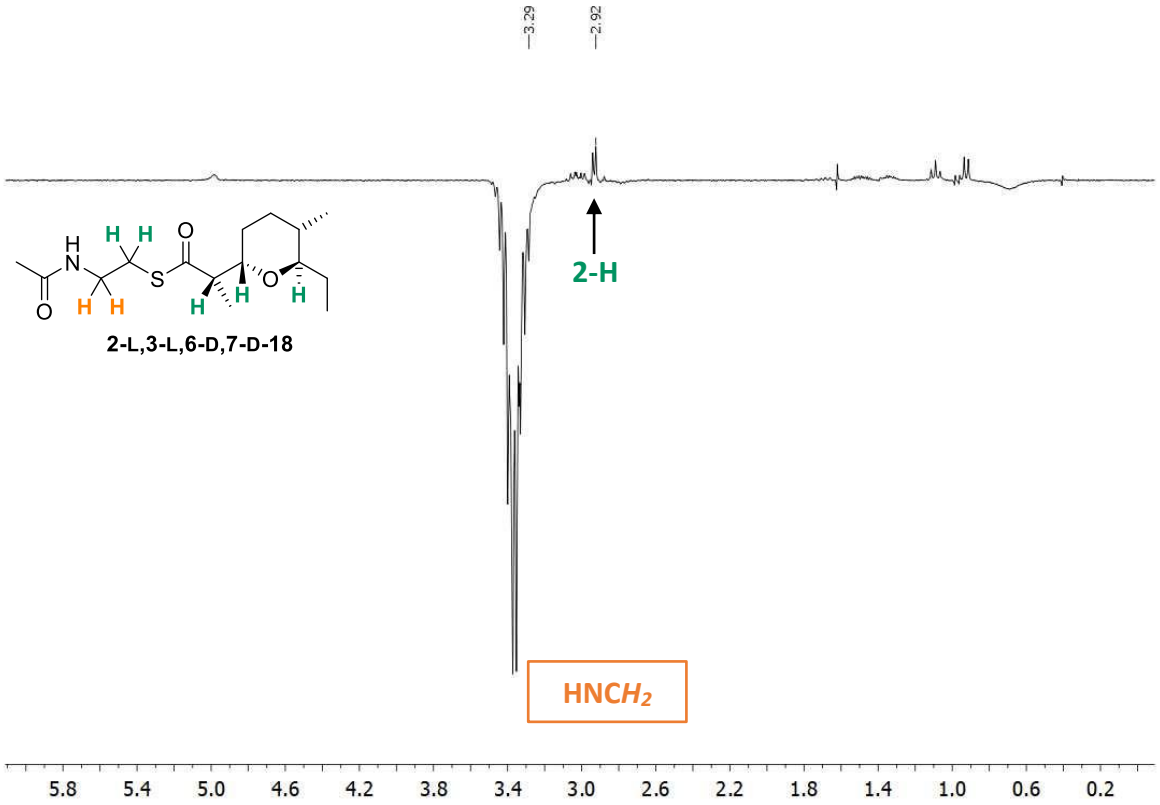

Figure S34. 1D-NOE spectrum of purified **2-L,3-L,6-D,7-D-18** with saturation at 3.29 ppm (**HNCH₂**) (C_6D_6, 300 MHz). Correlation with **CH₂S** at δ = 2.82 ppm and **2-H** at δ = 2.93 ppm is observed.

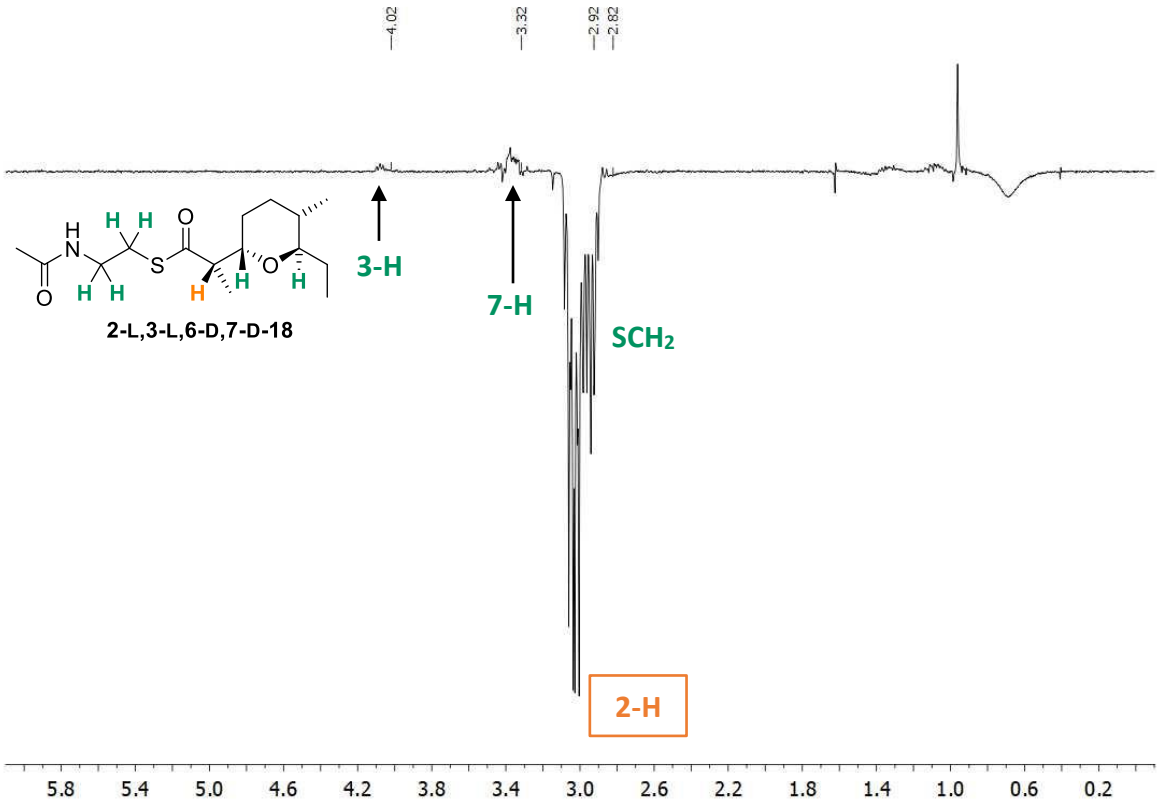

Figure S35. 1D-NOE spectrum of purified **2-L,3-L,6-D,7-D-18** with saturation at 2.93 ppm (2-H) (C_6D_6, 300 MHz). Correlation with 3-H at δ = 3.96 ppm and 7-H at δ = 3.31 ppm is observed.

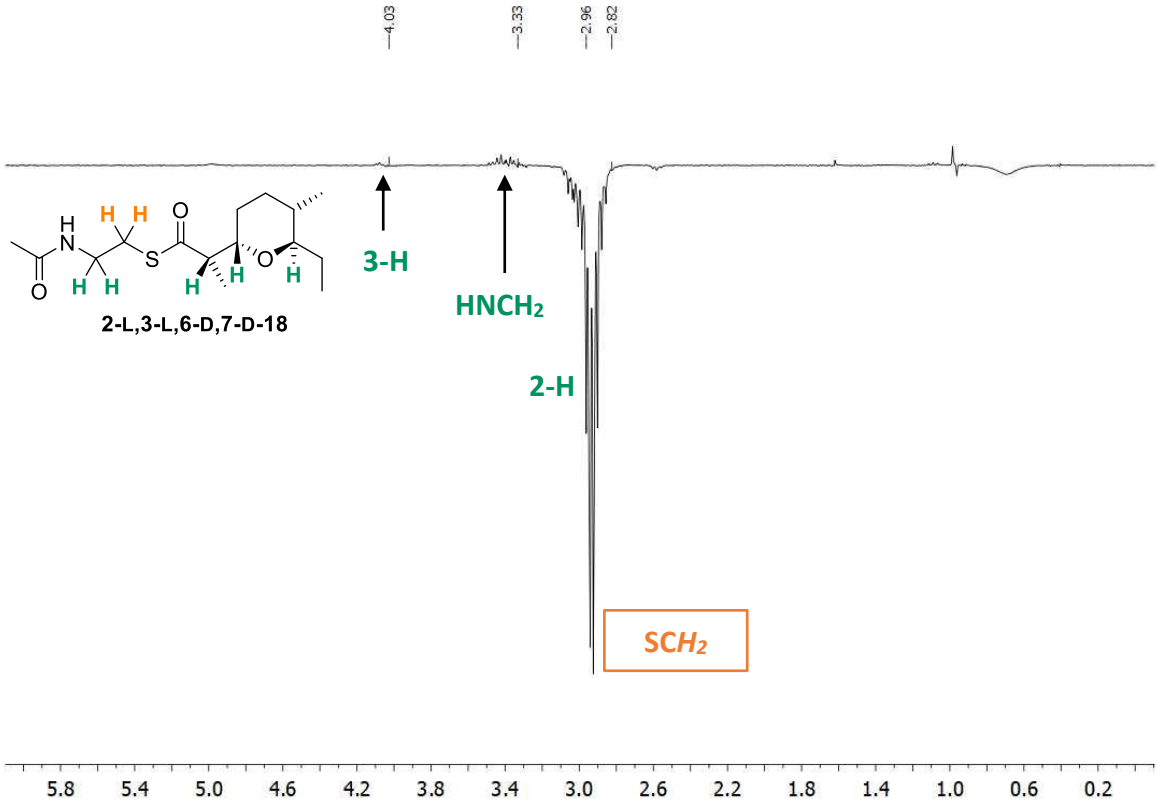

Figure S36. 1D-NOE spectrum of purified **2-L,3-L,6-D,7-D-18** with saturation at 2.82 ppm (SC*H*$_2$) (C_6D_6, 300 MHz). Correlation with NHCH$_2$ at δ = 3.29 ppm and weak correlation with 3-H at δ = 3.96 ppm is observed.

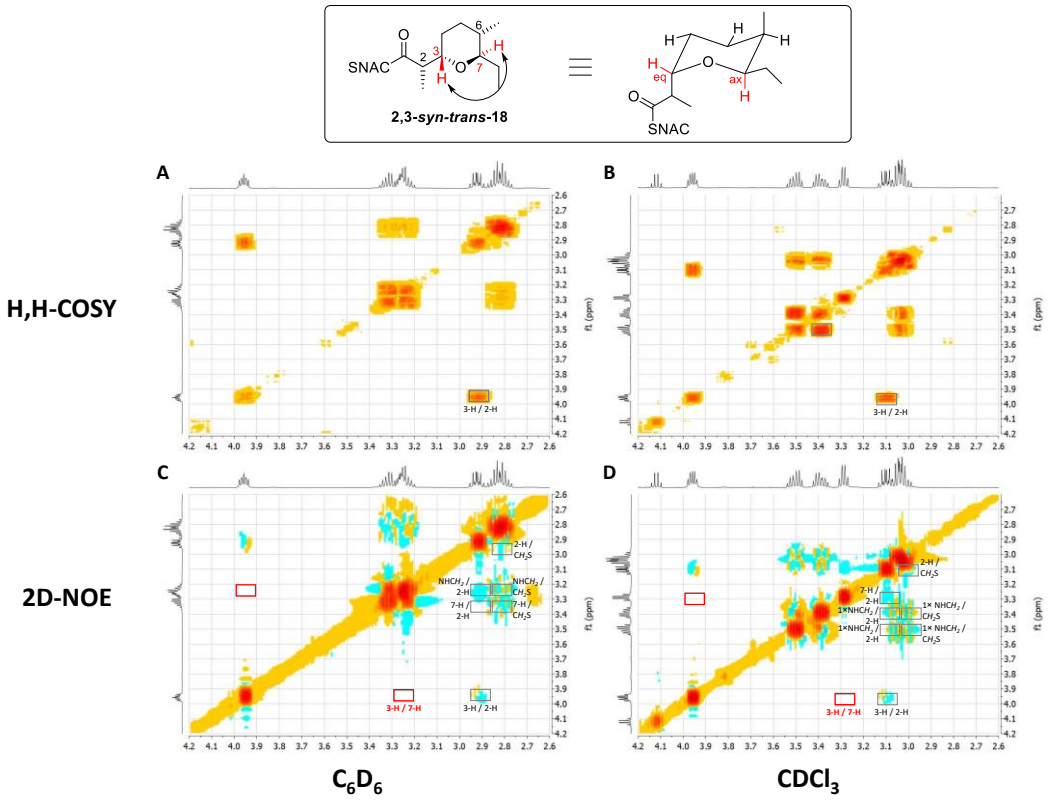

Figure S37. Section of the 2D-NOE spectra of purified **2-L,3-L,6-D,7-D-18**. **A+B)** *H,H*-COSY spectra; **C+D)** 2D-NOESY spectra (C_6D_6 (**A+C**) or $CDCl_3$ (**B+D**), 500 MHz). The full spectra are shown in Figure S38–Figure S41. The **red** boxes highlight regions in which a correlation should be visible in the 2D-NOE spectrum for a *cis*-THP, but not for a *trans*-THP. The corresponding *H,H*-COSY and 2D-NOE spectra for **2-D,3-D,6-D,7-D-18** are shown in Figure S44.

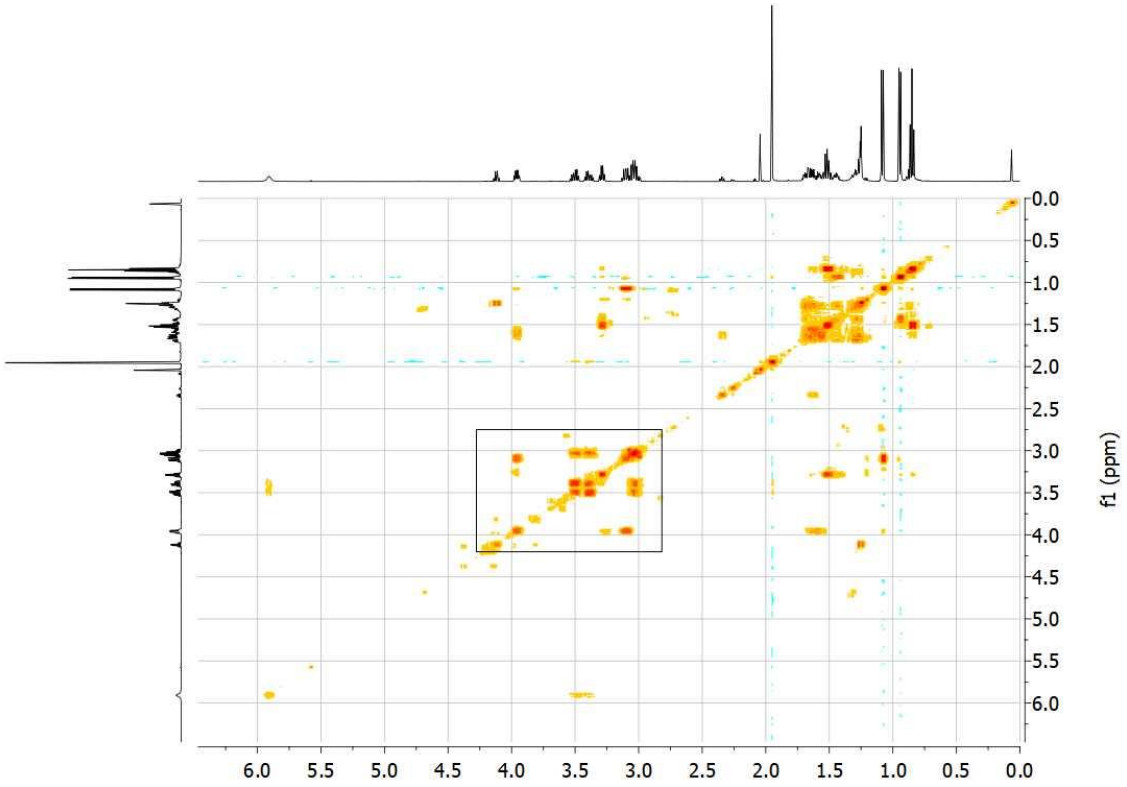

Figure S38. Full *H,H*-COSY spectrum of purified **2-L,3-L,6-D,7-D-18** ($CDCl_3$, 500 MHz).

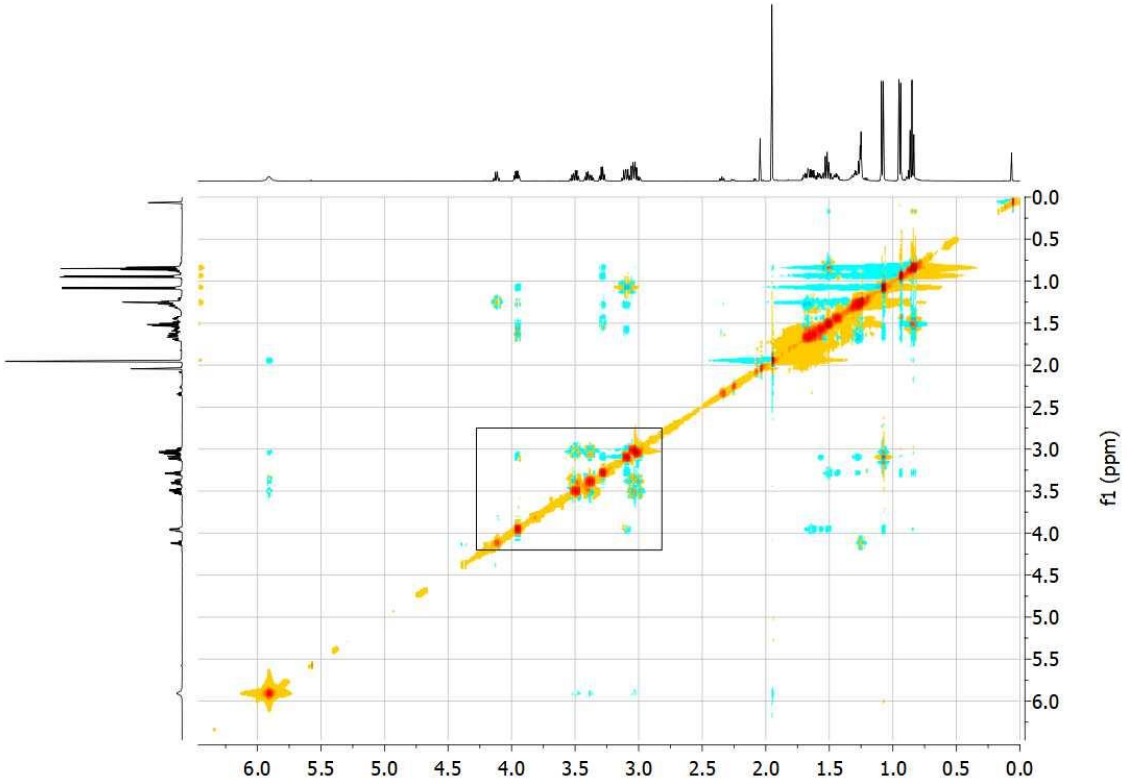

Figure S39. Full 2D-NOESY spectrum of purified **2-L,3-L,6-D,7-D-18** ($CDCl_3$, 500 MHz).

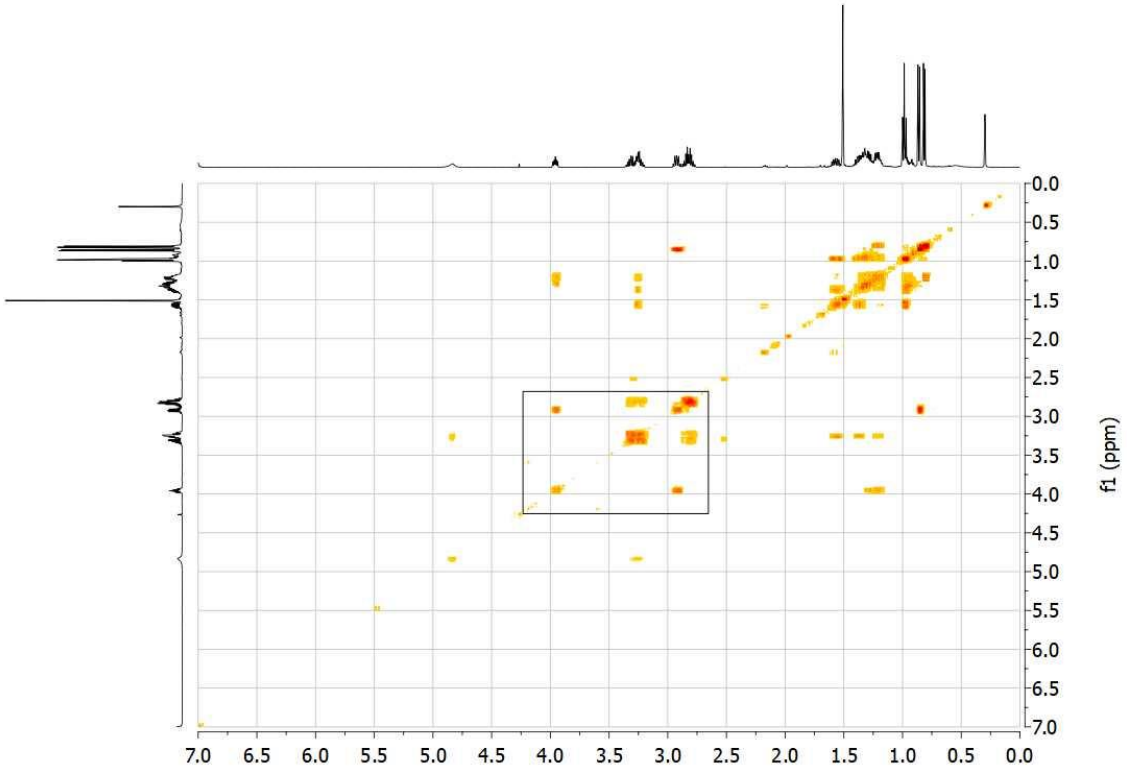

Figure S40. Full *H,H*-COSY spectrum of purified **2-L,3-L,6-D,7-D-18** (C_6D_6, 500 MHz).

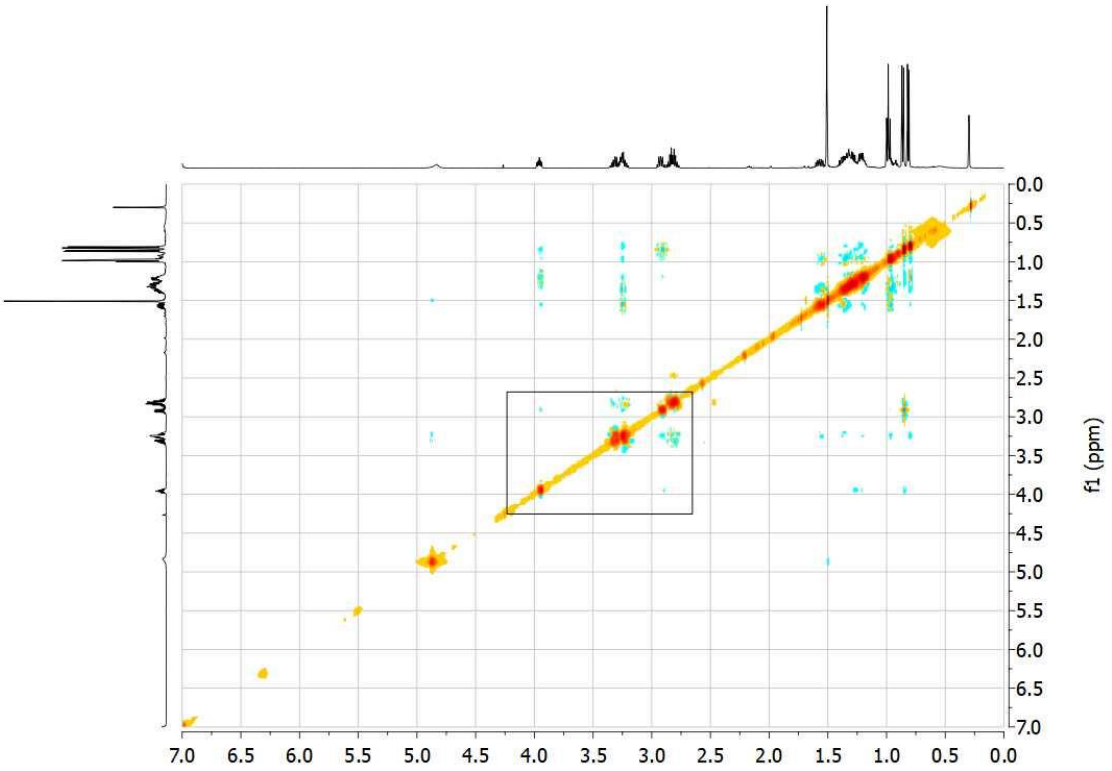

Figure S41. Full 2D-NOESY spectrum of purified **2-L,3-L,6-D,7-D-18** (C_6D_6, 500 MHz).

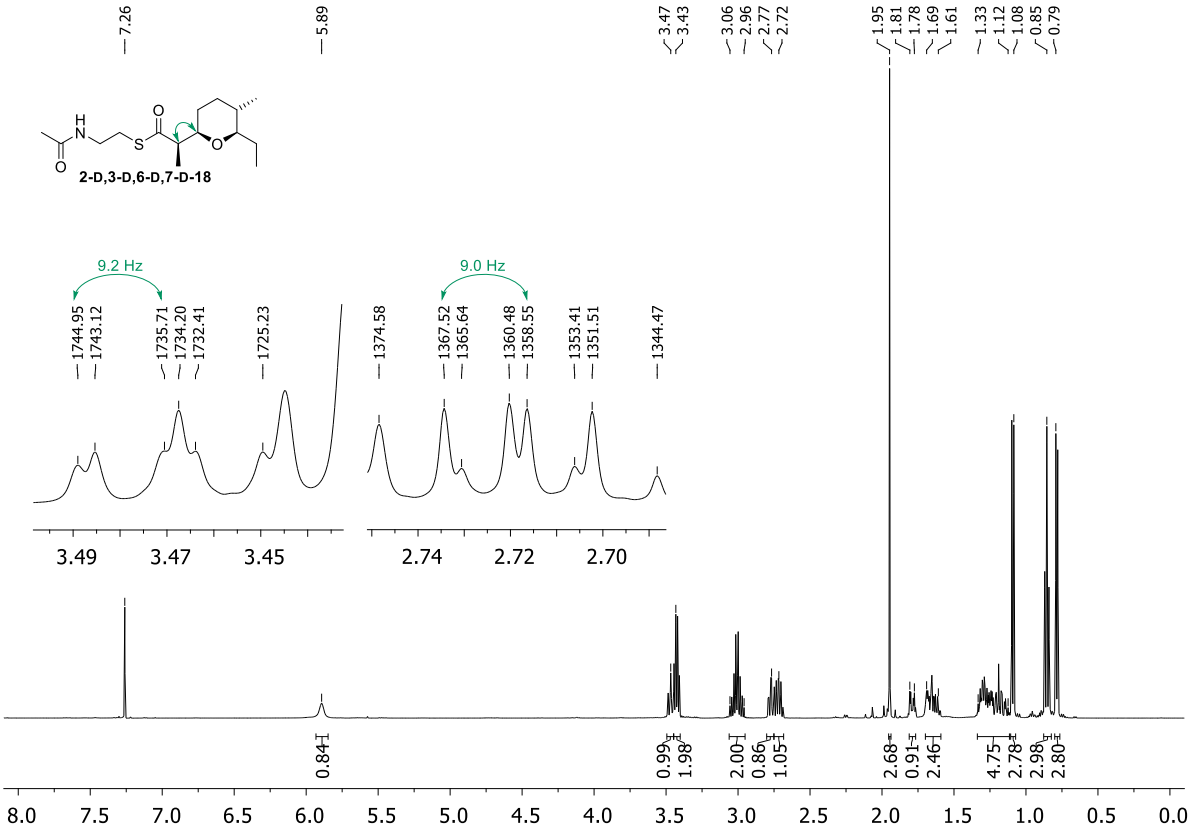

Figure S42. ^{1}H NMR analysis of **2-D,3-D,6-D,7-D-18** from incubation of **8** with AmbDH3 ($CDCl_3$, 500 MHz). It shows the 2,6-*cis*-THP characteristic shift of δ(**3-H**) = 3.47 and δ(**7-H**) = 2.77 ppm. The vicinal coupling constant $^3J_{2H\text{-}3H}$ = 9.1 Hz confirms the shown configuration at C-2.[2]

^{1}H NMR (500 MHz, $CDCl_3$): δ [ppm] = 5.89 (s, 1H, N*H*CH_2), 3.47 (ddd, *J* = 10.8, 9.2, 1.8 Hz, 1H, OC*H*CH_2CH_2), 3.45–3.40 (m, 2H, NHC*H*$_2$), 3.06–2.95 (m, 2H, C*H*$_2$S), 2.77 (td, *J* = 9.3, 2.7 Hz, 1H, OC*H*CH_2CH_3), 2.72 (dq, *J* = 9.0, 7.0 Hz, 1H, CC*H*CH_3), 1.95 (s, 3H, COC*H*$_3$), 1.82–1.76 (m, 1H, 1× C*H*$_2$$CHCH_3$), 1.70–1.59 (m, 2H, 1× C*H*$_2$$CH_3$, 1× OCHC*H*$_2$$CH_2$), 1.34–1.11 (m, 4H, CH_2C*H*CH_3, 1× OCHC*H*$_2$$CH_2$, 1× C*H*$_2$$CHCH_3$, 1× C*H*$_2$$CH_3$), 1.09 (d, *J* = 7.0 Hz, 3H, CCHC*H*$_3$), 0.85 (t, *J* = 7.4 Hz, 3H, CH_2C*H*$_3$), 0.79 (d, *J* = 6.6 Hz, 3H, CH_2CHC*H*$_3$).

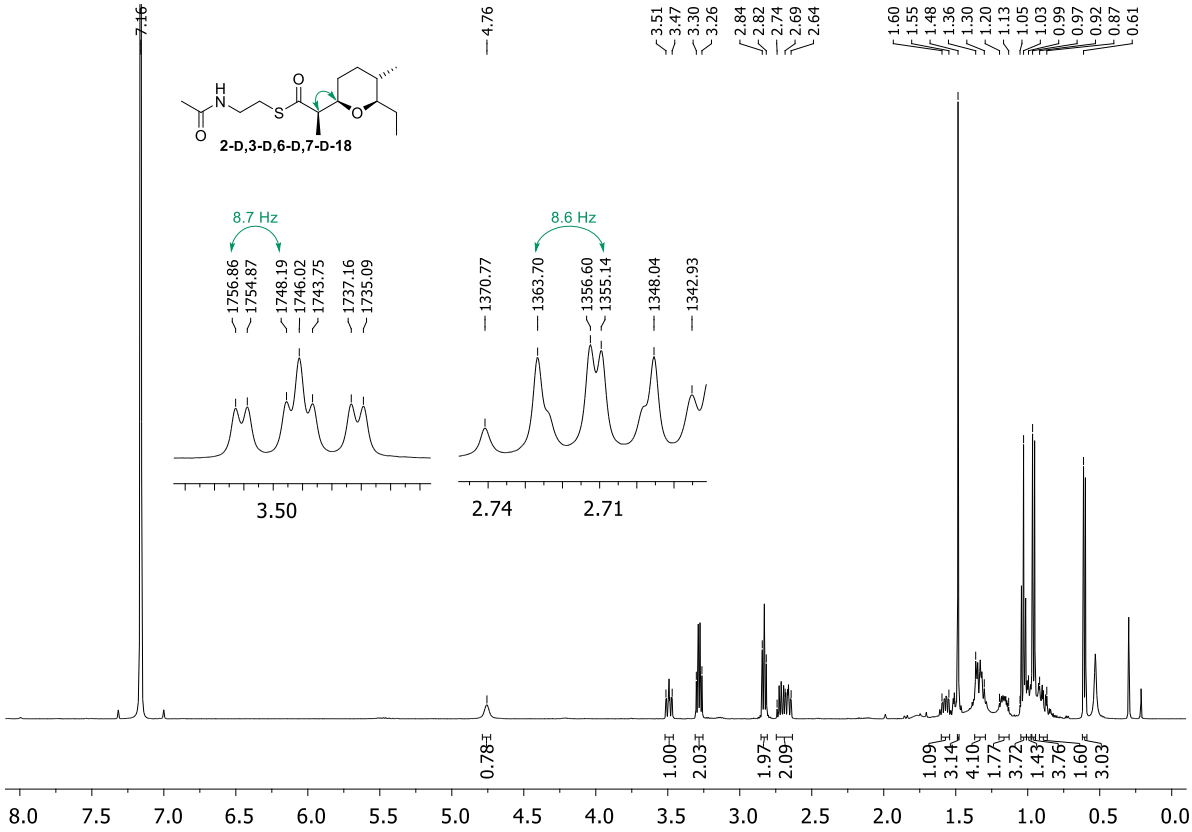

Figure S43. ^{1}H NMR analysis of purified **2-D,3-D,6-D,7-D-18** from incubation of **8** with AmbDH3 (C_6D_6, 500 MHz). It shows the 2,6-*cis*-THP characteristic shift of δ(**3-H**) = 3.49 and δ(**7-H**) = 2.66 ppm. The vicinal coupling constant $^3J_{2H\text{-}3H}$ of 8.7 Hz confirms the shown configuration at C-2.[2]

^{1}H NMR (500 MHz, C_6D_6): δ [ppm] = 4.76 (s, 1H, N*H*CH_2), 3.49 (ddd, *J* = 10.8, 8.7, 2.0 Hz, 1H, OC*H*CH_2CH_2), 3.28 (dd, *J* = 12.8, 6.7 Hz, 2H, NHC*H*$_2$), 2.86–2.80 (m, 2H, C*H*$_2$S), 2.71 (dq, *J* = 8.6, 7.1 Hz, 1H, CC*H*CH_3), 2.66 (td, *J* = 9.2, 2.5 Hz, 1H, OC*H*CH_2CH_3), 1.61–1.53 (m, 1H, 1× C*H*$_2$C*H*$_3$), 1.48 (s, *J* = 6.4 Hz, 3H, COC*H*$_3$), 1.36–0.61 (m, 6H, 1× C*H*$_2$$CH_3$, OCHC*H*$_2$$CH_2$, CH_2C*H*CH_3, C*H*$_2$$CHCH_3$), 1.03 (t, *J* = 7.4 Hz, 3H, CH_2C*H*$_3$), 0.96 (d, *J* = 7.1 Hz, 3H, CCHC*H*$_3$), 0.61 (d, *J* = 6.6 Hz, 3H, CH_2CHC*H*$_3$).

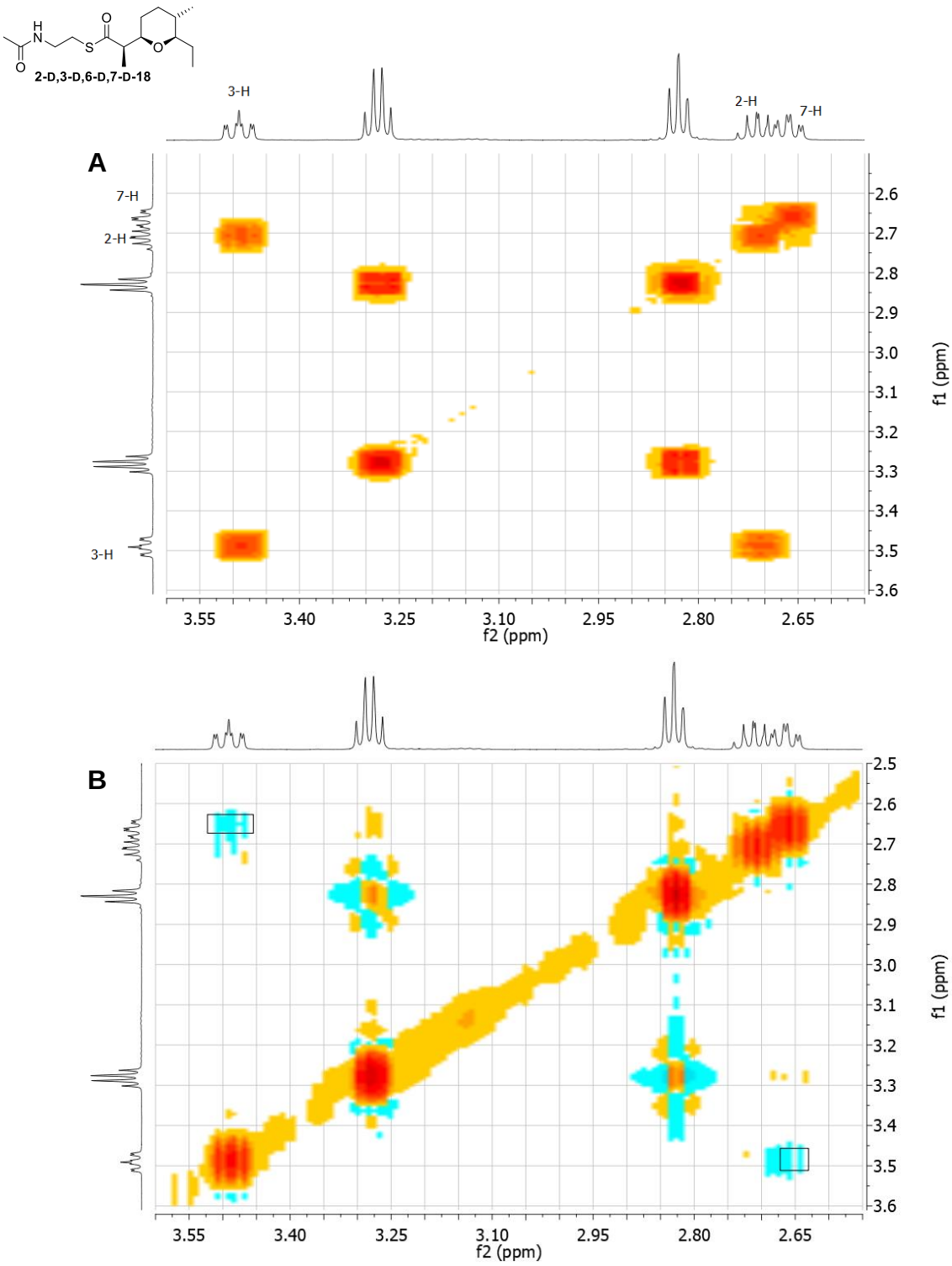

Figure S44. Section of the *H,H*-COSY spectrum (**A**) and 2D-NOE spectrum (**B**) of purified **2-D,3-D,6-D,7-D-18** (C_6D_6, 500 MHz). The relevant 2,3-*cis*-THP-characteristic correlation between **3-H** and **7-H** is highlighted with a box in the 2D-NOE spectrum. The full ^{1}H NMR spectrum is shown in Figure S43.

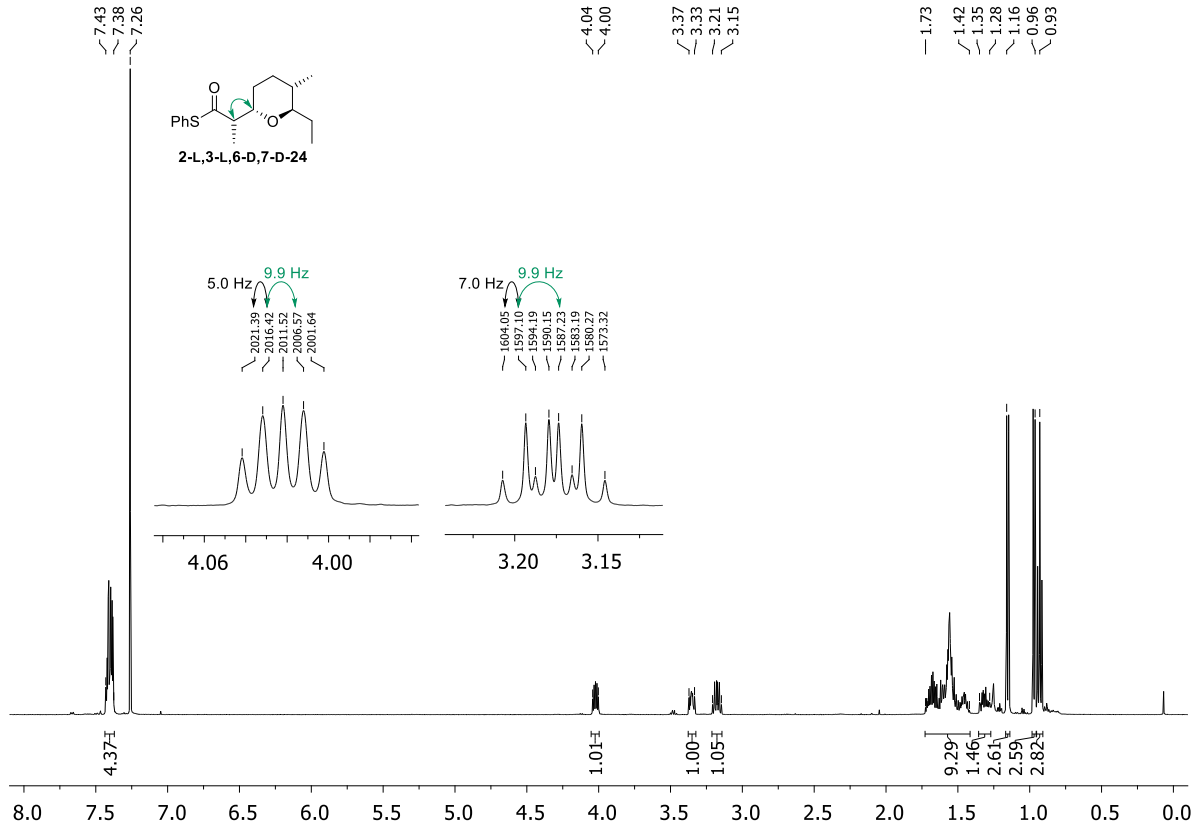

Figure S45. ^{1}H NMR analysis of the purified product **2-L,3-L,6-D,7-D-24** from the incubation of **14** with PedPS7 ($CDCl_3$, 500 MHz). It shows the 2,6-*trans*-THP characteristic shift of δ(**3-H**) = 4.02 and δ(**7-H**) = 3.35 ppm. The vicinal coupling constant $^{3}J_{2H\text{-}3H}$ of 9.9 Hz confirms the shown configuration at C-2.[4]

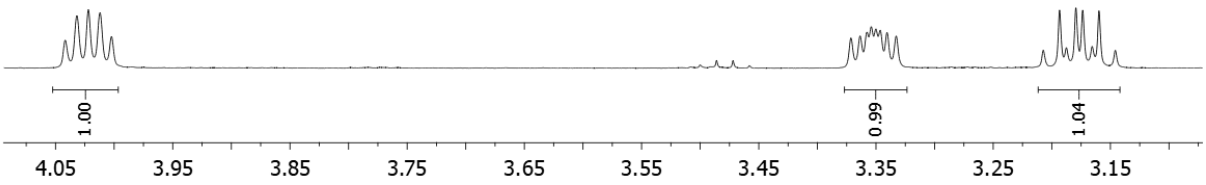

Figure S46. Section of the ^{1}H NMR spectrum of purified 2,3-*syn*-*trans*-**24** relevant for configurational analysis ($CDCl_3$, 500 MHz).

^{1}H NMR (500 MHz, $CDCl_3$): δ [ppm] = 7.44–7.37 (m, 5H, Ph), 4.02 (ddd, *J* = 9.9, 5.0, 4.9 Hz, 1H, CCHC*H*), 3.35 (ddd, *J* = 8.7, 6.8, 3.9 Hz, 1H, OC*H*CH_2CH_3), 3.18 (dq, *J* = 9.9, 7.0 Hz, 1H, CC*H*CH_3), 1.73–1.27 (m, 7H, CCHCHCH_2, CH_2CHCH_3, CHCH_2CH_3, CH_2C*H*CH_3), 1.15 (d, *J* = 7.0 Hz, 3H, CCHCH_3), 0.97 (d, *J* = 6.8 Hz, 3H, CH_2CHCH_3), 0.93 (t, *J* = 7.4 Hz, 3H, CHCH_2CH_3).

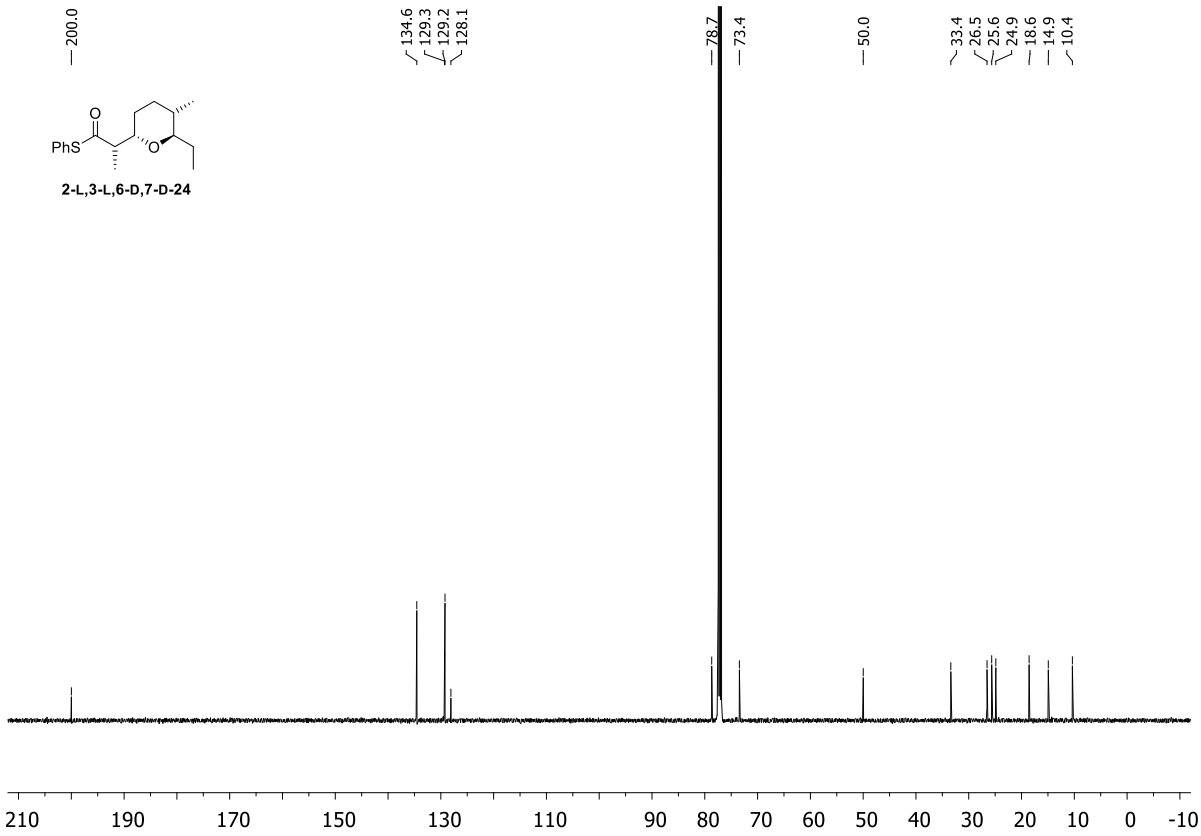

Figure S47. ^{13}C NMR analysis of the purified product **2-L,3-L,6-D,7-D-24** from the incubation of **14** with PedPS7 ($CDCl_3$, 125 MHz).

^{13}C NMR (125 MHz, $CDCl_3$): δ [ppm] = 200.0 (q, S*C*O), 134.6 (t, Ph), 129.3 (t, Ph), 129.2 (t, Ph), 128.1 (q, Ph), 78.7 (t, O*C*HCH$_2$CH$_3$), 73.5 (t, O*C*HCH$_2$CH$_2$), 50.0 (t, C*C*HCH$_3$), 33.4 (t, CH$_2$*C*HCH$_3$), 26.5 (s, OCH*C*H$_2$CH$_2$), 25.7 (s, *C*H$_2$CHCH$_3$), 24.9 (s, *C*H$_2$CH$_3$), 18.6 (p, CH$_2$*C*H$_3$), 14.9 (CCH*C*H$_3$), 10.4 (p, CH$_2$*C*H$_3$).

HRMS (ESI$^+$) *m/z* for $C_{17}H_{25}O_2S$ [M+H]$^+$: calculated 293.1575, found 293.1567.

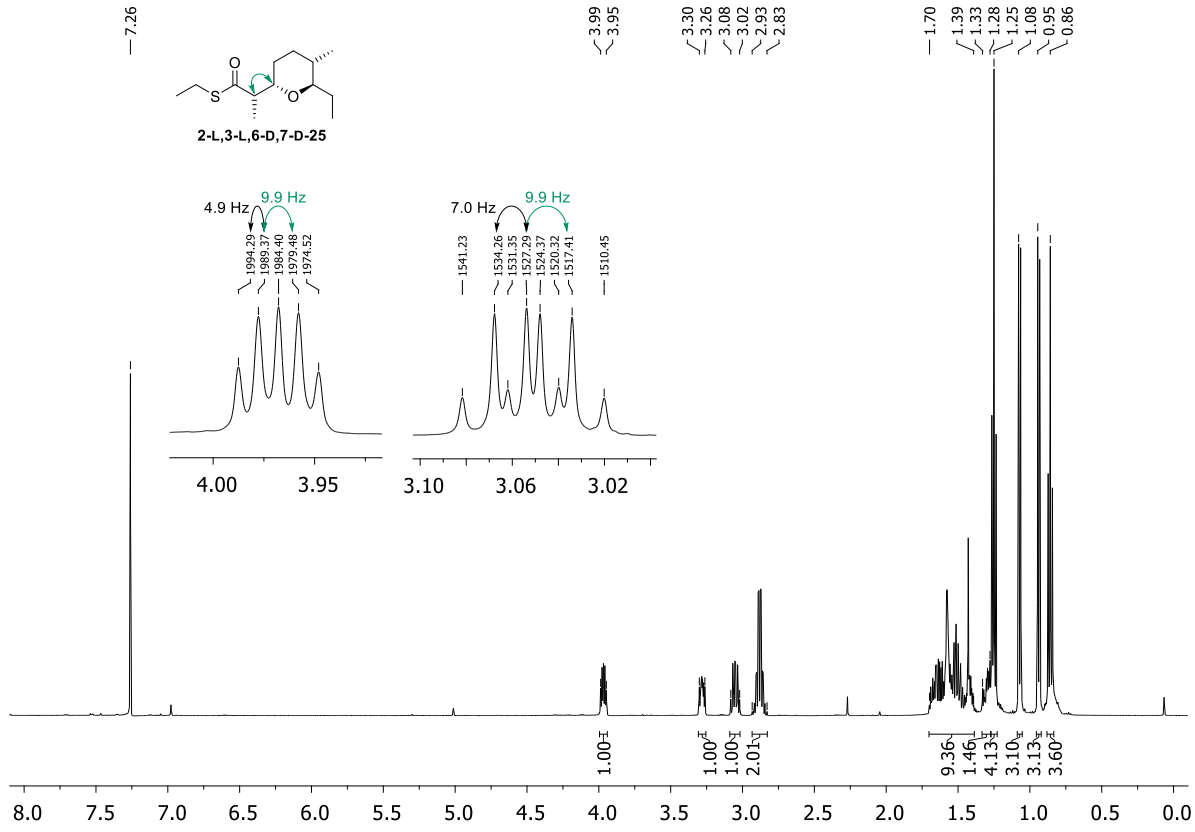

Figure S48. ^{1}H NMR analysis of the purified product **2-L,3-L,6-D,7-D-25** from the incubation of **15** with PedPS7 ($CDCl_3$, 500 MHz). It shows the 2,6-*trans*-THP characteristic shift of δ(**3-H**) = 3.97 and δ(**7-H**) = 3.28 ppm. The vicinal coupling constant $^{3}J_{2H\text{-}3H}$ of 9.9 Hz confirms the shown configuration at C-2.[4]

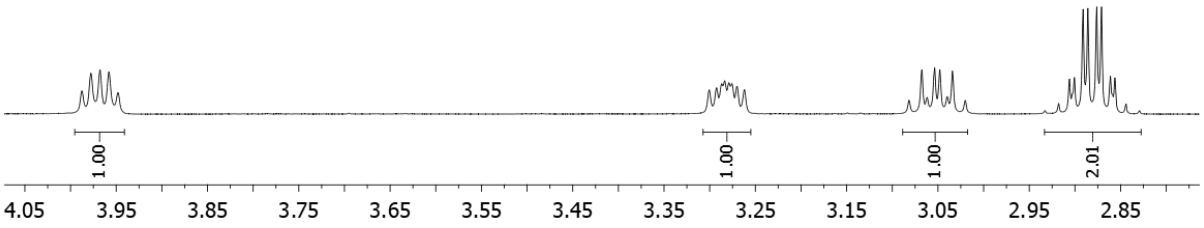

Figure S49. Section of the ^{1}H NMR analysis of purified **2-L,3-L,6-D,7-D-25** relevant for configurational analysis ($CDCl_3$, 500 MHz).

^{1}H NMR (500 MHz, $CDCl_3$): δ [ppm] = 3.97 (ddd, *J* = 9.9, 5.0, 4.9 Hz, 1H, CCHC*H*), 3.28 (ddd, *J* = 8.5, 6.8, 4.0 Hz, 1H, OC*H*CH_2CH_3), 3.05 (dq, *J* = 9.9, 7.0 Hz, 1H, CC*H*CH_3), 2.93–2.83 (m, 2H, C*H*$_2$S), 1.70–1.28 (m, 7H, CCHCHC*H*$_2$, C*H*$_2$CHCH$_3$, CHC*H*$_2$CH$_3$, CH$_2$C*H*CH$_3$), 1.25 (t, *J* = 7.4 Hz, 3H, C*H*$_3$CH$_2$S), 1.07 (d, *J* = 7.0 Hz, 3H, CCHC*H*$_3$), 0.94 (d, *J* = 6.8 Hz, 3H, CH$_2$CHC*H*$_3$), 0.86 (t, *J* = 7.4 Hz, 3H, CHCH$_2$C*H*$_3$).

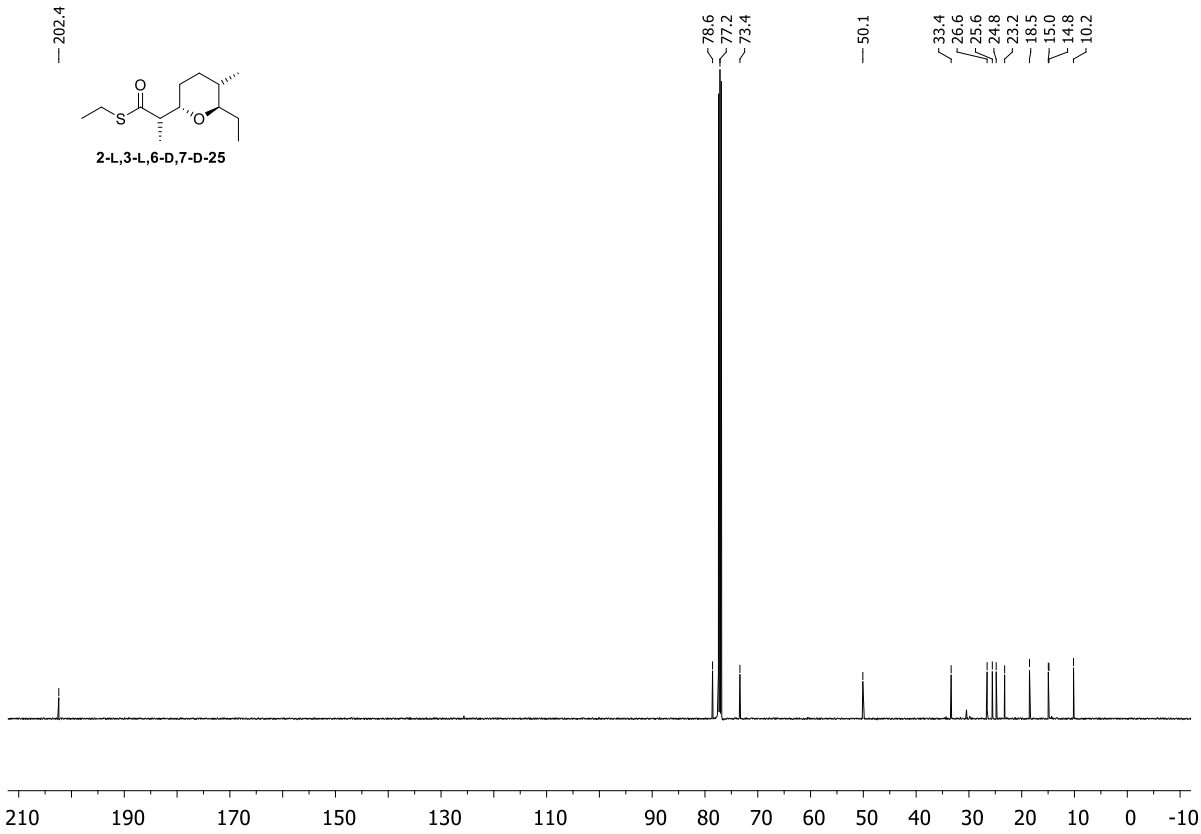

Figure S50. ^{13}C-NMR NMR analysis of the purified product **2-L,3-L,6-D,7-D-25** after conversion of PedPS7 and substrate **15** ($CDCl_3$, 125 MHz).

^{13}C NMR (125 MHz, $CDCl_3$): δ [ppm] = 202.4 (q, S*C*O), 78.6 (t, O*C*HCH$_2$CH$_3$), 73.4 (t, O*C*HCH$_2$CH$_2$), 50.1 (t, CCH*C*H), 33.4 (t, CH$_2$*C*HCH$_3$), 26.6 (s, *C*H$_2$CHCH$_3$), 25.6 (s, OCH*C*H$_2$CH$_2$), 24.8 (s, CHO*C*H$_2$CH$_3$), 23.2 (s, S*C*H$_2$CH$_3$), 18.5 (p, CH$_2$CH*C*H$_3$), 15.0 (p, COCH*C*H$_3$), 14.8 (p, SCH$_2$*C*H$_3$), 10.2 (p, CH$_2$*C*H$_3$).

HRMS (ESI$^+$) *m/z* for $C_{13}H_{25}O_2S$ [M+H]$^+$: calculated 245.1575, found 245.1568.

Stereoisomer discrimination and stereoselectivity of PedPS7

UPLC-MS analysis of crude reaction products

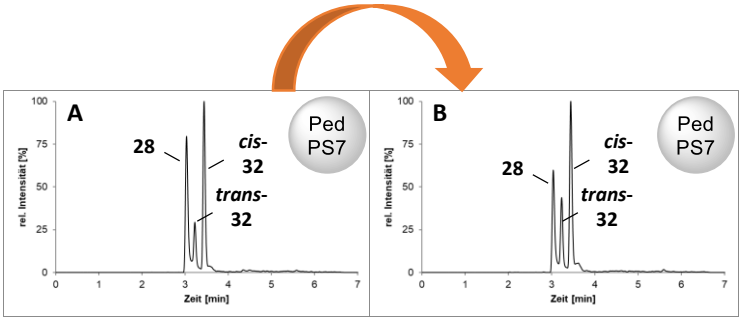

Figure S51. UPLC-MS analysis of conversion of **28** by PedPS7 after one (**A**) and two (**B**) reaction cycles. M(**28**)=310, M(**32**)=310, t_R(**28**)=3.03 min, t_R(*trans*-**32**)=3.23 min, t_R(*cis*-**32**)=3.44 min. Conditions of enzyme assay: 10× 0.1 mg (348 nmol) substrate **28** in HEPES buffer pH 7.2 (substrate concentration 2 mM) and 4.8–7.0 mg/mL His_6-PedPS7.

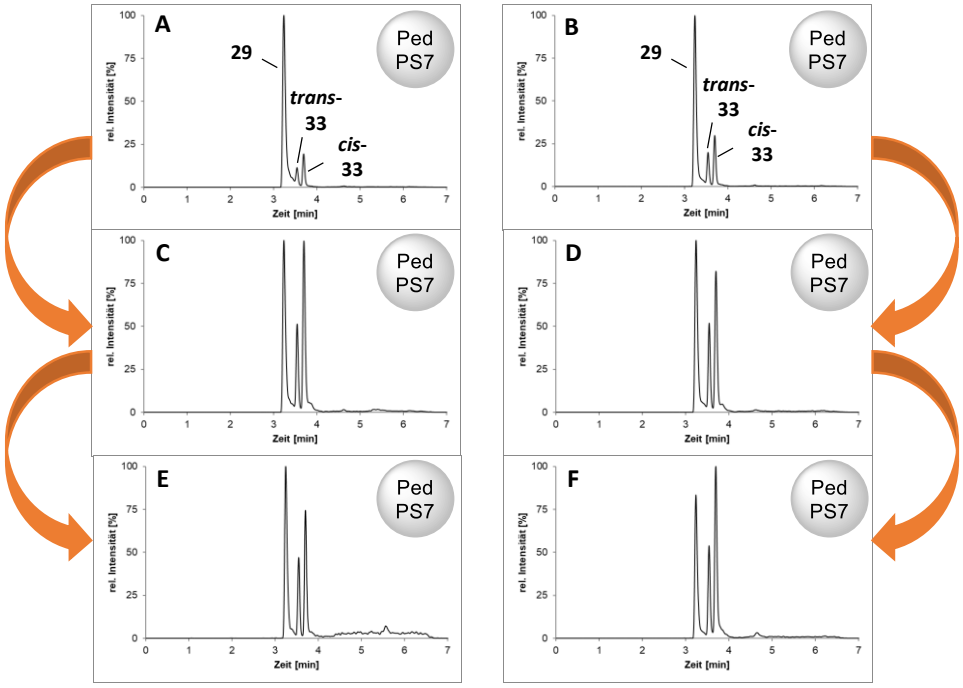

Figure S52. UPLC-MS analysis of conversion of **29** by PedPS7 after one (**A+B**), two (**C+D**) and three (**E+F**) reaction cycles. M(**29**)=388, M(**33**)=388, t_R(**29**)=3.24 min, t_R(*trans*-**33**)=3.54 min, t_R(*cis*-**33**)=3.70 min. Conditions of enzyme assay: 5× 0.1 mg (274 nmol) substrate **29** in HEPES buffer 6.8 (**A**), HEPES glycerol buffer pH 7.2 (**B**) and HEPES buffer pH 7.2 (**C–F**) (substrate concentration 2 mM) and 1.6–7.0 mg/mL His_6-PedPS7.

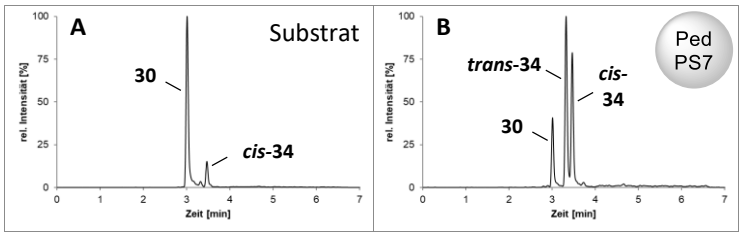

Figure S53. UPLC-MS analysis of (**A**) substrate **30**, (**B**) conversion of **30** by PedPS7. M(**30**)=374, M(**34**)=374, t_R(**30**)=3.01 min, t_R(*trans*-**34**)=3.21 min, t_R(*cis*-**34**)=3.47 min. Conditions of enzyme assay: 0.1 mg (285 nmol) substrate **30** in HEPES buffer (substrate concentration 2 mM) and 2.7 mg/mL His_6-PedPS7. No or only minimal spontaneous conversion of **30** into *cis*-**34** was observed under the reaction conditions in earlier studies.[2]

NMR analysis of crude reaction products

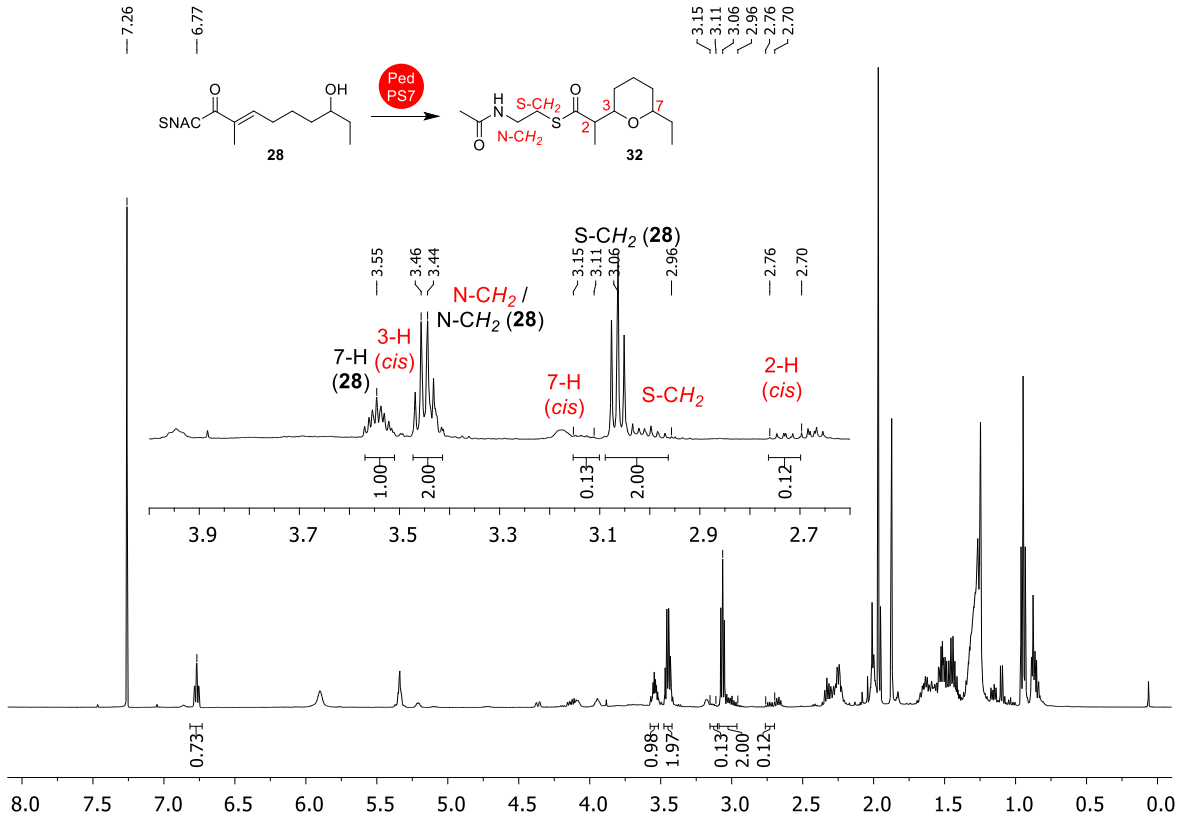

Figure S54. ^{1}H NMR analysis of the conversion experiment of PedPS7 and substrate **28** after one reaction cycle ($CDCl_3$, 500 MHz). The relevant signals of the starting material and the cyclised products are annotated in the enlarged section.

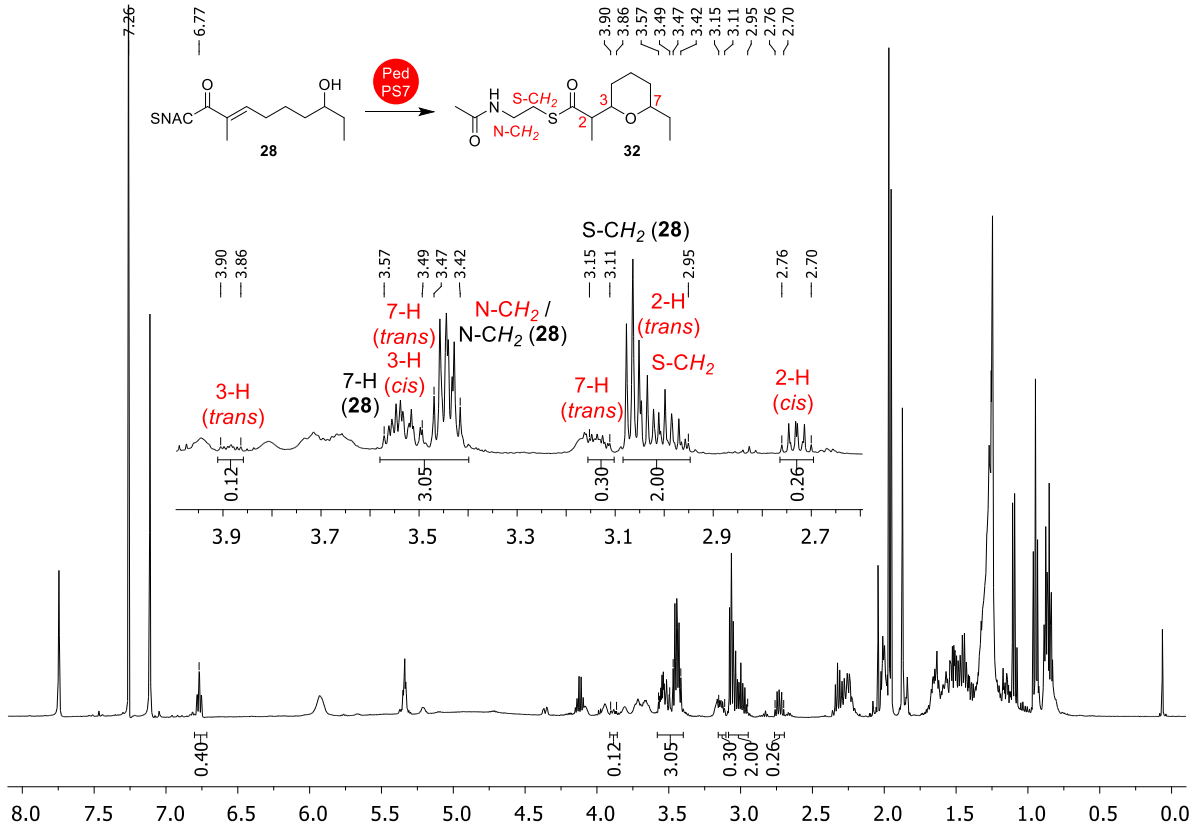

Figure S55. ^{1}H NMR analysis of the conversion experiment of PedPS7 and substrate **28** after two reaction cycles ($CDCl_3$, 500 MHz).

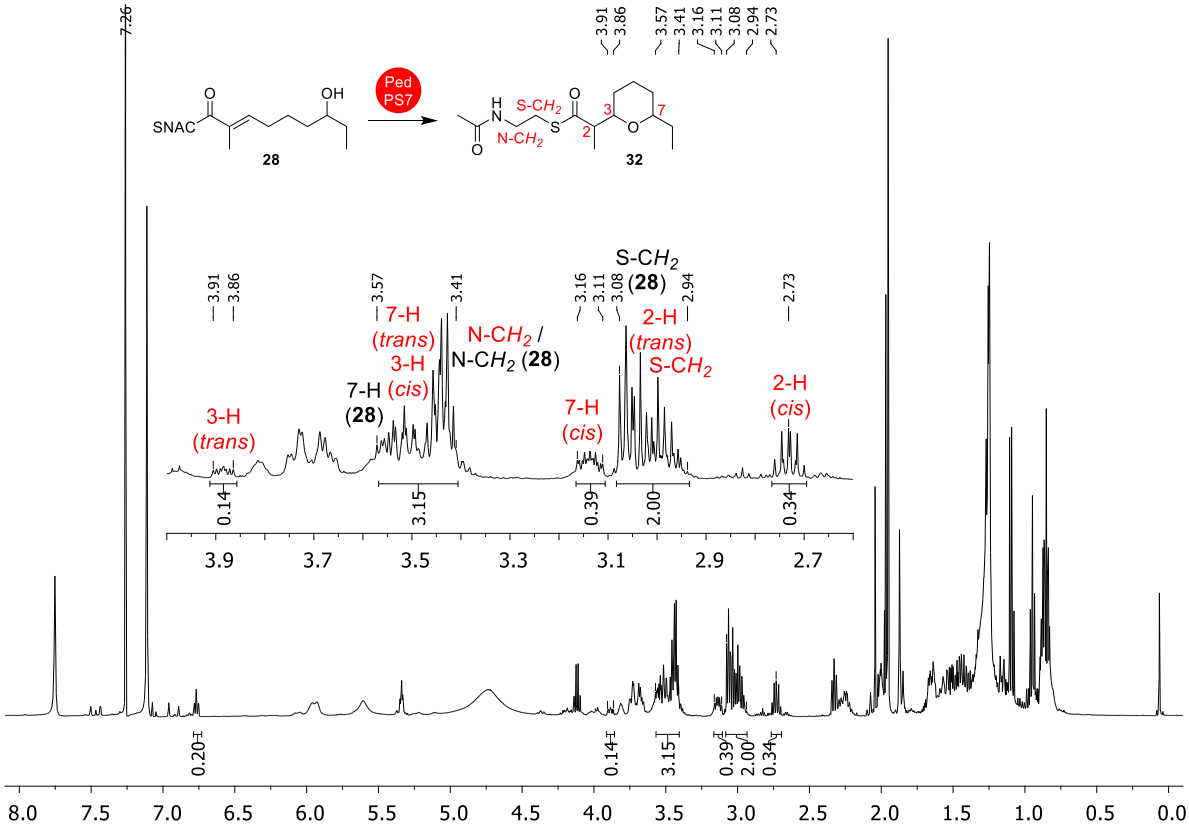

Figure S56. ^{1}H NMR analysis of the conversion experiment of PedPS7 and substrate **28** after three reaction cycles ($CDCl_3$, 500 MHz).

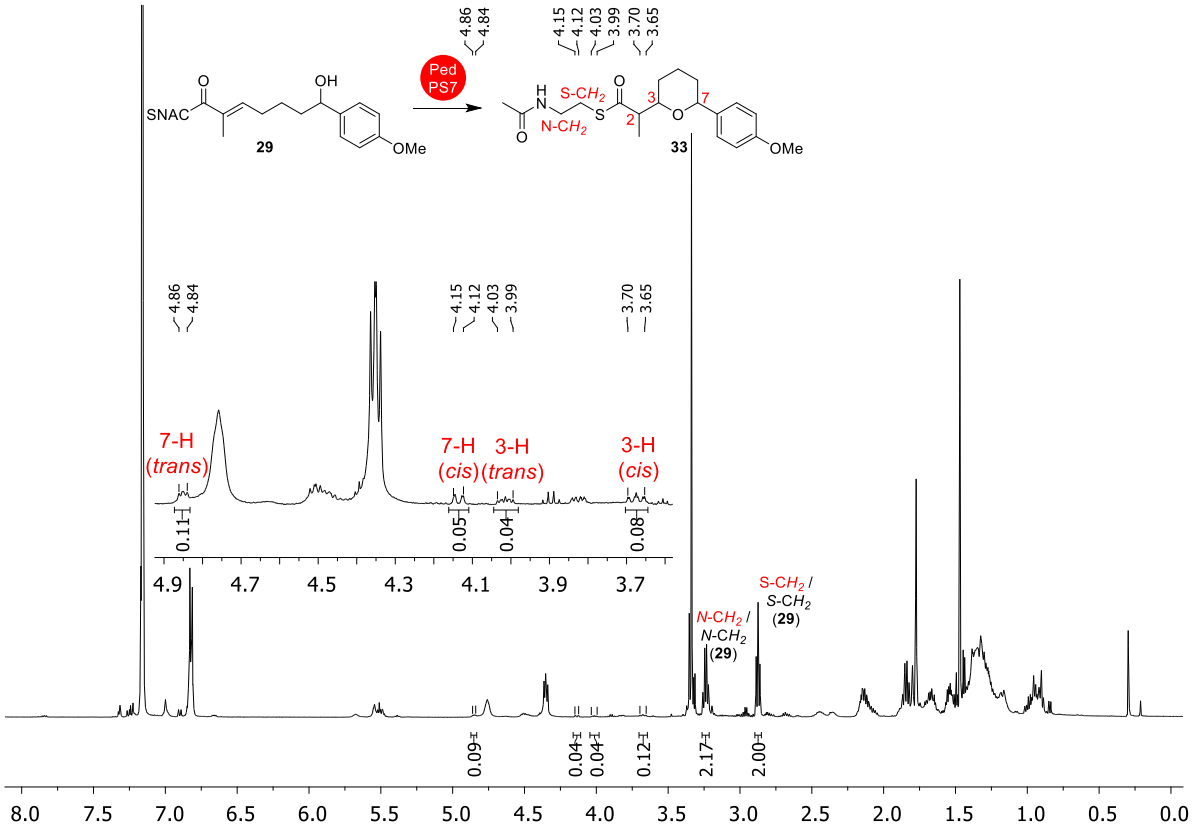

Figure S57. ^{1}H NMR analysis of the conversion experiment of PedPS7 and substrate **29** after one reaction cycle (C_6D_6, 500 MHz).

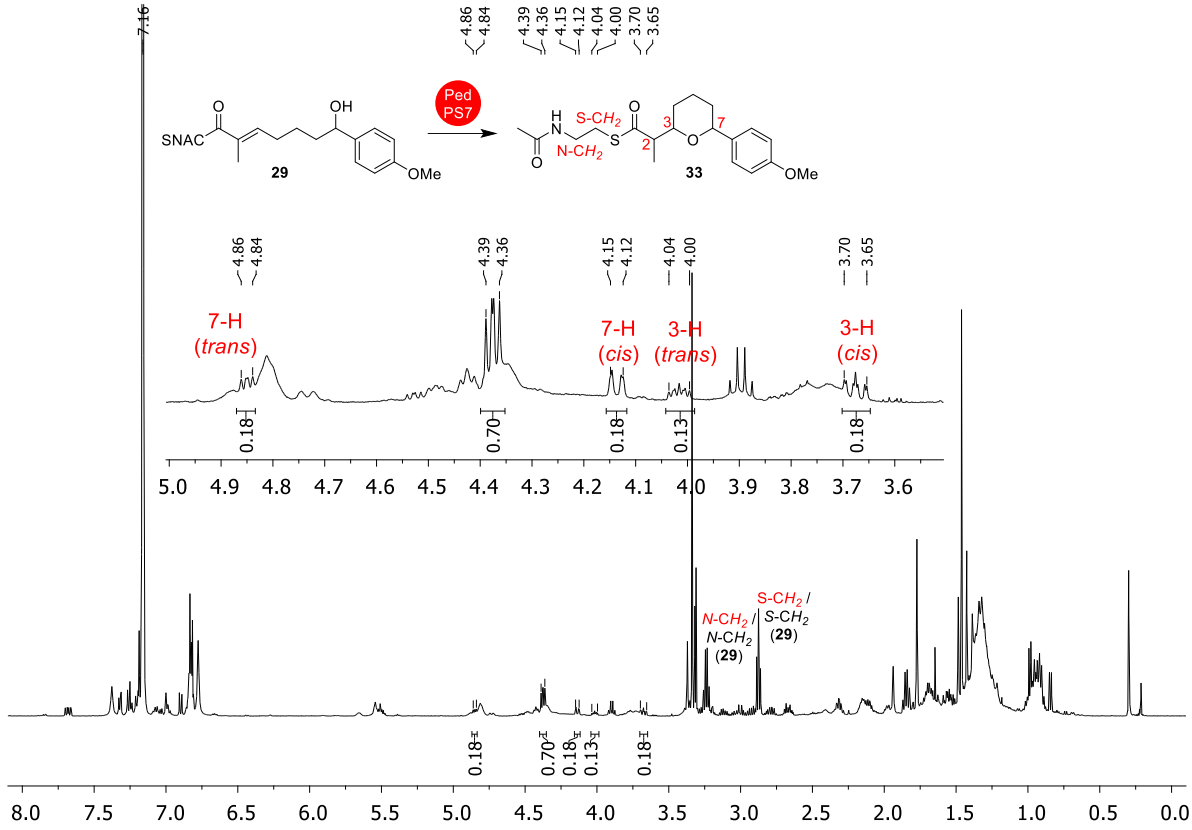

Figure S58. ^{1}H NMR analysis of the conversion experiment of PedPS7 and substrate **29** after two reaction cycles (C_6D_6, 500 MHz).

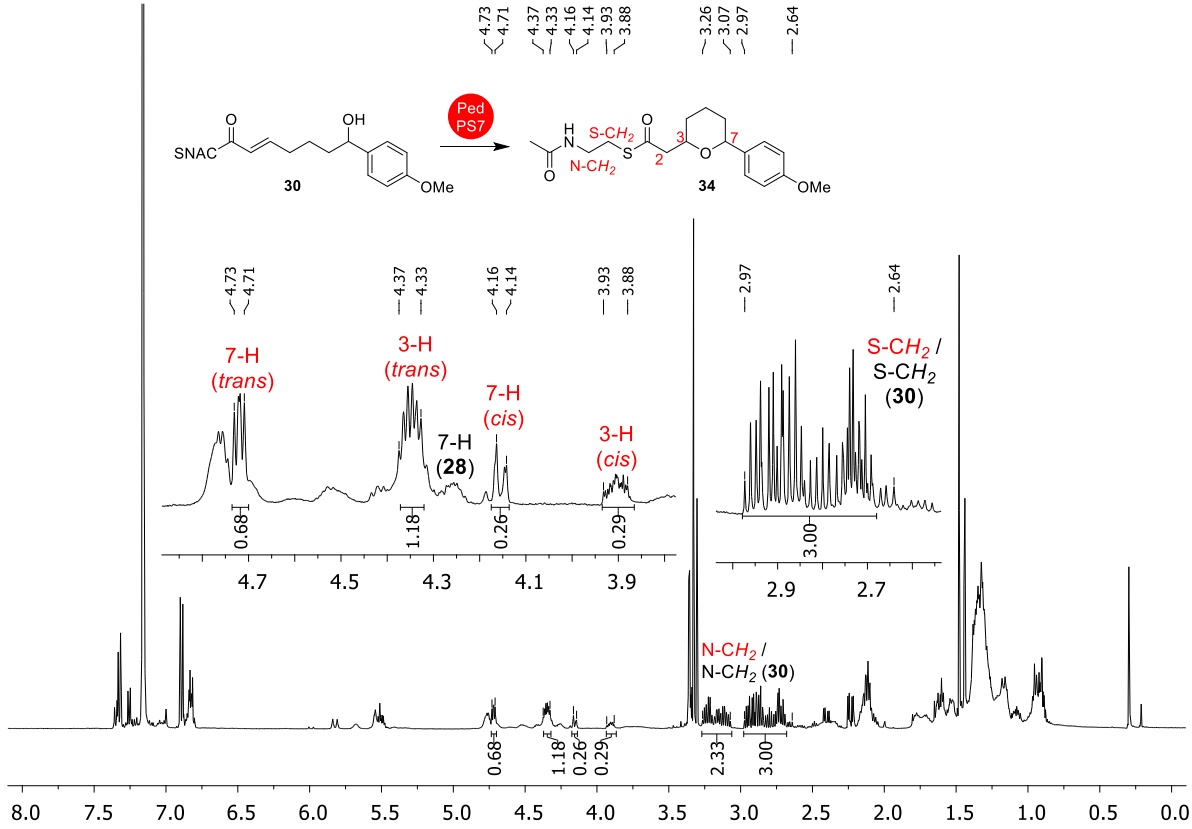

Figure S59. ^{1}H NMR analysis of the conversion experiment of PedPS7 and substrate **30** after one reaction cycle (C_6D_6, 500 MHz).

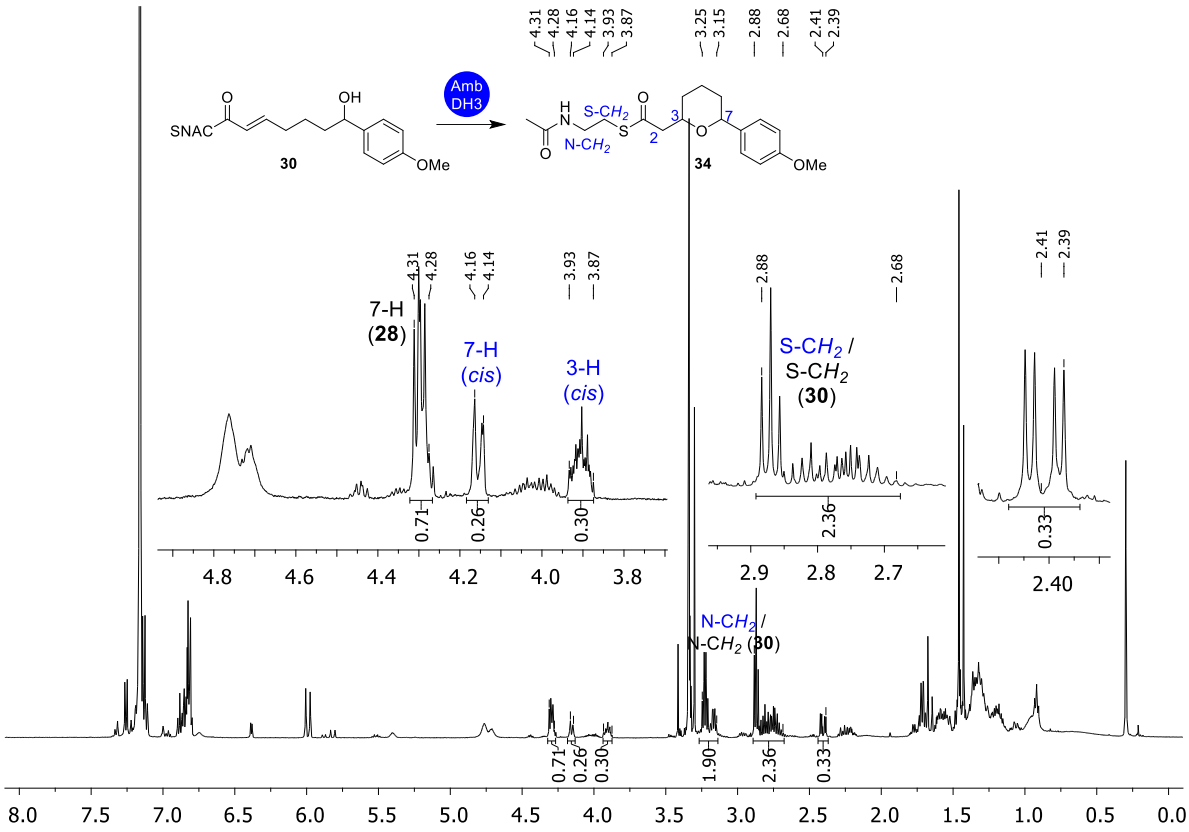

Figure S60. ^{1}H NMR analysis of the conversion experiment of AmbDH3 and substrate **30** after one reaction cycle (C_6D_6, 500 MHz).

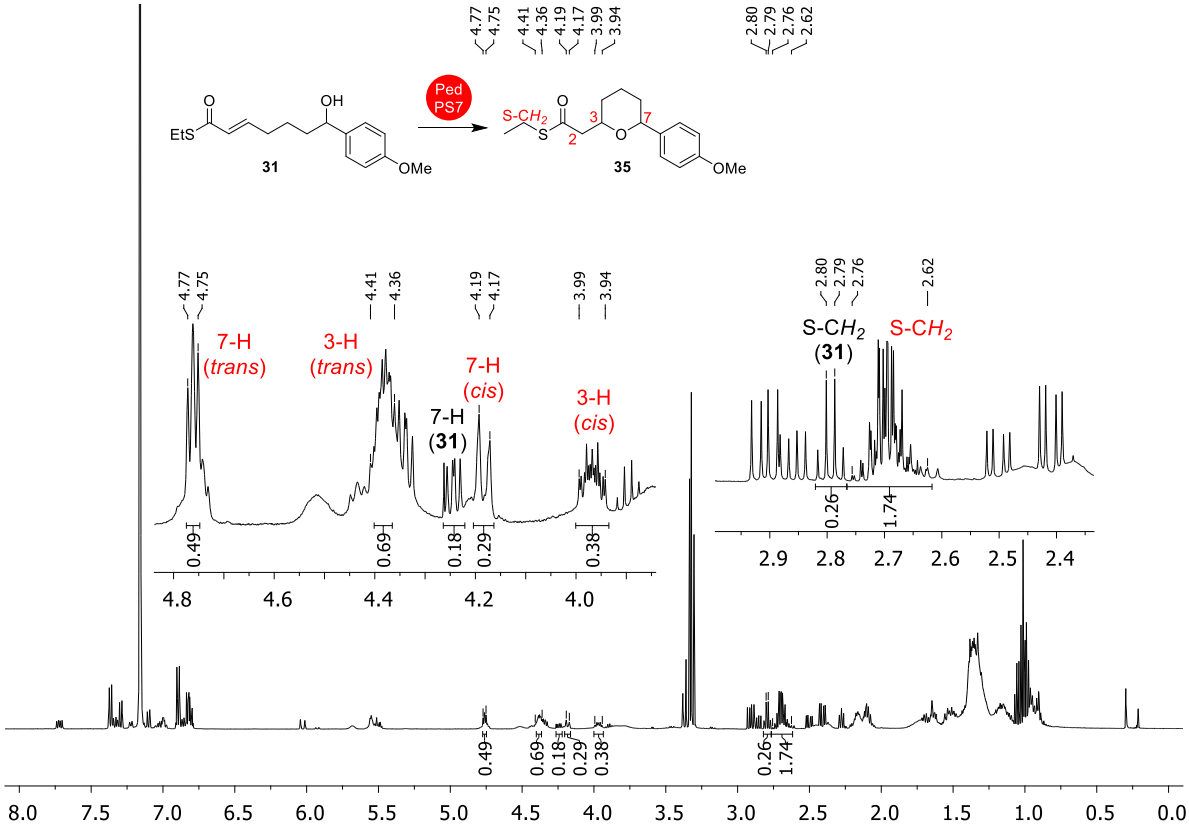

Figure S61. ^{1}H NMR analysis of the conversion experiment of PedPS7 and substrate **31** after one reaction cycle (C_6D_6, 500 MHz).

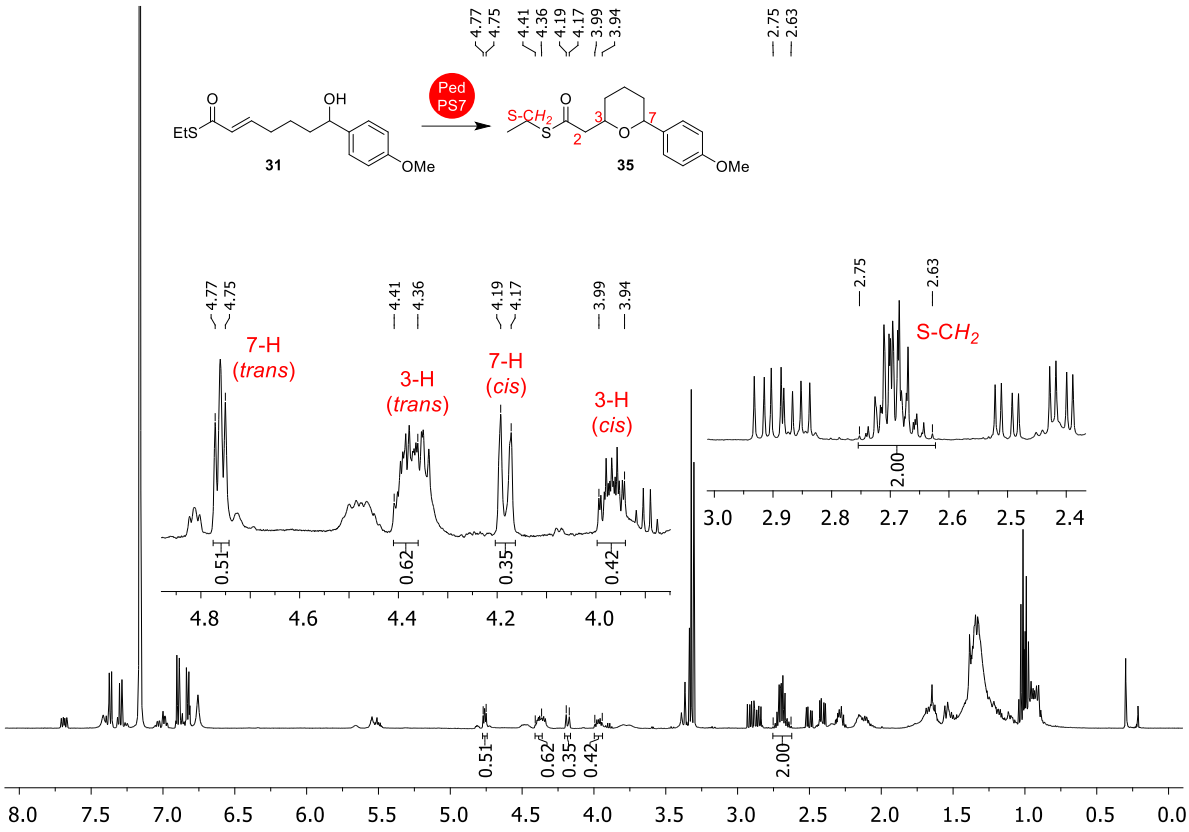

Figure S62. ^{1}H NMR analysis of the conversion experiment of PedPS7 and substrate **31** after two reaction cycles (C_6D_6, 500 MHz). The relevant signals of the starting material and the cyclised products are annotated in the enlarged section. The conversion could only be estimated due to overlapping signals.

Compound purification and configurational analysis

NMR analysis

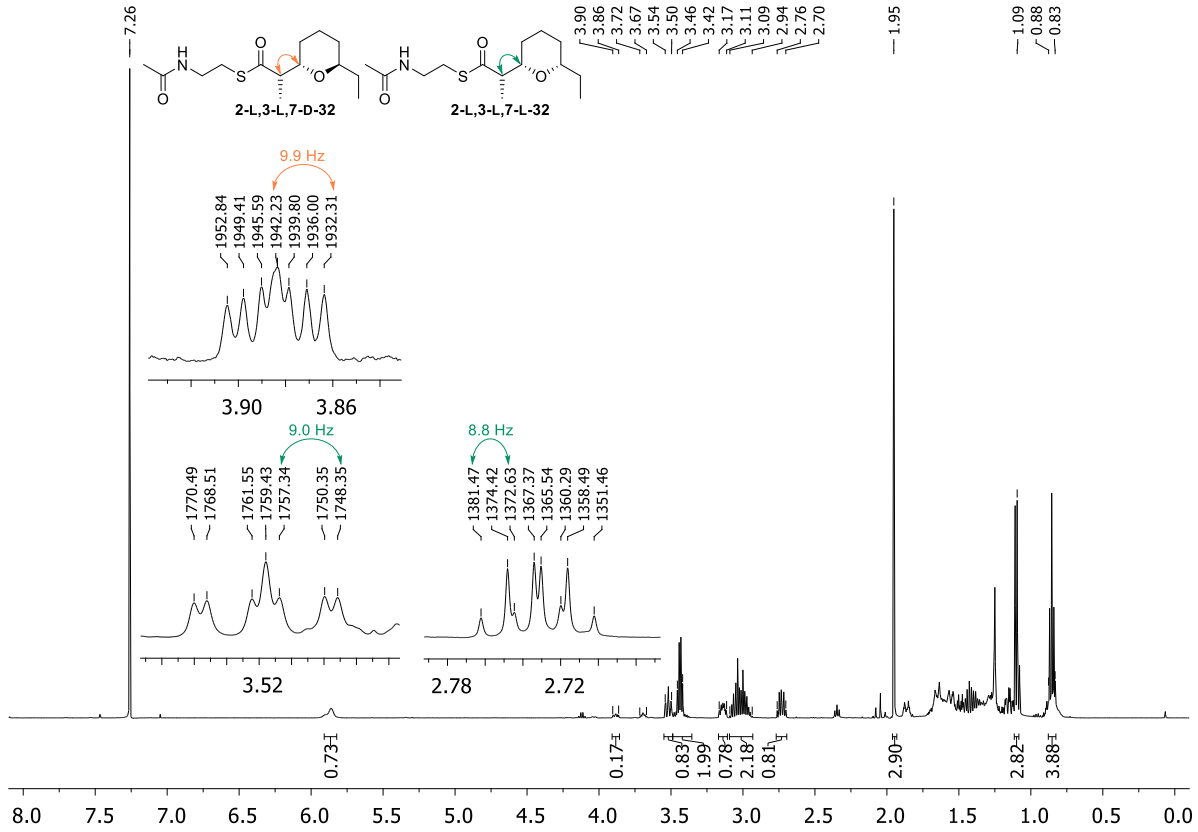

Figure S63. ^{1}H NMR analysis of the product mixture **2-L,3-L,7-D-32** and **2-L,3-L,7-L-32** after column chromatography ($CDCl_3$, 500 MHz). It shows the 2,6-*trans*-THP characteristic shifts of δ(**3-H**) = 3.89 and δ(**7-H**) = 3.50 ppm (collapsing with **3-H** (*cis*-THP) and NHC*H*$_2$) as well as the 3,7-*cis*-THP characteristic shifts of δ(**3-H**) = 3.52 and δ(**7-H**) = 2.73 ppm. The vicinal coupling constants $^{3}J_{2H\text{-}3H}$ of 9.9 Hz for **2-L,3-L,7-D-32** and 8.9 Hz for **2-L,3-L,7-L-32** confirm the shown configuration at C-2.[4]

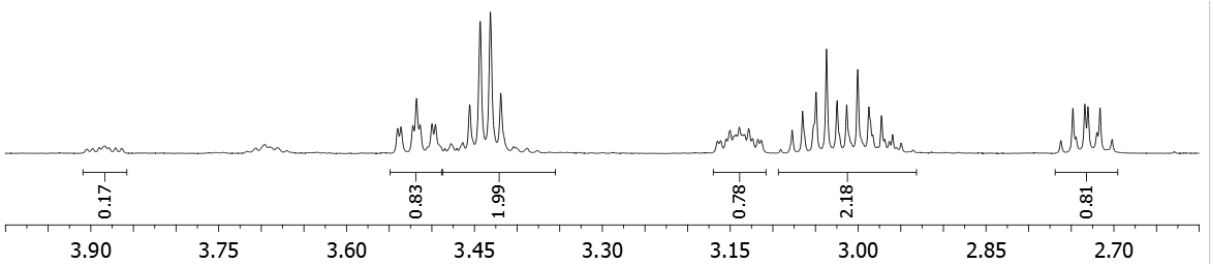

Figure S64. Section of the ^{1}H NMR analysis of the purified product mixture **2-L,3-L,7-D-32** and **2-L,3-L,7-L-32** relevant for configurational analysis ($CDCl_3$, 500 MHz).

HRMS (ESI$^+$) *m/z* for $C_{14}H_{26}NO_3S$ $[M+H]^+$: calculated 288.1633, found 288.1628.

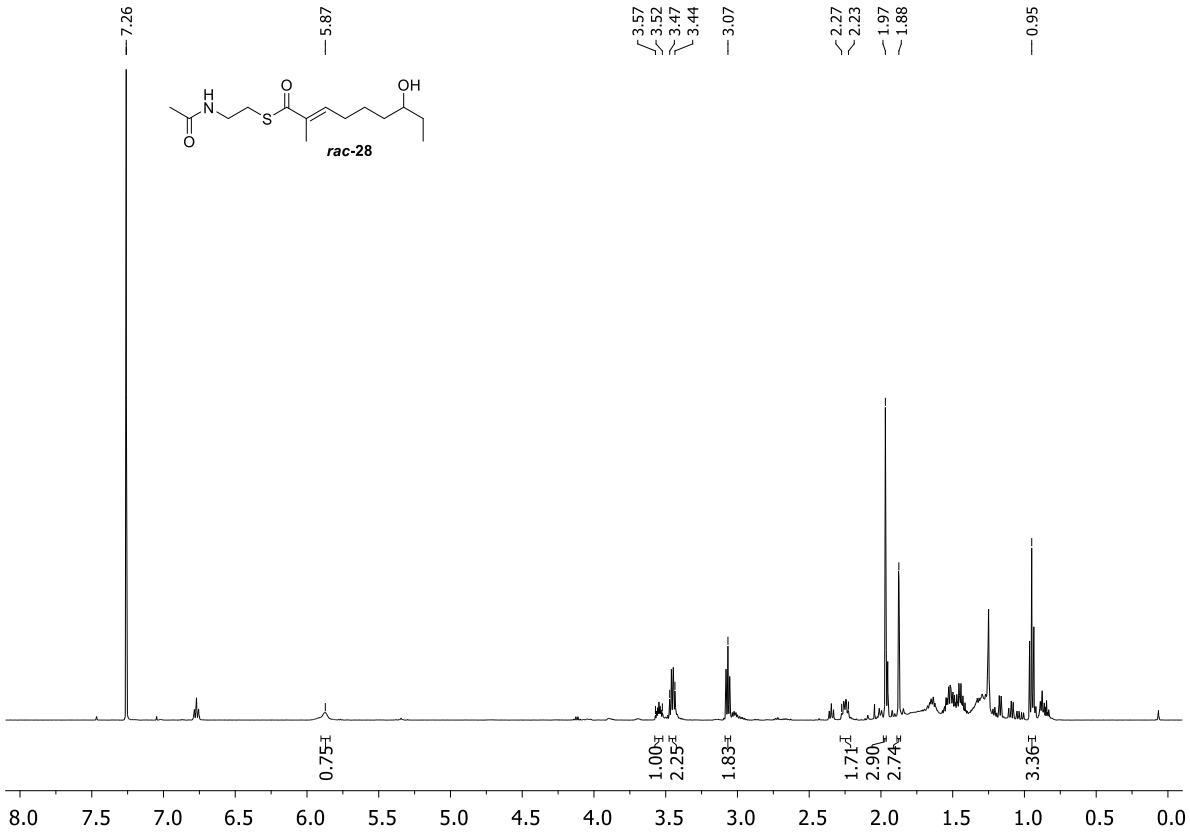

Figure S65. ^{1}H NMR analysis of the reisolated starting material *rac*-**28** along with a minor impurity of **2-L,3-L,7-D-32** ($CDCl_3$, 500 MHz).

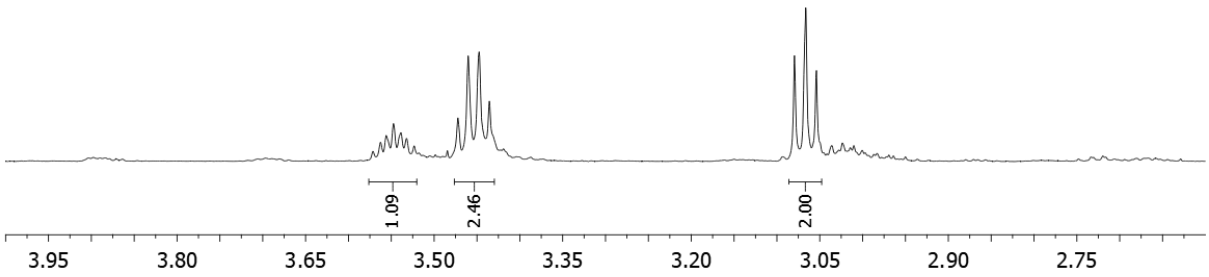

Figure S66. Section of the ^{1}H NMR analysis of the reisolated starting material *rac*-**28** from flash chromatography showing the signals for **7-H**, **NHC*H*$_2$** and **C*H*$_2$S** ($CDCl_3$, 500 MHz).

HRMS (ESI$^+$) *m/z* for $C_{14}H_{26}NO_3S$ $[M+H]^+$: calculated 288.1633, found 288.1628; for $C_{14}H_{25}NO_3SNa$ $[M+Na]^+$: calculated 310.1453, found 310.1447.

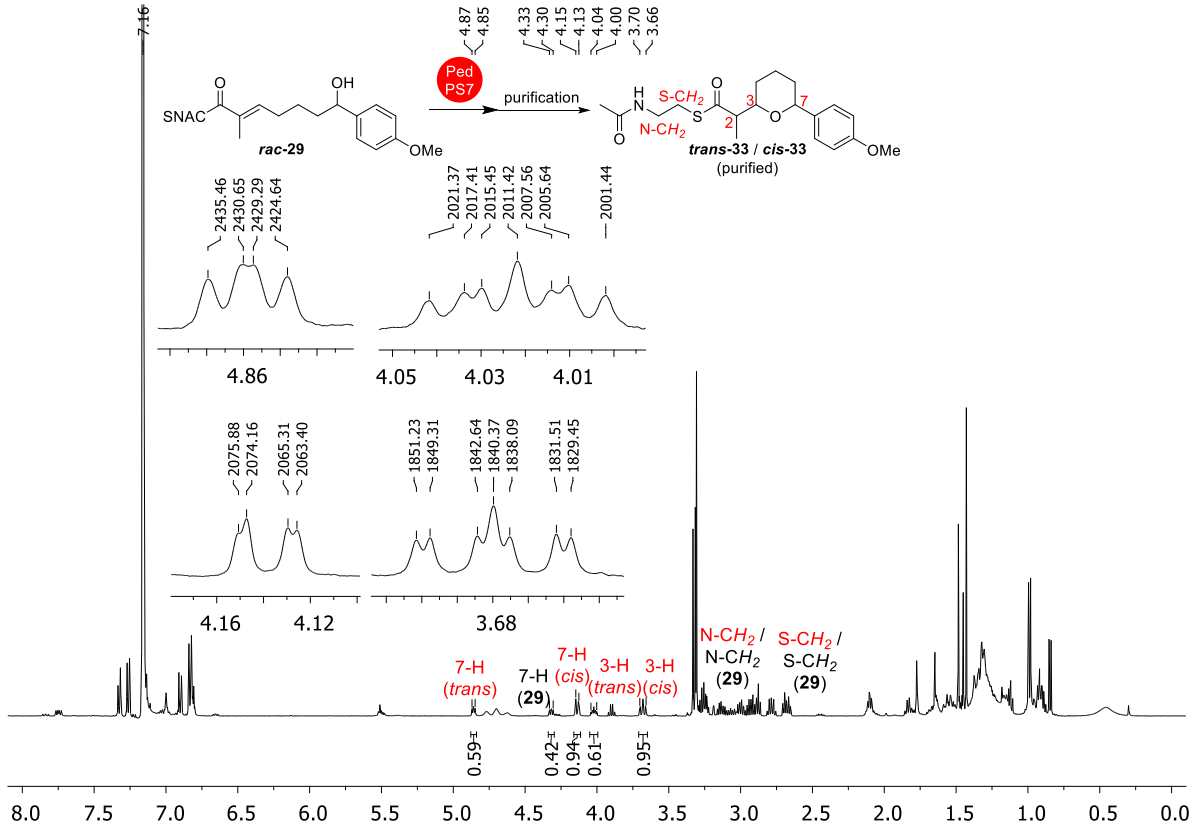

Figure S67. ^{1}H NMR analysis of the purified product mixture of *trans*-**33** and *cis*-**33** after conversion of PedPS7 and substrate *rac*-**29** (C_6D_6, 500 MHz). The ^{1}H NMR analysis of the starting material *rac*-**29** is shown in Figure S69. The sections of the NMR spectra for configuration determination are shown in Figure S68. It shows the 2,6-*trans*-THP characteristic shift of δ(**3-H**) = 4.02 and δ(**7-H**) = 4.86 ppm as well as the 2,6-*cis*-THP characteristic shift of δ(**3-H**) = 3.68 and δ(**7-H**) = 4.14 ppm. The vicinal coupling constants $^{3}J_{2H\text{-}3H}$ of 10.0 Hz for *trans*-**33** and 8.6 Hz for *cis*-**33** confirm the shown relative configuration along C-2–C-3.[2,4]

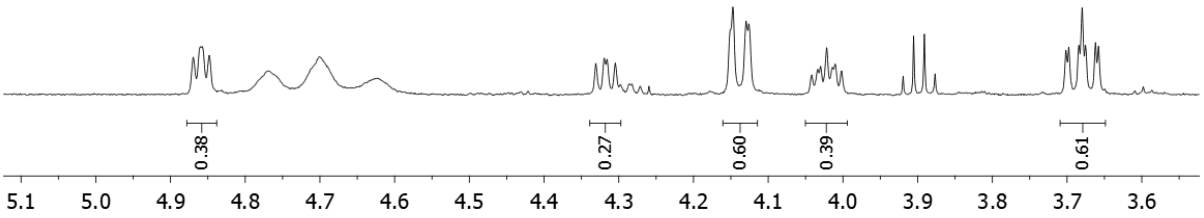

Figure S68. Section of the ^{1}H NMR analysis of the purified product mixture *trans*-**33** and *cis*-**33** after conversion of PedPS7 and substrate *rac*-**29** (C_6D_6, 500 MHz).

HRMS (ESI^{+}) *m/z* for $C_{19}H_{28}NO_4S$ $[M+H]^{+}$: calculated 366.1739, found 366.1728.

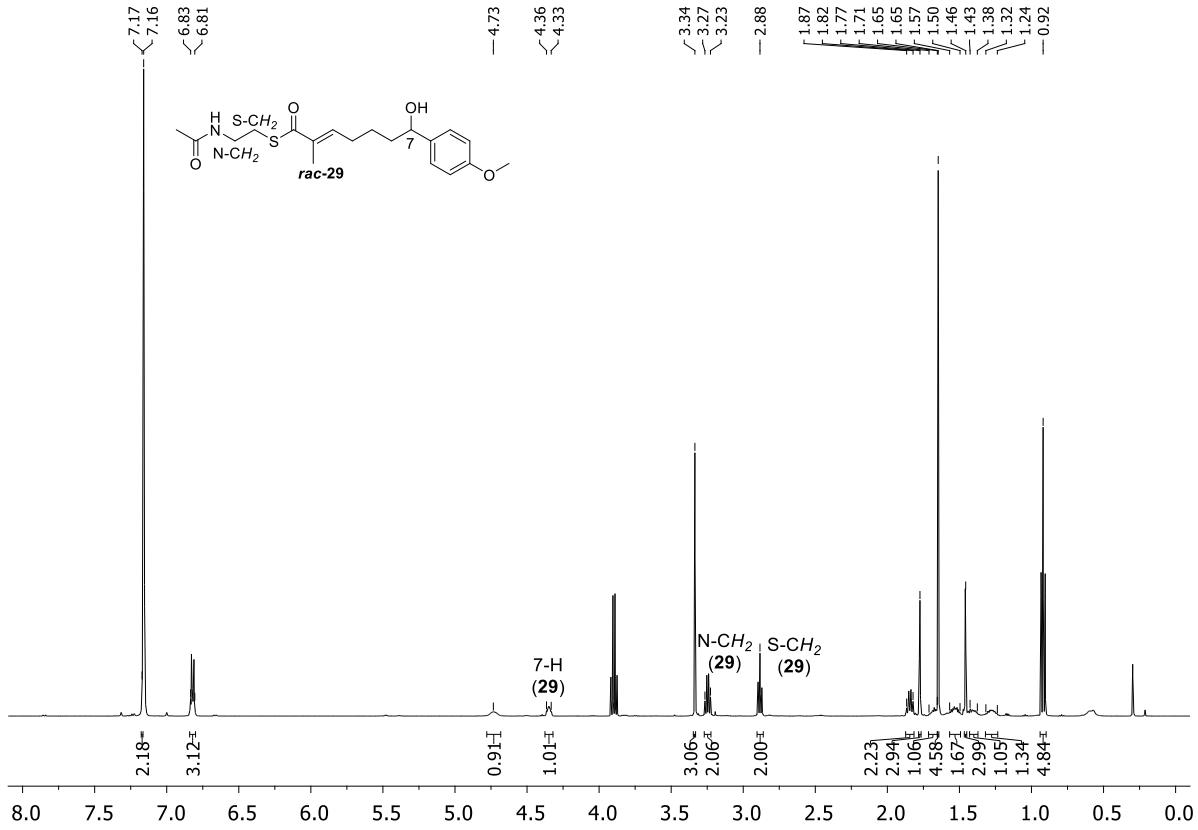

Figure S69. ^{1}H NMR analysis of the starting material *rac*-**29** (C_6D_6, 500 MHz). Impurities of EtOAc are visible at 3.90, 1.65 and 0.92 ppm.

^{1}H NMR (500 MHz, C_6D_6): δ [ppm] = 7.18–7.17 (m, 2H, 2× C*H*$_{Ar}$OMe), 6.84–6.80 (m, 3H, 2× C*H*$_{Ar}$OMe, CH_3CCH), 4.73 (s, 1H, CH_2NH), 4.37–4.32 (m, 1H, C*H*OH), 3.34 (s, 3H, OCH_3), 3.27–3.22 (m, 2H, $NHCH_2$), 2.88 (t, *J* = 6.7 Hz, 2H, CH_2S), 1.87–1.82 (m, 2H, $CCHCH_2$), 1.77 (s, 3H, CH_3CO), 1.71–1.66 (m, 1H, 1× CH_2COH), 1.57–1.49 (m, 1H, 1× CH_2COH), 1.46 (d, *J* = 1.4 Hz, 3H, CH_3CCO), 1.43 – 1.36 (m, 1H, 1× $CH_2CH_2CH_2$), 1.32–1.22 (m, 1H, 1× $CH_2CH_2CH_2$).

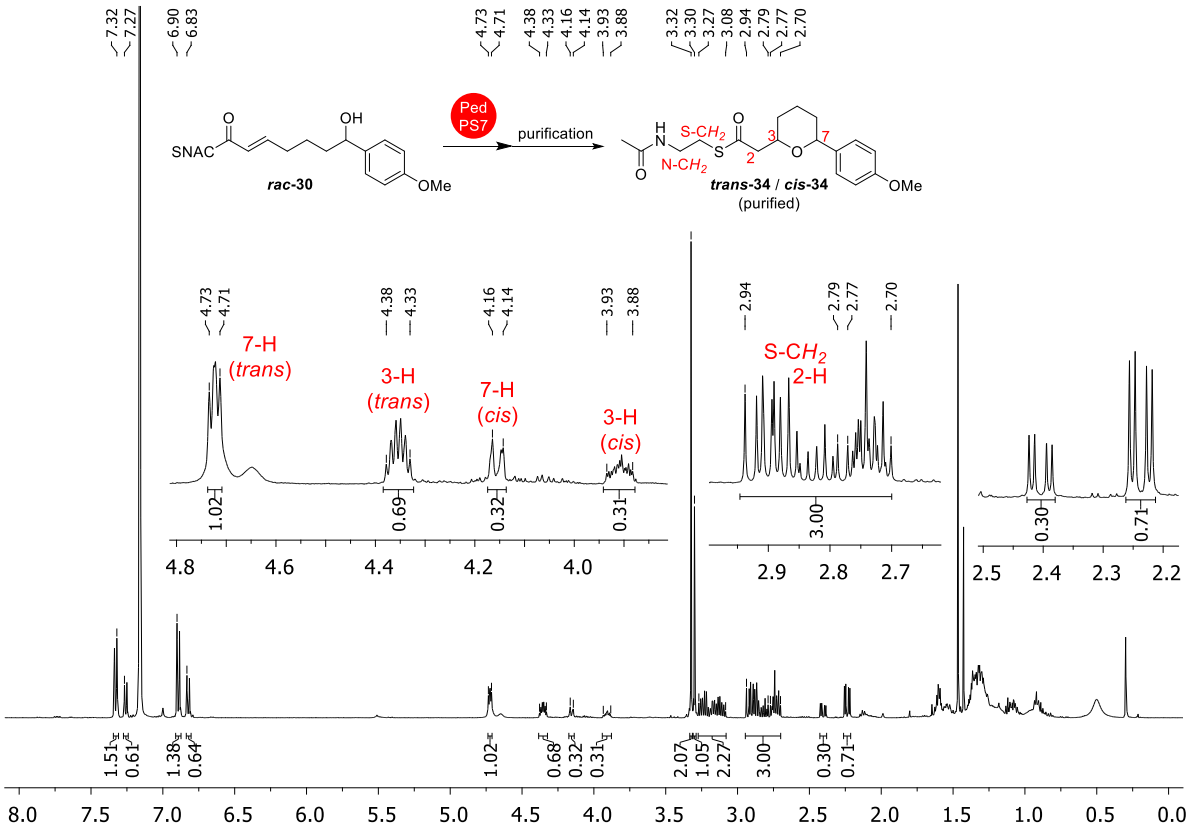

Figure S70. ^{1}H NMR analysis of the product mixture *trans*-**34** and *cis*-**34** obtained from the incubation of *rac*-**30** and PedPS7 after flash chromatography (C_6D_6, 500 MHz). It shows the 2,6-*trans*-THP characteristic shifts of δ(**7-H**) = 4.72 and δ(**3-H**) = 4.36 ppm as well as the 2,6-*cis*-THP characteristic shifts of δ(**7-H**) = 4.15 and δ(**3-H**) = 3.91 ppm.

HRMS (ESI$^+$) *m/z* for $C_{18}H_{26}NO_4S$ $[M+H]^+$: calculated 352.1583, found 352.1573.

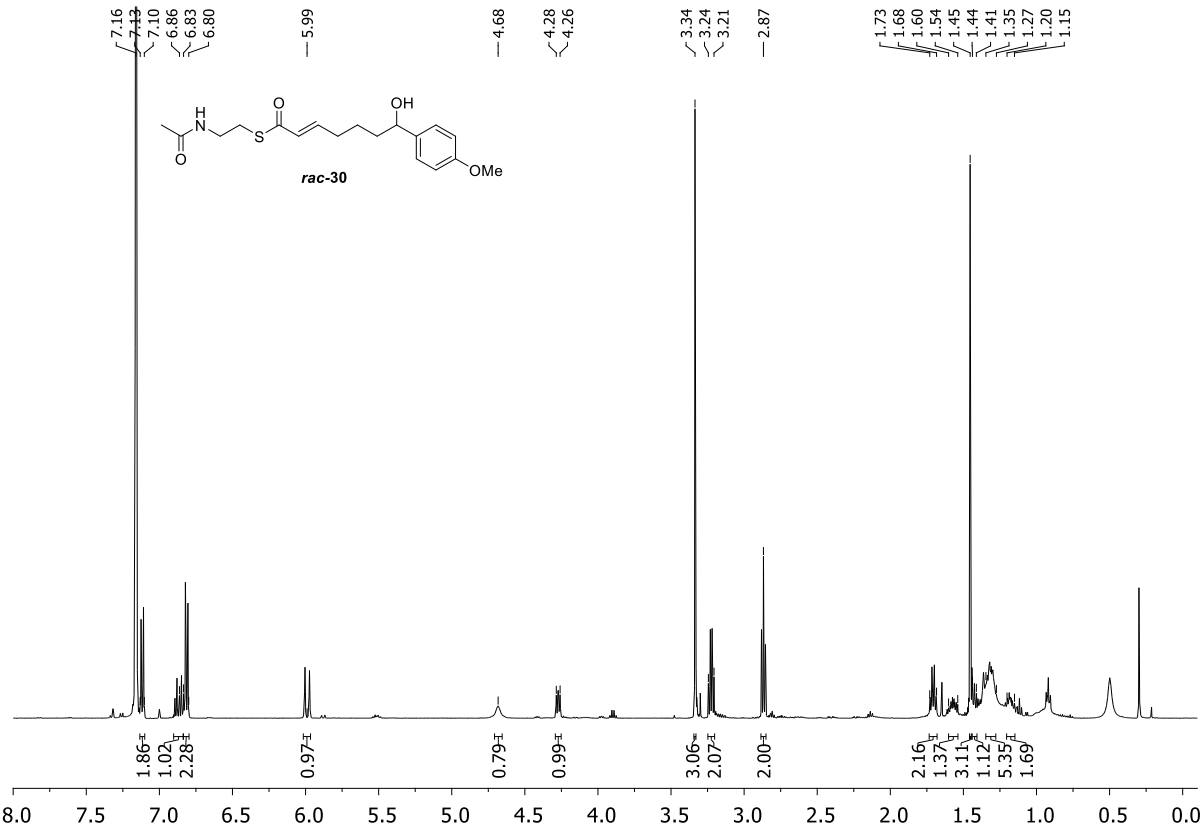

Figure S71. ^{1}H NMR analysis of synthetic *rac*-**30** (C_6D_6, 500 MHz).

^{1}H NMR (500 MHz, C_6D_6): δ [ppm] = 7.13–7.10 (m, 2H, *m*-C*H*ArOMe), 6.86 (dt, *J* = 13.3, 5.9 Hz, 1H, OCCHC*H*), 6.83–6.79 (m, 2H, *o*-C*H*ArOMe), 5.99 (dt, *J* = 15.5, 1.5 Hz, 1H, OCC*H*CH), 4.68 (s, 1H, CH_2N*H*), 4.29–4.25 (m, 1H, C*H*OH), 3.34 (s, 3H, OCH_3), 3.25–3.20 (m, 2H, NCH_2), 2.87 (t, *J* = 6.7 Hz, 2H, CH_2S), 1.73–1.68 (m, 2H, CHCHCH_2), 1.61–1.54 (m, 1H, 1× OHCHCH_2), 1.44–1.41 (m, 1H, 1× OHCHCH_2), 1.45 (s, 3H, OCCH_3), 1.36–1.28 (m, 1H, 1× CH_2C$H_2$$CH_2$), 1.21–1.14 (m, 1H, 1× CH_2C$H_2$$CH_2$).

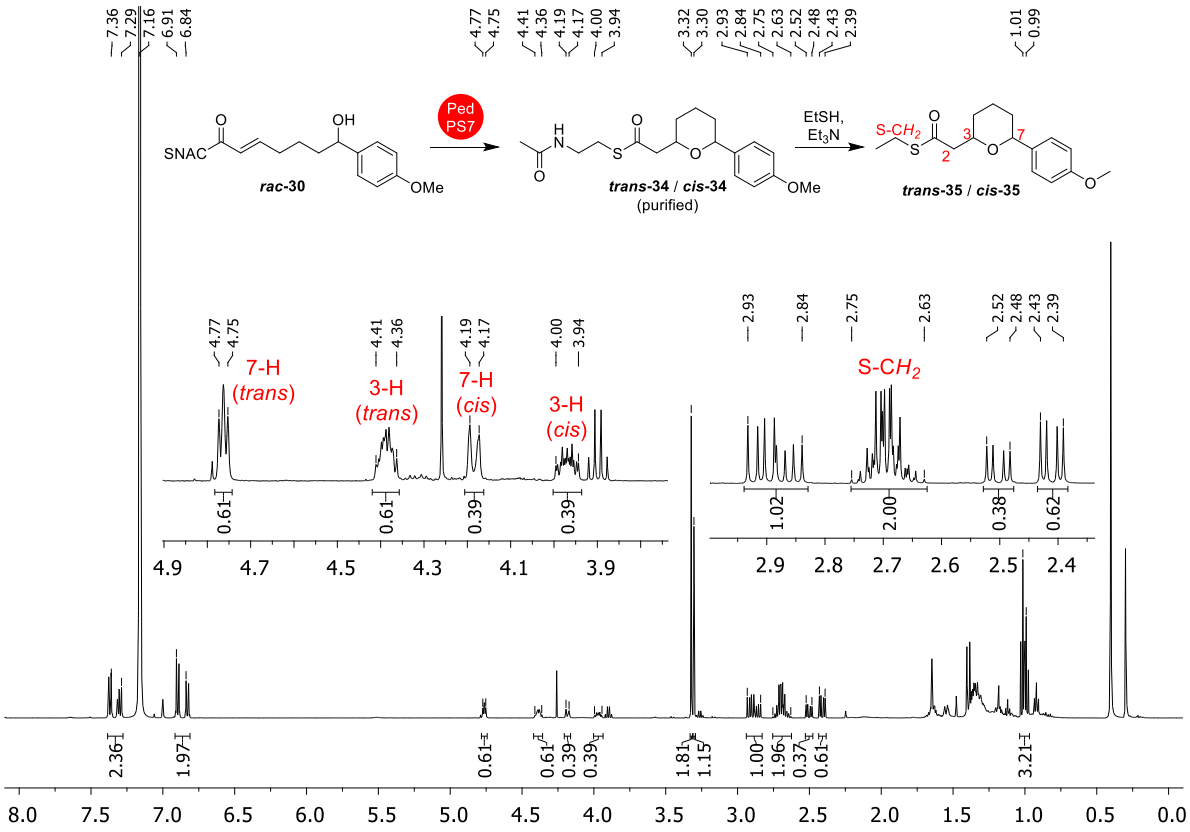

Figure S72. ^{1}H NMR analysis of the mixture of *trans*-**35** and *cis*-**35** resulting from transesterification of the SNAC thioesters **34** shown in Figure S70 to the corresponding SEt thioesters (C_6D_6, 500 MHz). It shows the 2,6-*trans*-THP characteristic shift of δ(**7-H**) = 4.76 and δ(**3-H**) = 4.39 ppm as well as the 2,6-*cis*-THP characteristic shift of δ(**7-H**) = 4.18 and δ(**3-H**) = 3.97 ppm.

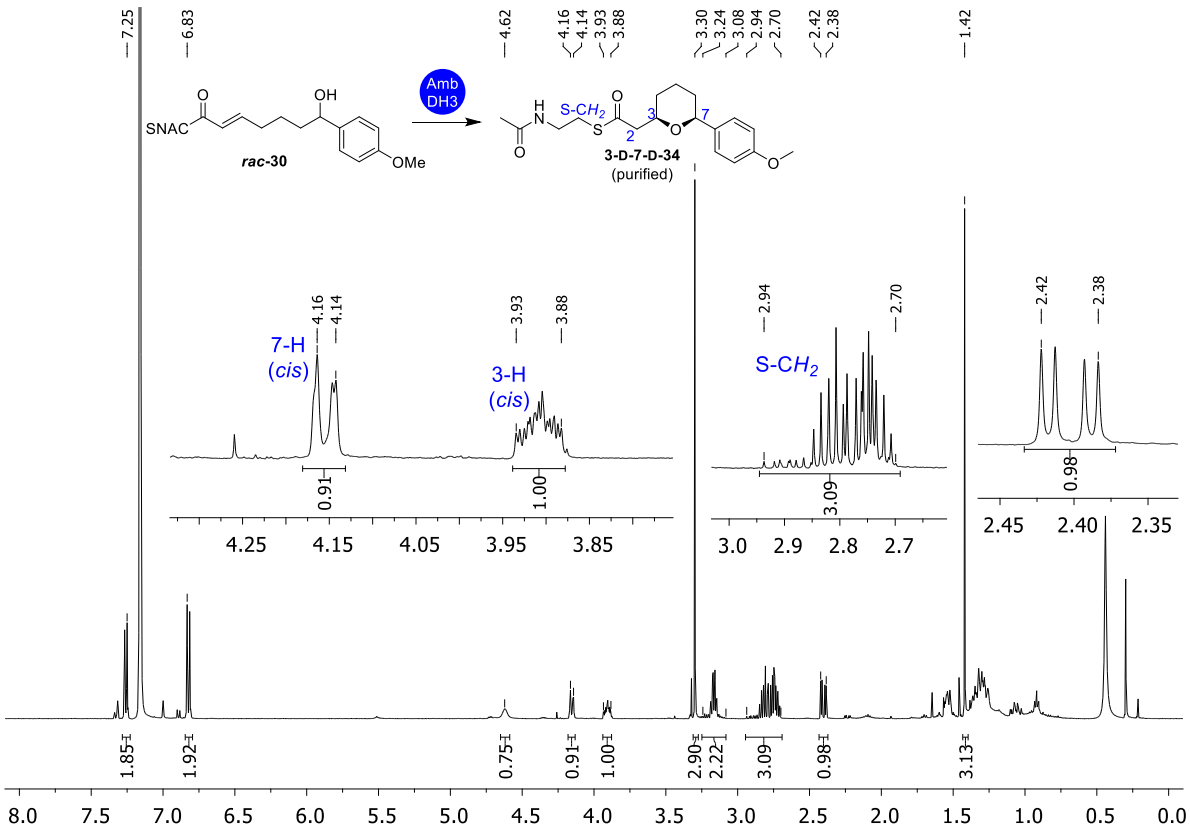

Figure S73. ^{1}H NMR analysis of the purified product of the incubation reaction of *rac*-**30** and AmbDH3 (C_6D_6, 500 MHz). It shows the 2,6-*cis*-THP characteristic shift of δ(**7-H**) = 4.15 and δ(**3-H**) = 3.91 ppm.

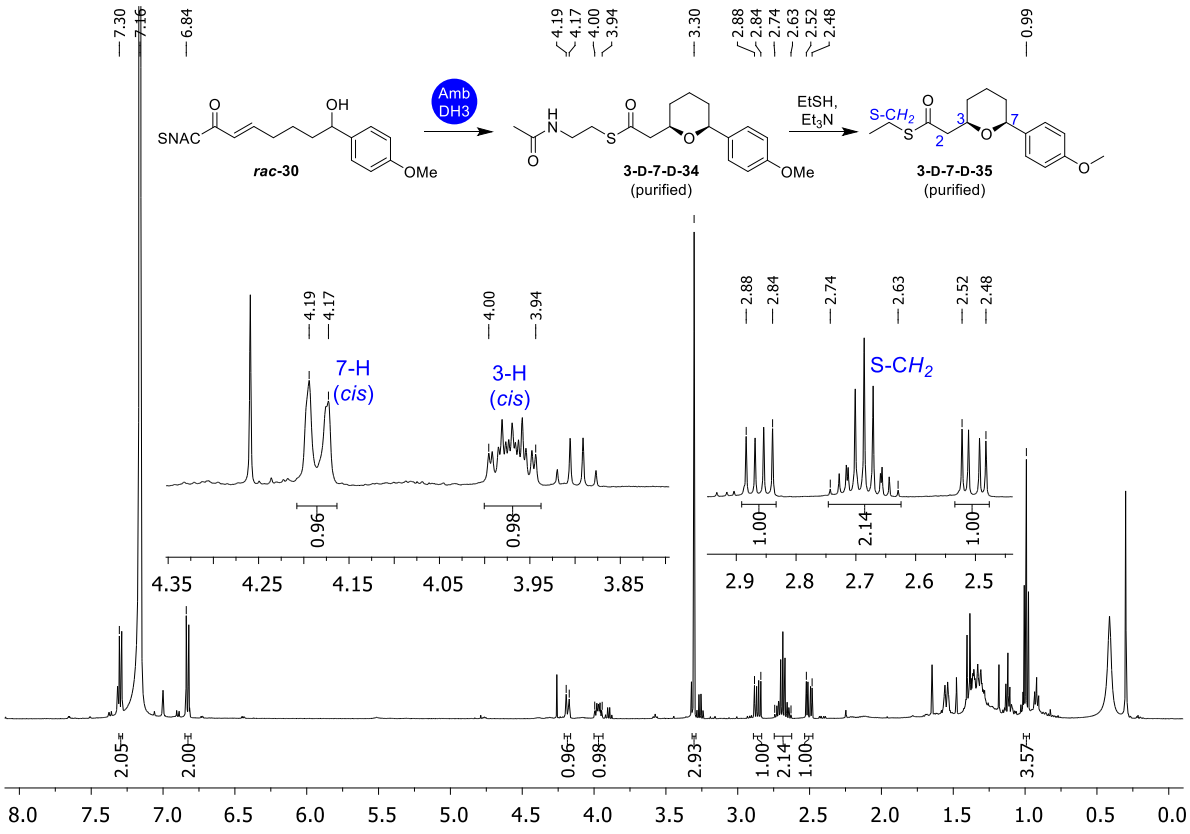

Figure S74. ^{1}H NMR analysis of the SEt thioester resulting from the transesterification of the SNAC thioester shown in Figure S73 (C_6D_6, 500 MHz). It shows the 2,6-*cis*-THP characteristic shift of δ(**7-H**) = 4.18 and δ(**3-H**) = 3.97 ppm.

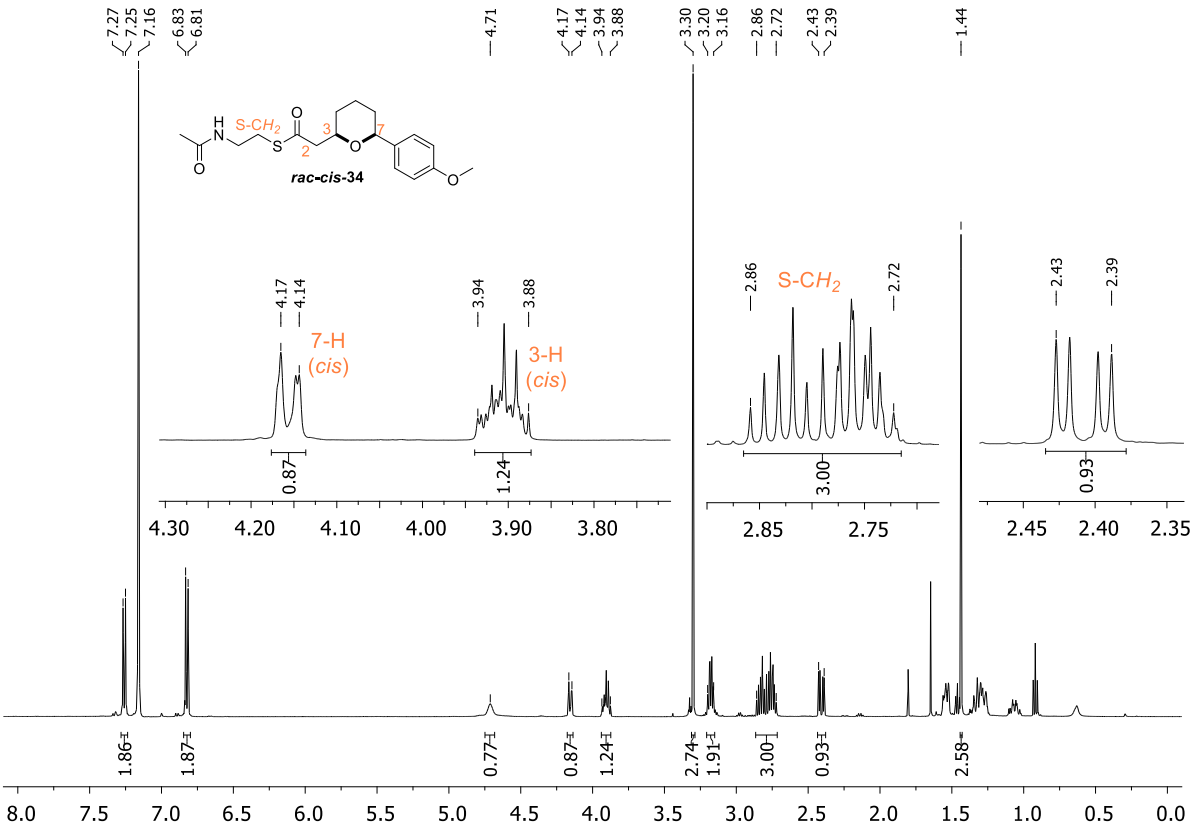

Figure S75. ^{1}H NMR analysis of the synthetic reference compound *cis-rac*-**34** (C_6D_6, 500 MHz). It shows the 2,6-*cis*-THP characteristic shift of δ(**7-H**) = 4.16 and δ(**3-H**) = 3.91 ppm.

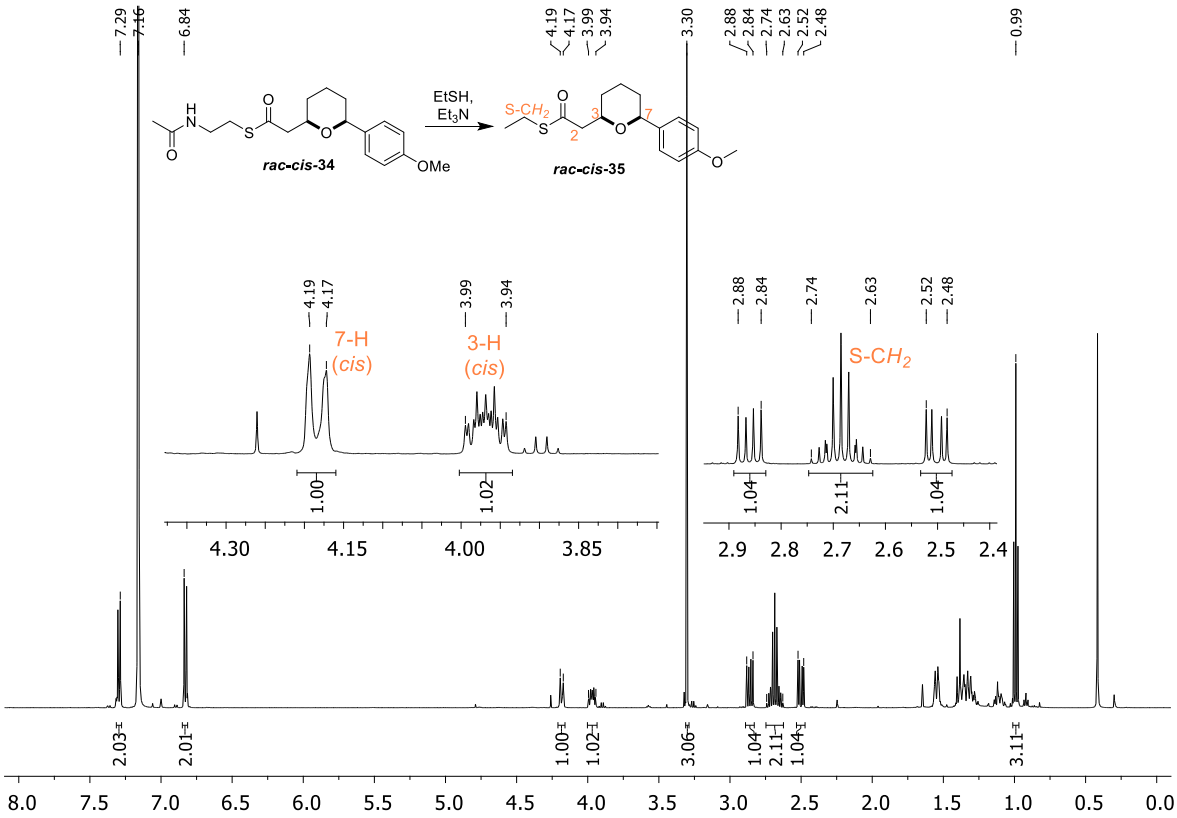

Figure S76. ^{1}H NMR analysis of the SEt thioester resulting from the transesterification of the reference compound shown in Figure S75 (C_6D_6, 500 MHz). It shows the 2,6-*cis*-THP characteristic shift of δ(**7-H**) = 4.18 and δ(**3-H**) = 3.97 ppm.

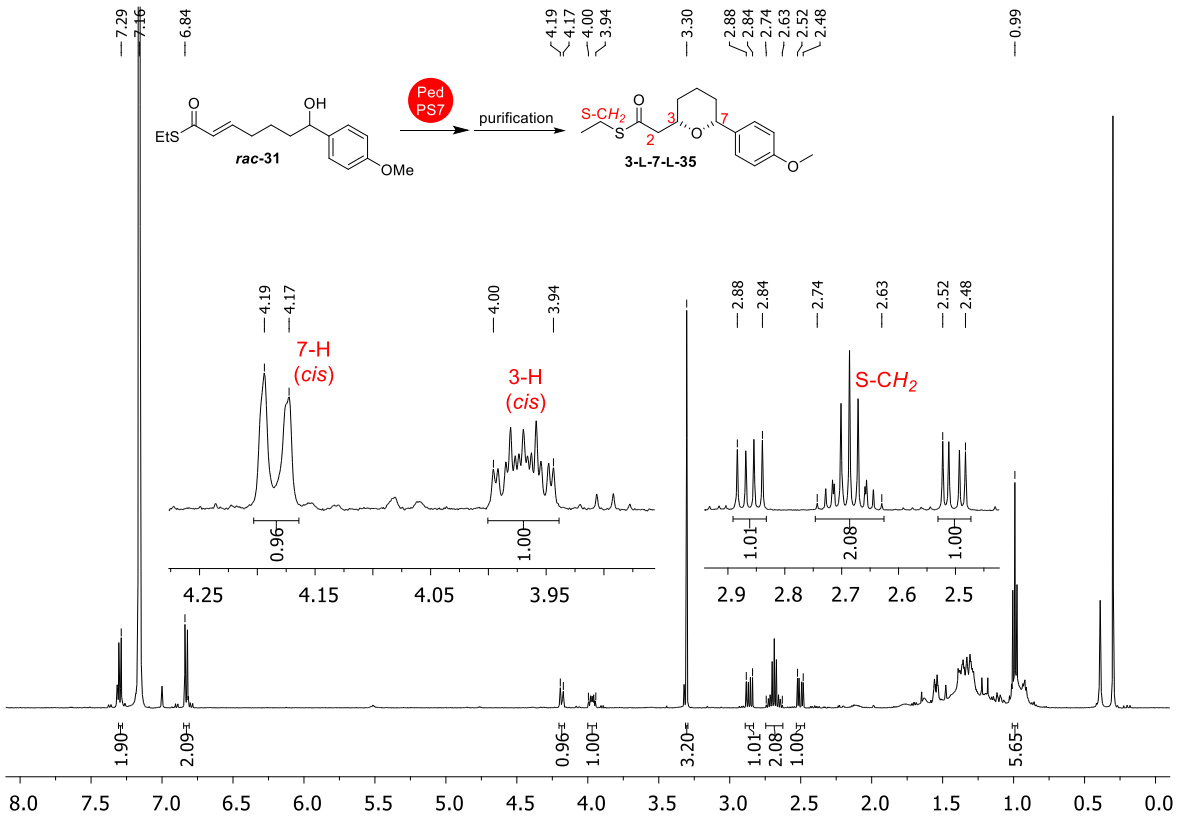

Figure S77. ^{1}H NMR analysis of the purified *cis*-**39** diastereomer from the incubation of PedPS7 and **22** (C_6D_6, 500 MHz). It shows the 2,6-*cis*-THP characteristic shift of δ(**7-H**) = 4.18 and δ(**3-H**) = 3.97 ppm.

HRMS (ESI$^+$) *m/z* for $C_{16}H_{23}O_3S$ $[M+H]^+$: calculated 295.1368, found 295.1359.

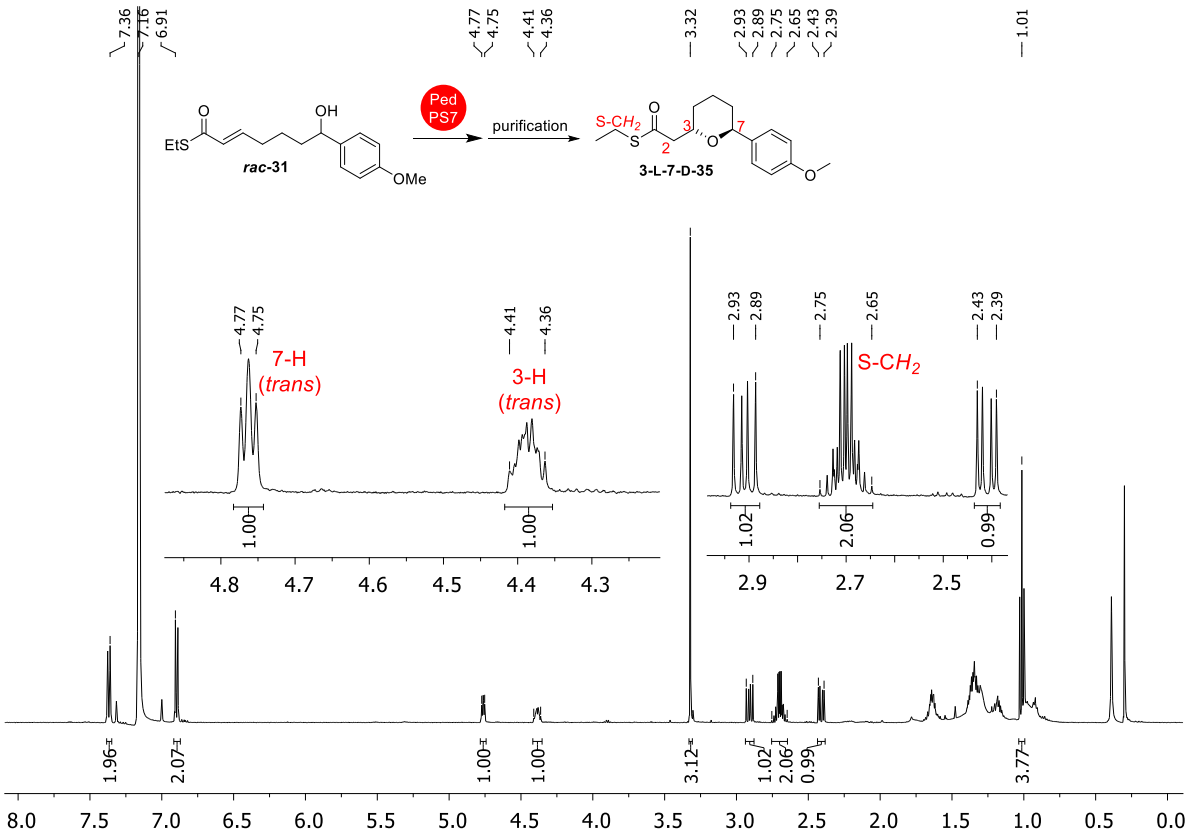

Figure S78. ^{1}H NMR analysis of the purified *trans*-**39** diastereomer from the incubation of PedPS7 and **31** ($CDCl_3$, 500 MHz). It shows the 2,6-*trans*-THP characteristic shift of δ(**7-H**) = 4.76 and δ(**3-H**) = 4.39 ppm.

HRMS (ESI$^+$) *m/z* for $C_{16}H_{23}O_3S$ $[M+H]^+$: calculated 295.1368, found 295.1358.

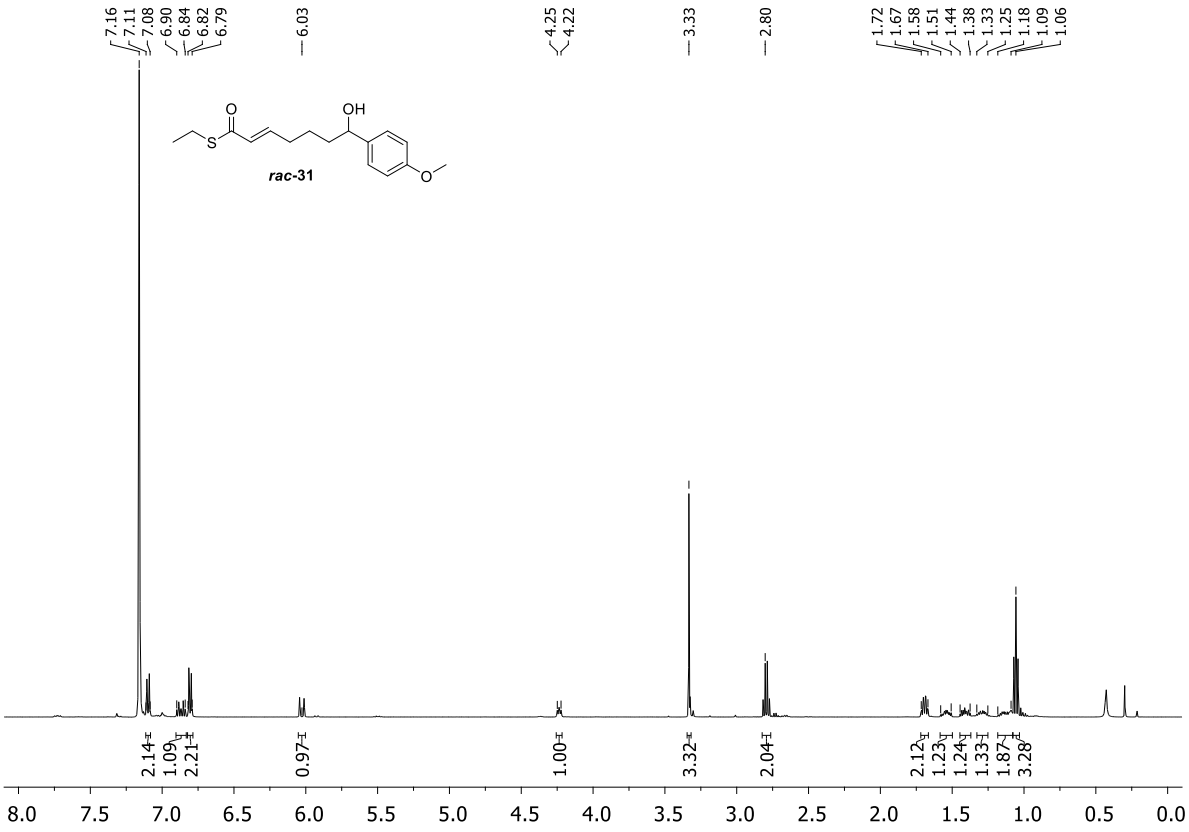

Figure S79. ^{1}H NMR analysis of the starting material *rac*-**31** (C_6D_6, 500 MHz).

^{1}H NMR (500 MHz, C_6D_6): δ [ppm] = 7.11–7.08 (m, 2H, *m*-C*H*$_{Ar}$OMe), 6.87 (dt, *J* = 15.5, 7.0 Hz, 1H, OCCHC*H*), 6.82–6.78 (m, 2H, *o*-C*H*$_{Ar}$OMe), 6.03 (dt, *J* = 15.5, 1.5 Hz, 1H, OCC*H*CH), 4.26–4.22 (m, 1H, C*H*OH), 3.33 (s, 3H, OC*H*$_3$), 2.79 (q, *J* = 7.4 Hz, 2H, C*H*$_2$S), 1.72–1.67 (m, 2H, CHCHC*H*$_2$), 1.58–1.50 (m, 1H, 1× C*H*$_2$COH), 1.45–1.37 (m, 1H, 1× C*H*$_2$COH), 1.32–1.25 (m, 1H, 1× CH_2C*H*$_2CH_2$), 1.18–1.09 (m, 2H, 1× CH_2C*H*$_2CH_2$, O*H*), 1.06 (t, *J* = 7.4 Hz, 3H, C*H*$_3CH_2$S).

Chiral HPLC analysis and reference experiments

An estimation of the individual stereoisomers of **28**, **30** and **31** in the starting material and in purified products after enzymatic assays was made by chiral HPLC (Figure S80-Figure S92). The individual stereoisomers of **28** migrated in the order **7-L-28** and **7-D-28**, according to reference [2].

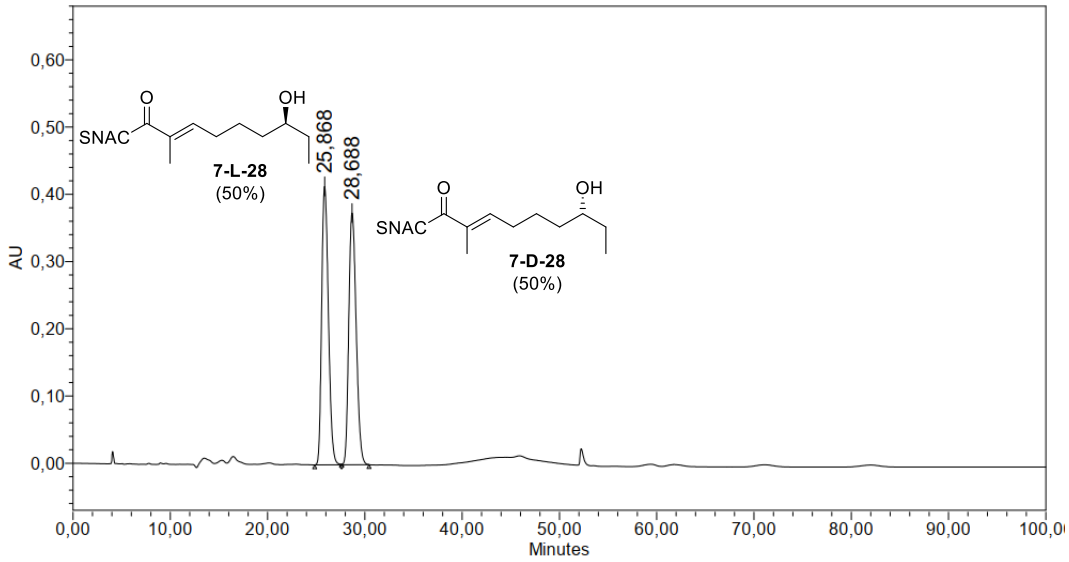

	Ret. Time	Start (min)	End (min)	Height	% Height	Area	% Area
1	25,87	24,85	30,43	414188	52,52	19867073	50,08
2	28,69	24,85	30,43	374466	47,48	19805989	49,92

Figure S80. Chiral HPLC analysis of *rac*-**28**. t_R(**7-L-28**)=25.87 min, t_R(**7-D-28**)=28.69 min. The elution order was established based on the chiral HPLC profiles in reference [2].

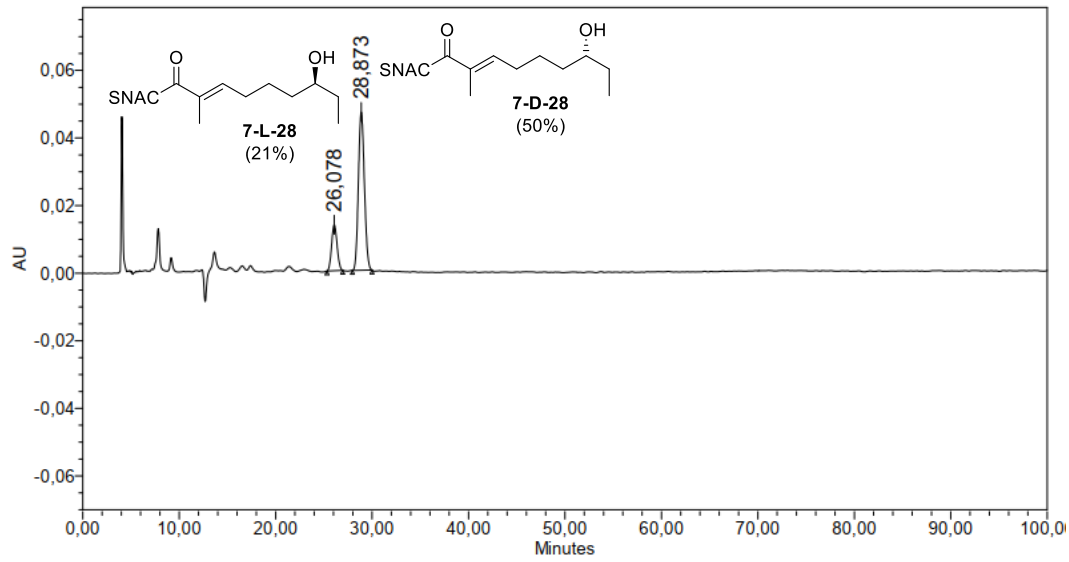

	Ret. Time	Start (min)	End (min)	Height	% Height	Area	% Area
1	26,08	25,33	26,95	13583	22,48	534366	20,93
2	28,87	27,96	29,98	46837	77,52	2018198	79,07

Figure S81. Chiral HPLC analysis of the resiolated mixture of **7-L-28** and **7-D-28** after three incubation cycles of PedPS7 and *rac*-**28** and flash chromatography (see NMR spectrum in Figure S65). **7-L-28** was consumed by the PedPS7 to a larger extent. t_R(**7-L-28**)=26.08 min, t_R(**7-D-28**)=28.87 min.

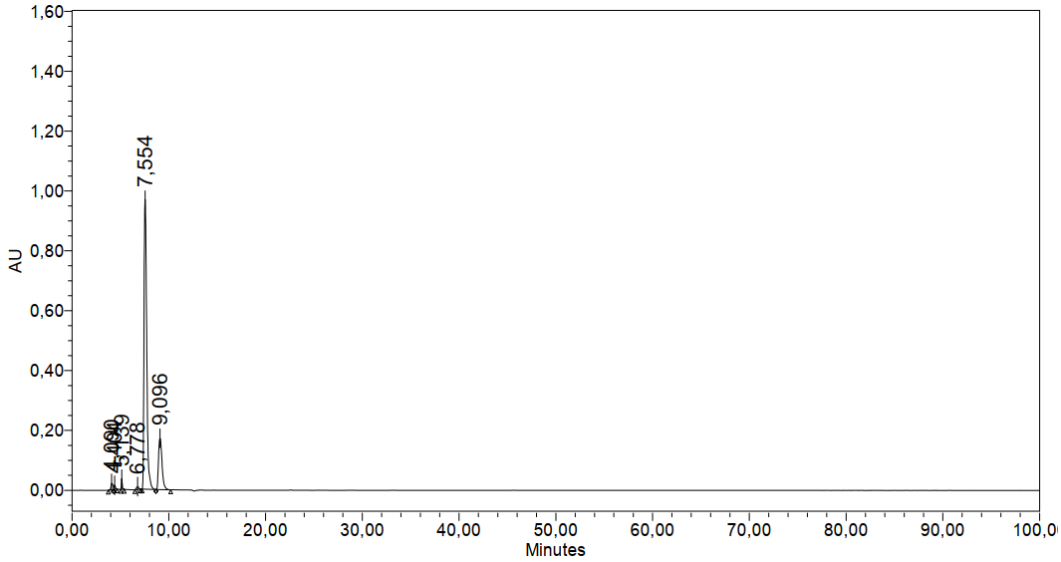

	Ret. Time	Start (min)	End (min)	Height	% Height	Area	% Area
1	4,09	3,75	4,67	21478	1,76	324132	1,35
2	4,40	3,75	4,67	14070	1,15	146082	0,61
3	5,14	5,03	5,40	35195	2,88	231684	0,97
4	6,78	6,50	7,08	9391	0,77	153608	0,64
5	7,55	7,25	10,20	968247	79,36	18782367	78,35
6	9,10	7,25	10,20	171612	14,07	4335950	18,09

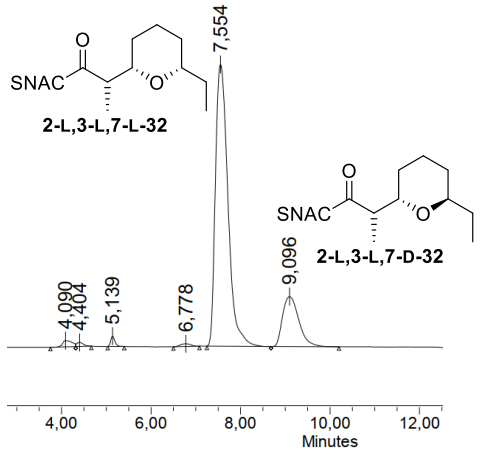

Figure S82. Chiral HPLC analysis of the product mixture after three reaction cycles of PedPS7 and substrate *rac*-**28** and subsequent flash chromatography (see NMR spectrum in Figure S63). t_R(**2-L,3-L,7-L-32**)=7.55 min, t_R(**2-L,3-L,7-D-32**)=9.10 min. The product stereoisomers were annotated based on the established 2-L,3-L,7-D-selectivity of PedPS7, the *syn*-THP:*anti*-THP ratio in the UPLS-MS chromatograms and NMR spectra as well as by comparison to chiral HPLC elution profiles of the product from the reaction of **28** and AmbDH3.[2]

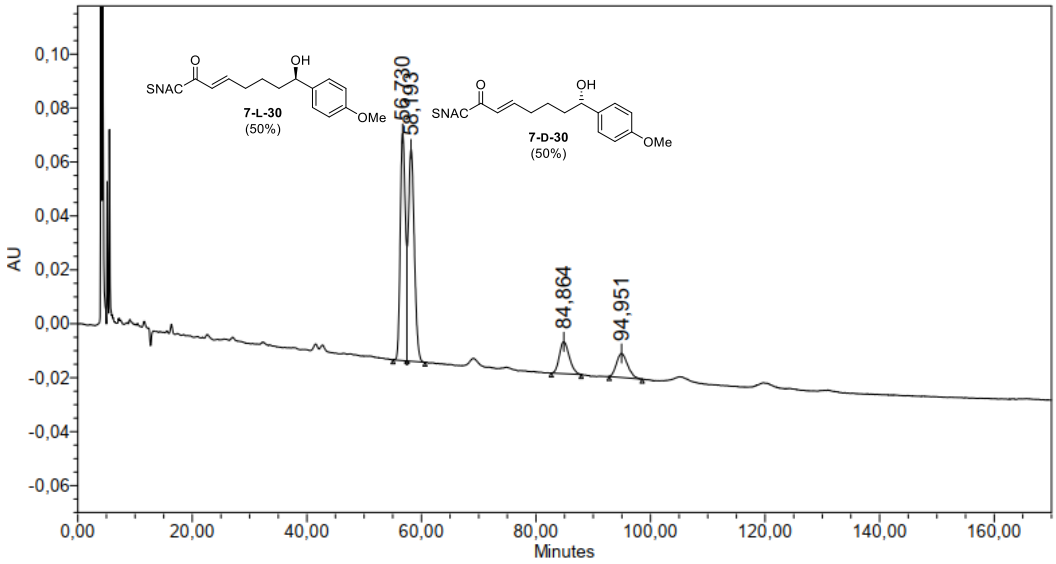

	Ret. Time	Start (min)	End (min)	Height	% Height	Area	% Area
1	56,73	55,07	60,63	84272	45,85	5286873	38,57
2	58,19	55,07	60,63	78753	42,85	5782459	42,18
3	84,86	82,67	87,90	11840	6,44	1435026	10,47
4	94,95	92,78	98,55	8929	4,86	1203732	8,78

Figure S83. Chiral HPLC analysis of synthetic *rac*-**30**. t_R(**7-L-30**)=56.73 min, t_R(**7-D-30**)=58.19 min. Minor amounts of the *cis*-THP products resulting from spontaneous cyclisation after long-time storage are visible at 84.86 min and 94.95 min.

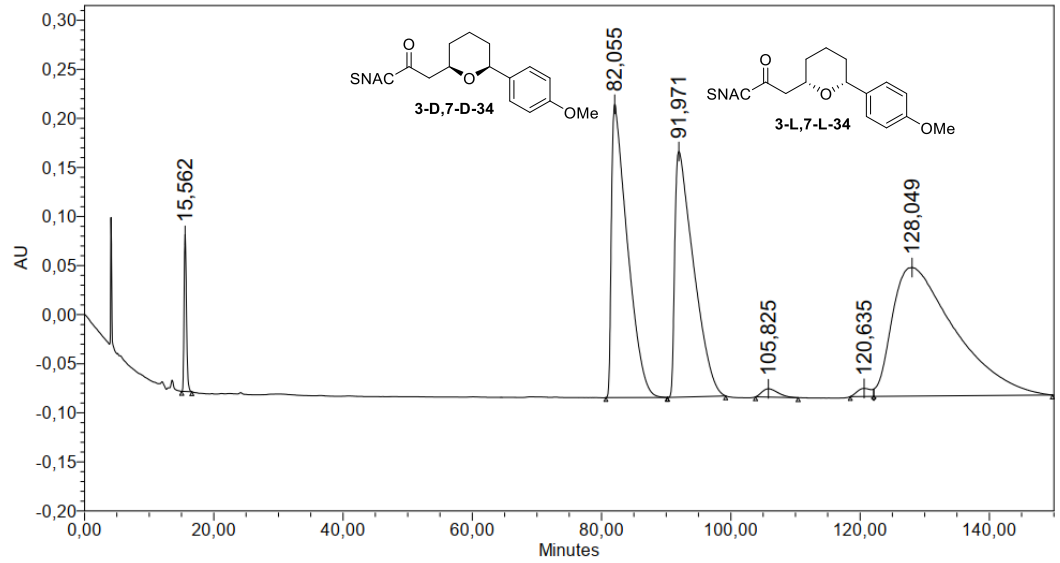

	Ret. Time	Start (min)	End (min)	Height	% Height	Area	% Area
1	15,56	15,03	16,60	159854	18,66	4057802	2,06
2	82,05	80,68	90,17	298827	34,89	51208078	26,00
3	91,97	90,20	99,20	250257	29,22	50629096	25,70
4	105,83	103,82	110,42	8433	0,98	1449298	0,74
5	120,64	118,48	149,78	8180	0,96	1263843	0,64
6	128,05	118,48	149,78	130989	15,29	88360114	44,86

Figure S84. Chiral HPLC analysis of synthetic *rac-cis*-**34**. t_R(**3-D,7-D-34**)=82.06 min, t_R(**3-L,7-L-34**)=91.97 min. Minor amounts of the *trans* diastereomers of **34** are visible at 105.83 min and 120.64 min. The peak at 128.05 min is associated to an impurity that is non-related to the sample (see Figure S75 for confirmation).

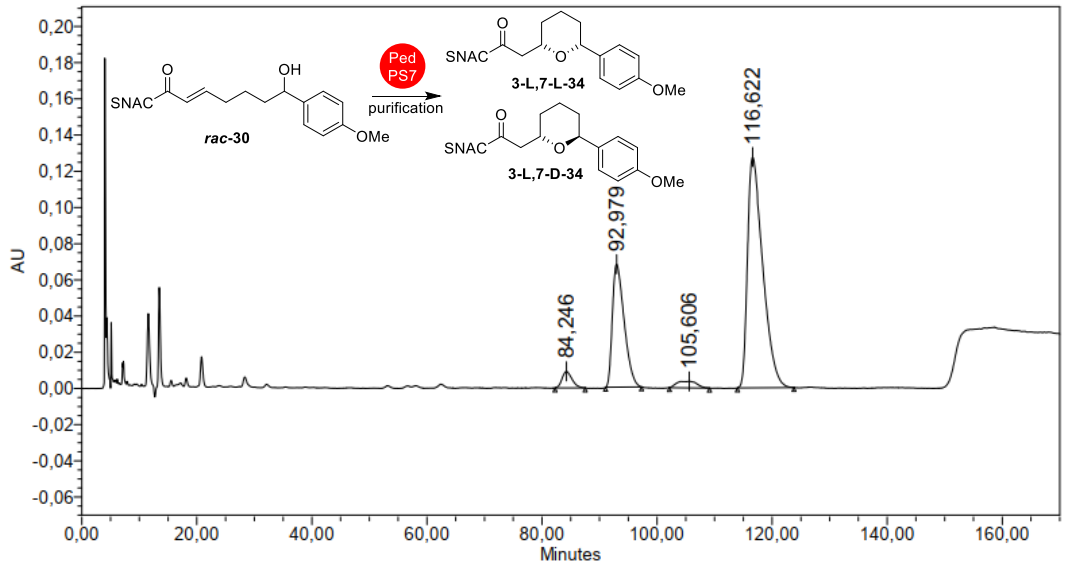

	Ret. Time	Start (min)	End (min)	Height	% Height	Area	% Area
1	84,25	82,27	87,50	9137	4,39	1092839	3,11
2	92,98	91,05	97,30	67927	32,63	9656055	27,50
3	105,61	102,15	109,10	3583	1,72	872789	2,49
4	116,62	113,98	123,82	127521	61,26	23486679	66,90

Figure S85. Chiral HPLC analysis of the purified product mixture of **3-L,7-L-34** and **3-L,7-D-34** after one reaction cycle of PedPS7 and substrate **30.** t_R(**3-L,7-L-34**)=92.98 min, t_R(**3-D,7-L-34** or **3-L,7-D-34**)=116.62 min. (see Figure S70).

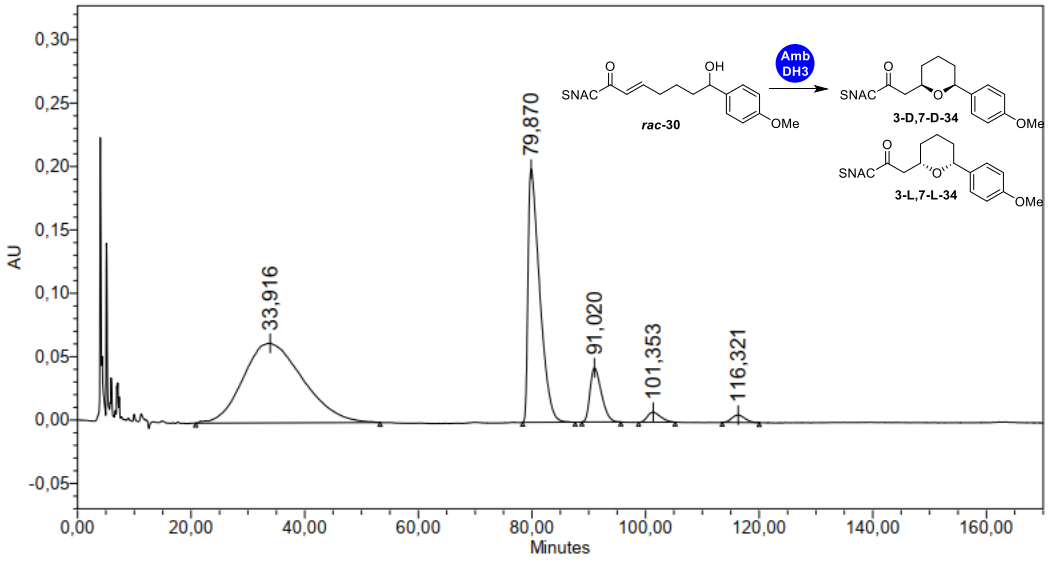

	Ret. Time	Start (min)	End (min)	Height	% Height	Area	% Area
1	33,92	20,82	53,27	62808	19,69	45968040	55,73
2	79,87	78,37	87,62	199701	62,59	28360353	34,38
3	91,02	88,78	95,65	42774	13,41	5933094	7,19
4	101,35	98,77	105,20	7930	2,49	1285199	1,56
5	116,32	113,50	120,00	5848	1,83	940429	1,14

Figure S86. Chiral HPLC analysis of the purified product mixture of **3-D,7-D-34** and **3-L,7-L-34** after one reaction cycle of of AmbDH3 and substrate **30**. t_R(**3-D,7-D-34**)=79.87 min, t_R(**3-L,7-L-34**)=91.02 min.

The SNAC thioester shown in Figure S84–Figure S86 were converted into the respective EtS thioesters to provide a reference for the configurational assignment of the products from the incubation of **31** with PedPS7.

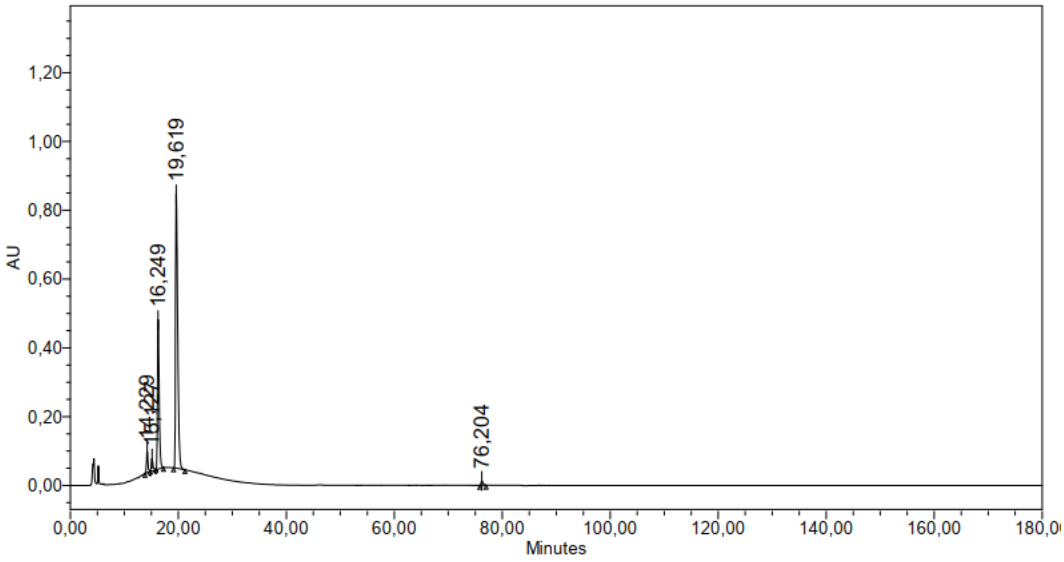

	Ret. Time	Start (min)	End (min)	Height	% Height	Area	% Area
1	14,23	13,83	17,27	61996	4,61	1121572	3,31
2	15,13	13,83	17,27	36774	2,73	812866	2,40
3	16,25	13,83	17,27	434831	32,34	9555804	28,17
4	19,62	19,12	21,22	798070	59,35	22110406	65,18
5	76,20	75,85	77,00	12951	0,96	319065	0,94

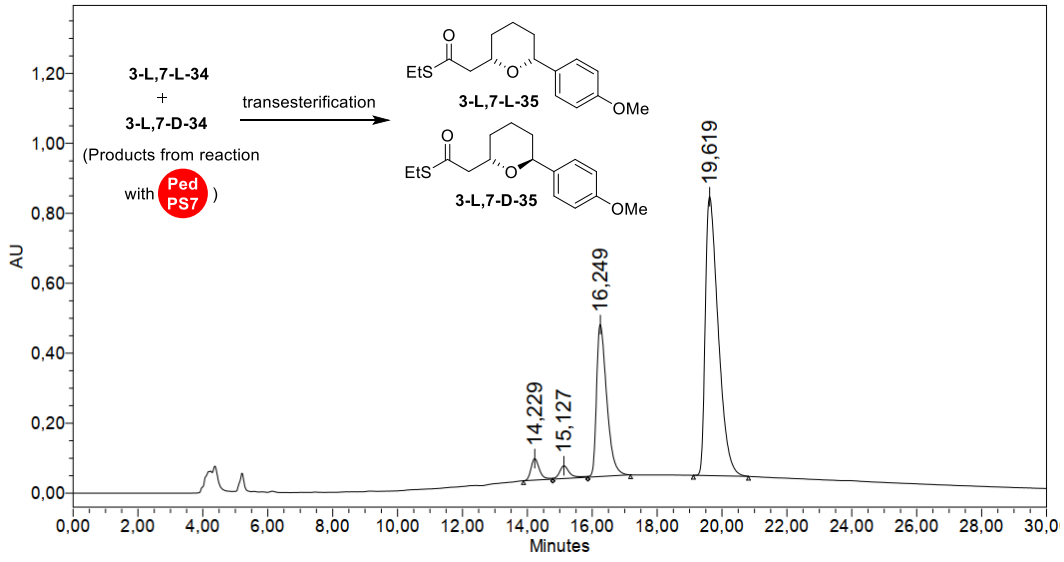

Figure S87. Chiral HPLC analysis of the purified product mixture of **3-L,7-L-34** and **3-L,7-D-34** after SNAC→SEt transesterification of the PedPS7 reaction product to **3-L,7-L-35** and **3-L,7-D-35** (Figure S85). t_R(**3-L,7-L-35**)=16.25 min, t_R(**3-L,7-D-35**)=19.62 min.

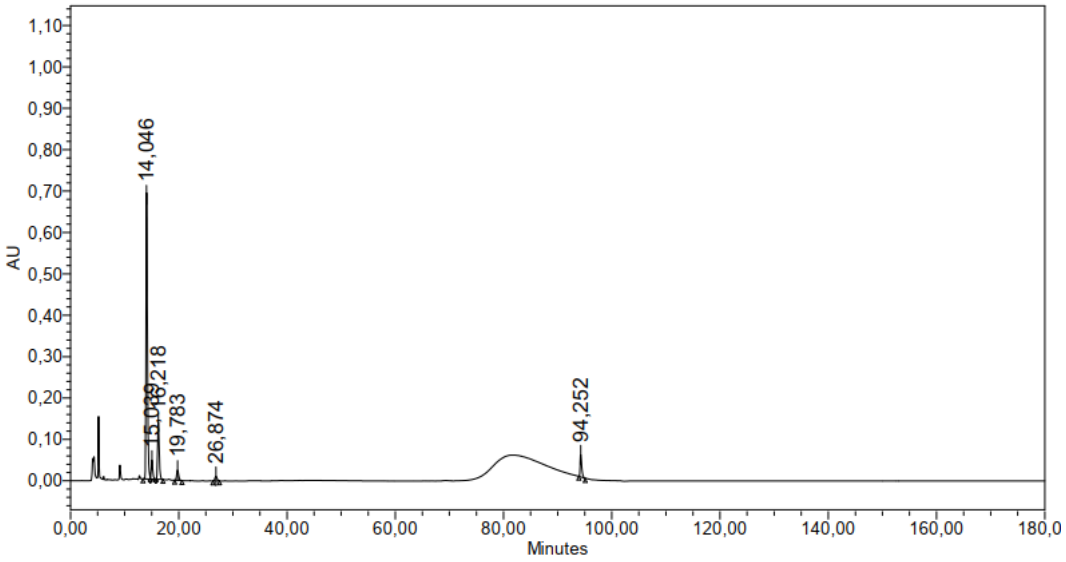

	Ret. Time	Start (min)	End (min)	Height	% Height	Area	% Area
1	14,05	13,42	17,10	691567	71,65	12872539	68,66
2	15,04	13,42	17,10	45987	4,76	937989	5,00
3	16,22	13,42	17,10	138232	14,32	2903519	15,49
4	19,78	19,25	20,60	24737	2,56	610444	3,26
5	26,87	26,32	27,53	11249	1,17	317071	1,69
6	94,25	93,93	95,10	53443	5,54	1106471	5,90

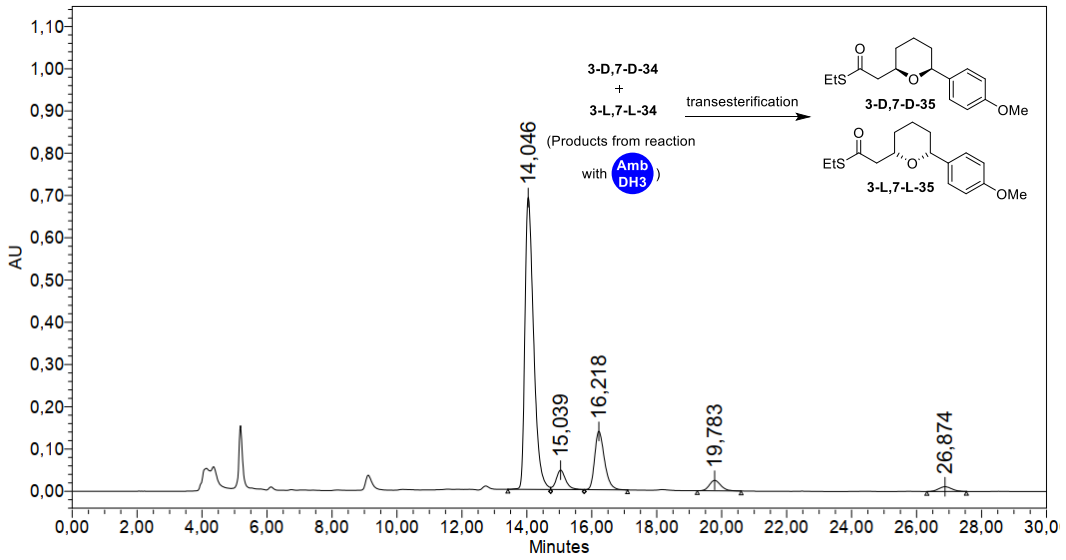

Figure S88. Chiral HPLC analysis of the purified product mixture of **3-D,7-D-34** and **3-L,7-L-34** after SNAC→SEt transesterification of the product from AmbDH3 incubation to **3-D,7-D-35** and **3-L,7-L-35** (Figure S86). t_R(**3-D,7-D-35**)=14.05 min, t_R(**3-L,7-L-35**)=16.22 min.

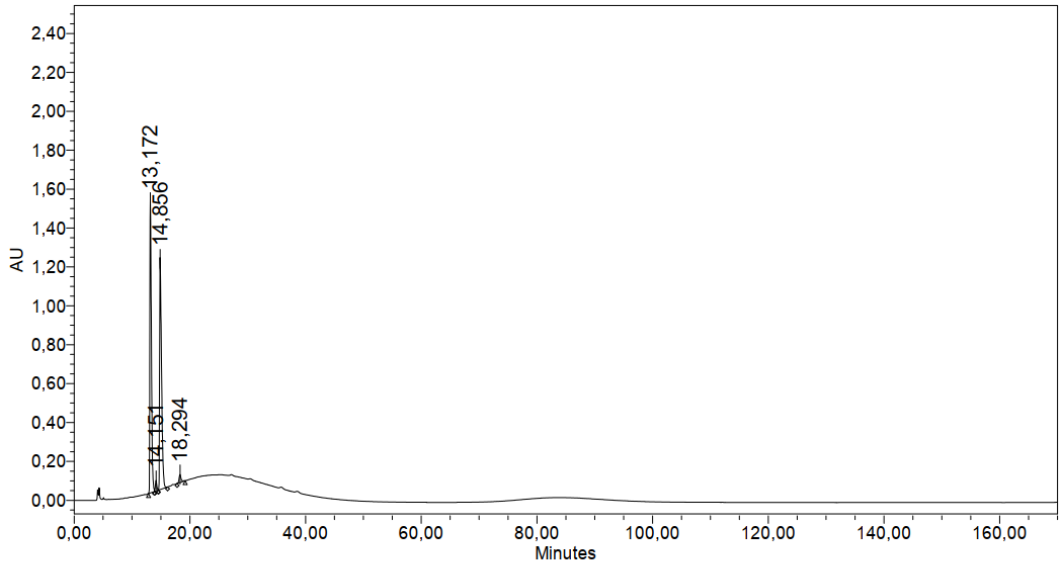

	Ret. Time	Start (min)	End (min)	Height	% Height	Area	% Area
1	13,17	12,87	19,18	1507858	53,90	27314082	47,86
2	14,15	12,87	19,18	54456	1,95	921672	1,62
3	14,86	12,87	19,18	1194044	42,68	27840242	48,78
4	18,29	12,87	19,18	41402	1,48	991548	1,74

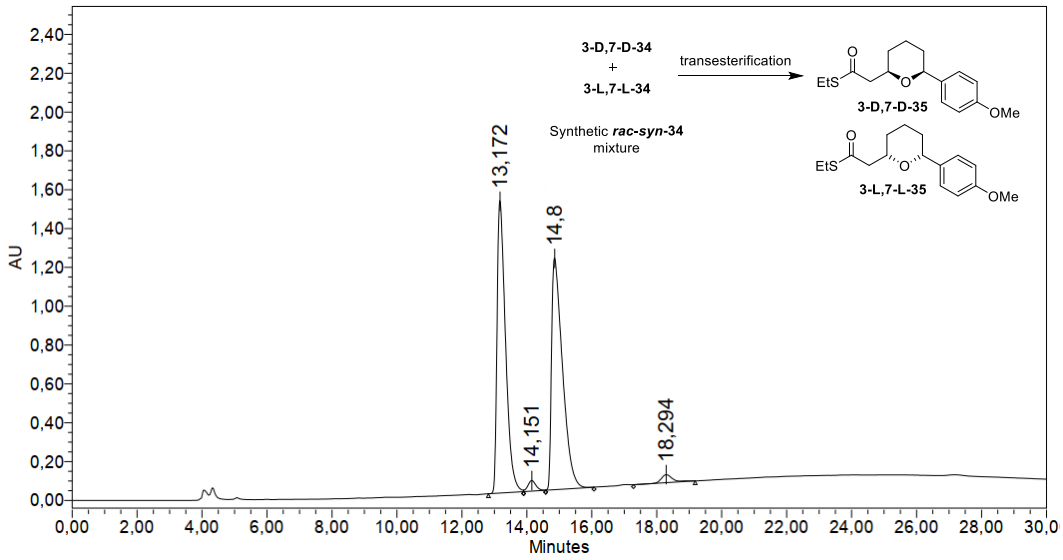

Figure S89. Chiral HPLC analysis of the reference *cis*-products of **3-D,7-D-34** and **3-L,7-L-34** after SNAC→SEt transesterification of the synthetic *syn-rac*-mixture to **3-D,7-D-35** and **3-L,7-L-35** (Figure S87). t_R(**3-D,7-D-35**)=13.17 min, t_R(**3-L,7-L-35**)=14.86 min.

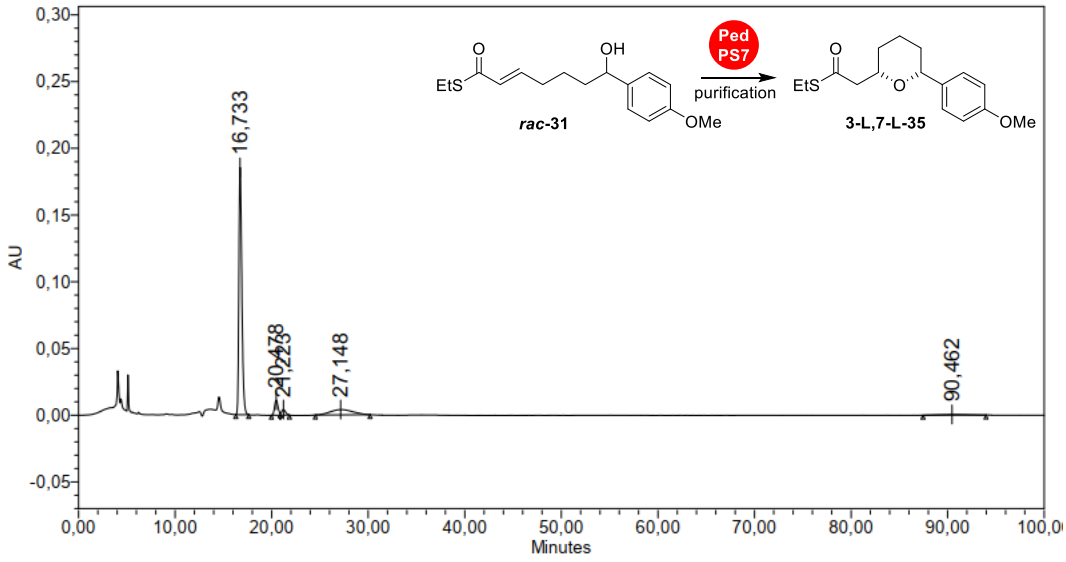

	Ret. Time	Start (min)	End (min)	Height	% Height	Area	% Area
1	16,73	16,28	17,63	185248	90,24	3948186	77,22
2	20,48	19,98	21,83	11284	5,50	279161	5,46
3	21,22	19,98	21,83	4196	2,04	122367	2,39
4	27,15	24,53	30,20	3987	1,94	647178	12,66
5	90,46	87,45	93,98	572	0,28	116176	2,27

Figure S90. Chiral HPLC analysis of the purified *cis*-THP product **3-L,7-L-35** after two reaction cycles of PedPS7 and substrate *rac*-**31** (see Figure S77). t_R(**3-L,7-L-35**)=16.73 min.

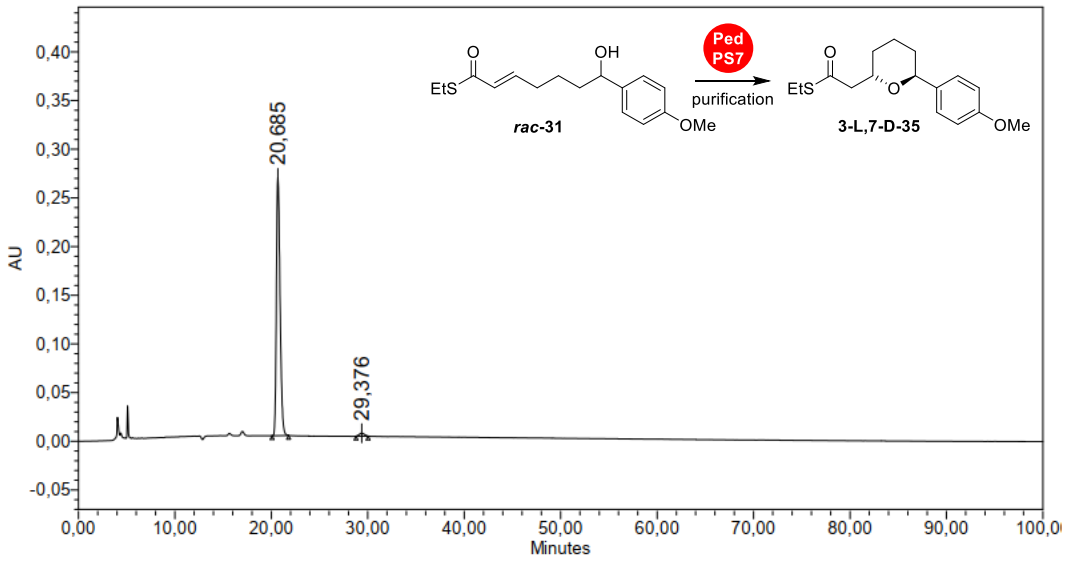

	Ret. Time	Start (min)	End (min)	Height	% Height	Area	% Area
1	20,68	20,08	21,80	264821	98,87	6985843	98,40
2	29,38	28,78	30,03	3018	1,13	113354	1,60

Figure S91. Chiral HPLC analysis of the purified *trans*-THP product **3-D,7-L-35** or **3-L,7-D-35** after two reaction cycles of PedPS7 and substrate **31** (see Figure S78). t_R(**3-D,7-L-35** or **3-L,7-D-35**)=20.69 min.

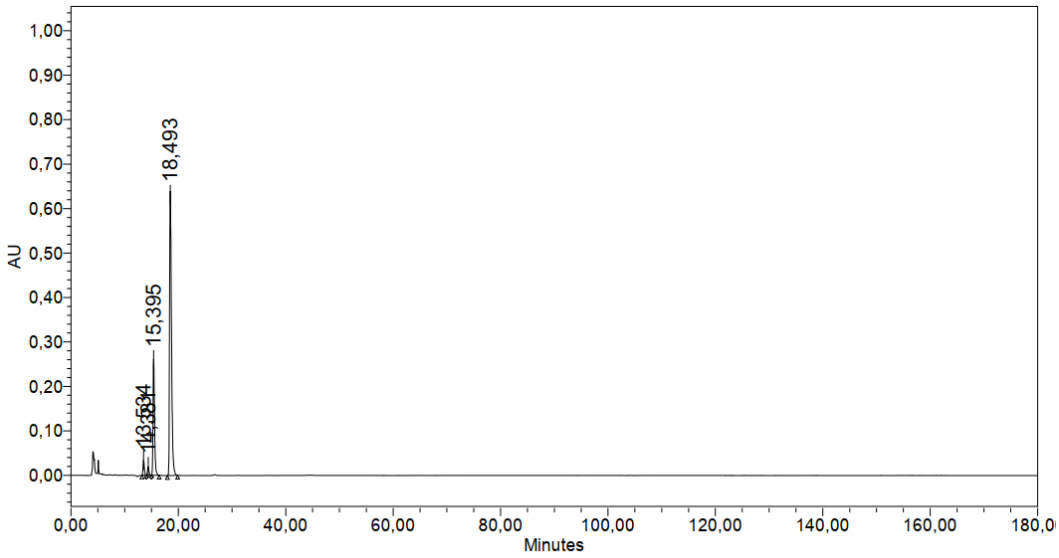

	Ret. Time	Start (min)	End (min)	Height	% Height	Area	% Area
1	13,53	13,25	16,43	33767	3,54	550314	2,49
2	14,38	13,25	16,43	19437	2,04	345558	1,56
3	15,39	13,25	16,43	261713	27,40	5247427	23,76
4	18,49	17,95	19,87	640144	67,03	15938000	72,18

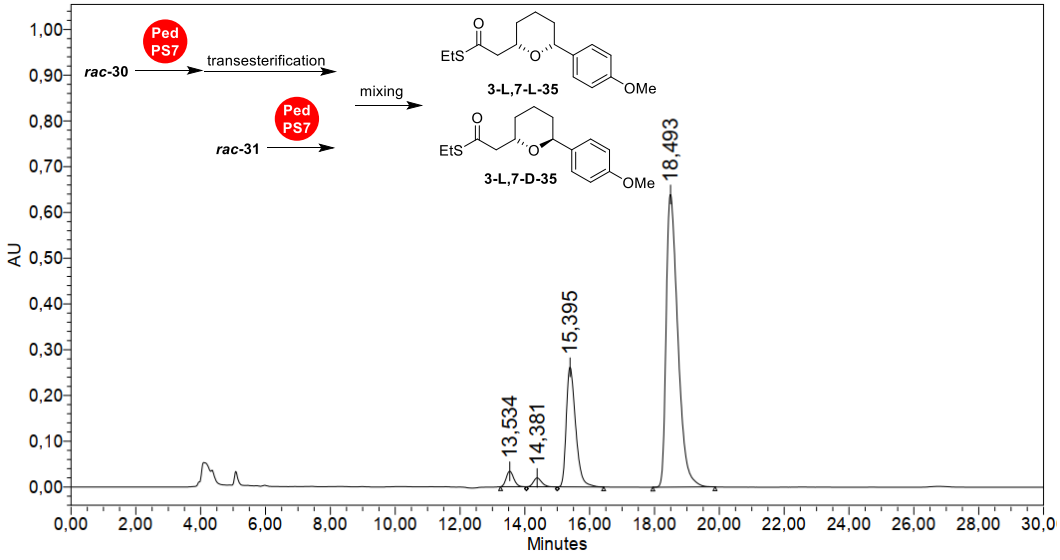

Figure S92. Chiral HPLC analysis after mixing of the product from incubation of *rac*-**30** with PedPS7 followed by transesterification and from the incubation of *rac*-**31** with PedPS7. The individual chiral HPLC analysis are shown in Figure S87, Figure S90 and Figure S91. This spiking experiment confirms that the configuration of the reaction products from incubation of PedPS7 and *rac*-**30** or *rac*-**31**, respectively, is identical. t_R(**3-L,7-L-35**)=15.40 min, t_R(**3-D,7-L-35** or **3-L,7-D-35**)=18.49 min.

References

1 G. Berkhan and F. Hahn, *Angew. Chem. Int. Ed.*, 2014, **53**, 14240–14244.

2 T. Hollmann, G. Berkhan, L. Wagner, K. H. Sung, S. Kolb, H. Geise and F. Hahn, *ACS Catal.*, 2020, **10**, 4973–4982.

3 G. H. Lonca, D. Y. Ong, T. M. H. Tran, C. Tejo, S. Chiba and F. Gagosz, *Angew. Chem. Int. Ed.*, 2017, **56**, 11440–11444.

4 Z. Song, R. P. Hsung, T. Lu and A. G. Lohse, *J. Org. Chem.*, 2007, **72**, 9722–9731.

5 T. J. Harrison, S. Ho and J. L. Leighton, *J. Am. Chem. Soc.*, 2011, **133**, 7308–7311.

6 P. J. Kocieński, R. C. D. Brown, A. Pommier, M. Procter and B. Schmidt, *J. Chem. Soc. Perkin 1*, 1998, **0**, 9–40.